Cape Peninsula University of Technology

Synthesis of zeolite (ZSM-5 and Faujasite) and geopolymer from South African coal fly ash

By

Nkululeko Zenzele Neville, Ndlovu

Thesis submitted in fulfilment of the requirements for the degree

Master of Engineering: Chemical Engineering

In the Faculty of Engineering

At the Cape Peninsula University of Technology

Supervisor: Prof. Tunde, V. Ojumu

Co-supervisor: Prof Leslie, F.Petrik

Bellville Campus

September 2016

DECLARATION

I, Nkululeko Zenzele Neville Ndlovu, declare that the contents of this thesis represent my own unaided work, and that the thesis has not previously been submitted for academic examination towards any qualification. Furthermore, it represents my own opinions and not necessarily those of the Cape Peninsula University of Technology.

…… ……

Signed Date

ABSTRACT

Population growth in South Africa has led to a direct increase in electricity demand. Due to the abundance of coal in the country, most of the energy requirement is met through coal combustion. Although there is a vast coal resource, the natural high grade coal is mainly exported, while the low grade coal is exploited for electricity generation. The combustion of low grade coal during electricity production results in huge quantities of coal fly ash (CFA) that require careful disposal, due to its toxicity. Poor management of this waste constitutes serious human and environmental problems, such as respiratory diseases, contamination of soil, surface water and groundwater. This is in part due to the fact that only a small percentage of fly ash is utilised efficiently in the construction industry. Several studies have recently been conducted into the use of CFA as a starting material for the synthesis of zeolites and geopolymers, due to its high silicon and aluminium content. However, the synthesis of zeolites from CFA has been subject to criticism, because the synthesis of zeolites from the bulk CFA results in zeolite products that are mixed with non-reacted fly ash and toxic elements. On the other hand, pure phase zeolites can only be synthesised from CFA extracts, which results in a small yield of the zeolite products and a huge amount of solid waste. Therefore, this does not facilitate either the use of fly ash-based zeolites as catalysts in advanced chemical processes or scaling up of the synthesis process.

This study seeks to make optimal use of CFA by developing a method for optimal extraction of Si and Al for the synthesis of ZSM-5 and faujasite zeolites, and use the resulting solid waste for the synthesis of geopolymers such that the resultant waste is minimised or completely eliminated. Two distinct processes are employed in this study to synthesise ZSM-5 or faujasite zeolite from CFA extracts, while the solid residue is transformed into a geopolymer. In the first process, an alkaline leaching method is employed for extraction of Si from CFA using 8 M NaOH at 150 ^{0}C for 24 h. It was found that the Si extract contained a certain amount of Al, enough for the synthesis of a high silica zeolite such as ZSM-5. However, the Si extract had to be treated with oxalic acid in order to remove the excess Na in the extract, since this could prevent the formation of ZSM-5. The obtained Si extract was then used as a feedstock for the synthesis of Zeolite ZSM-5 with NaOH and tetraethyl ammonium hydroxide (TEAOH) as mineralising and structure directing agents respectively. The obtained gel underwent hydrothermal synthesis at 160 °C for 72 h, while the solid residue obtained after Si extraction was used in the synthesis of geopolymer at 70 °C for 5 days. The obtained ZSM-5 and geopolymer products were characterised using ICP, XRD, SEM, FTIR and NMR techniques.

The results obtained from Process 1 showed that ZSM-5 and a geopolymer were successfully synthesised with only CFA as source of Si and Al, with a yield of synthesised ZSM-5 of 35.9%.

The second process involved the acid leaching method for the extraction of Al from CFA using H_2SO_4 at 250 ^oC for 6 h; aluminium sulphate was precipitated and recovered over a period of 24 hours, followed by calcination at 800 ^0C for 2 h. Thereafter, the solid residue was used for the extraction of Si using 8 M NaOH at 150 ^0C for 24 h. The obtained Si extract was also treated with oxalic acid, in the same manner as the Si extract in the first process. The obtained Al and Si extracts were then used as feedstocks in the synthesis of faujasite zeolite at 100 °C for 6 h. It was found that the yield of synthesised faujasite zeolite was 43.28%. Subsequently, the resulting solid residue obtained after Al and Si extraction was used in synthesis of geopolymer at 70 °C for 5 days. The fly ash-based faujasite and geopolymer were also characterised using ICP, XRD, SEM, FTIR and NMR techniques. The results obtained showed that zeolite faujasite and a geopolymer were successfully synthesised from CFA.

The success of this project constitutes a breakthrough in the valorisation of CFA through the synthesis of pure and high value zeolites namely ZSM-5 and faujasite with an acceptable yield and geopolymers. Indeed, ZSM-5 and faujasite are widely used as catalysts in several petrochemical processes and geopolymers are used as construction materials. Therefore, CFA that is considered by many as waste product can be used as feedstock in the synthesis of high value products without further generation of waste.

DEDICATION

This thesis is dedicated to my closest family members for their indefatigable support throughout the course of this study:

- Simon Dlamini (Late grandfather)
- Delsy Wistence Ndlovu (Mother)
- Rolihlahla Nandipha Ndlovu (Brother)
- Xolani Kyalami Munene Ndlovu (Brother)

ACKNOWLEDGEMENTS

I would like to acknowledge the Lord God in His supremacy for the strength, inspiration, and the ability to carry out this study, and his love and provision whenever I needed Him. Indeed, apart from Him we can do nothing (John 15:5).

Also, I would like to thank:

- My supervisor Prof T.V Ojumu for giving the opportunity to accomplish my postgraduate studies under his supervision. I thank him for his continuous support and insight throughout the duration of the project, for his advice, mentorship, guidance and for always being willing to listen. For being passionate and always willing to assist.

- Co-supervisor Prof L.F Petrik for believing in me when I did not, for showing me love, care and support, for making herself available every time I needed her assistance. I would like to thank her for her motivation, advice, courage, and most importantly for the financial support she provided throughout the course of the study. I would like to acknowledge her excellent supervision and the insightful contribution throughout the research.

- Roland Missengue for his assistance in lab work, data acquisition and analysis (FTIR). I would like to thank him for believing in me and for the support, motivation, advice, courage and for the spiritual support.

- Miranda Waldron from the Physics department at UCT, for her help in SEM analysis.

- Remy Bucher from iThemba labs for his help in XRD analysis.

- Dr Edith Beukes from the University of the Western Cape for her help with NMR analysis.

- Ilse Wells and Rallston Richards from the Environmental and Nanoscience Department at UWC for their assistance with ICP analysis.

- ENS Research Group, my second family, for their love, encouragement, support and all the interaction that made my Master's journey interesting.

- My close family members for their love, support and motivation and advice.

- My friends (Vuyokazi Mama, Wasiu Olalekan Afolabi, Sandile Jongile, Lydia Jaceni and Dunani Malefane) for their support, aspiration, care and love.

- And finally my sincere gratitude to the National Research Foundation (NRF) for the financial support that made this study possible.

LIST OF PRESENTATIONS

Oral flash presentation

Ndlovu, N.Z.N., Missengue, R., Ojumu, T.V., and Leslie F. Petrik. 2015. Synthesis of Zeolite Faujasite and geopolymer from coal fly ash. Catalysis Society of South Africa, Cape Town, Arabella Western Cape, South Africa. 15-18 Nov 2015.

Poster presentation

Ndlovu, N.Z.N., Missengue, R., Ojumu, T.V., and Leslie F. Petrik. 2015. Synthesis of Zeolite Faujasite and geopolymer from coal fly ash. Catalysis Society of South Africa, Cape Town, Arabella Western Cape, South Africa. 15-18 Nov 2015.

TABLE OF CONTENTS

LIST OF FIGURES

LIST OF TABLES

LIST OF ABBREVIATIONS

Abbreviation	Meaning
A	Aluminium Oxide
An	Anhydrite
C	Calcite
Ca	Calcium
CFA	Coal fly ash
CFAAE	Coal fly ash alumina extract
CFASE-ATT	Coal fly ash silica extract after oxalic acid treatment
CFASE-BAT	Coal fly ash silica extract before oxalic acid treatment
Cr	Chromium
Fe	Iron
FTIR	Fourier transform infrared spectroscopy
FUA	Faujasite
G	Geopolymer
H (small letter)	Hour
H	Hematite
He	Hematite
Hex	Hexahydrite
HGC	High grade coal
ICP-AES	Inductively coupled plasma atomic emission
K	Potassium
LGC	Low grade coal
M	Millosevichite
M	Mullite
Mg	Magnesium

Mi	Mirabilite
Mn	Manganese
N	Nitrite
Na	Sodium
NaOH	Sodium hydroxide
NMR	Nuclear magnetic resonance spectroscopy
ɒ	Extraction efficiency
P	Phillipsite
PPM	Parts per million
Ps	Pseudobrookite
Q	Quartz
S	Sodium Hydrogen Oxalate Hydrate
SA	Sodium Aluminium Silicate Hydrate
SEM	Scanning electron microscope
SH	Sodium aluminium silicate hydroxide hydrate
Si	Silicon
SR	Solid Residue
Th	Thenardite
Ti	Titanium
XRD	X-ray diffraction spectroscopy
W	Weight
XRF	X-ray Fluorescent Spectroscopy
Z	ZSM-5

CHAPTER ONE

1.1. Introduction

South Africa is largely dependent on coal mining for power generation. The coal can be classified into two categories, high grade coal (HGC) with less inorganic minerals mainly composed of clays, calcite, dolomite, pyrites and silica, and low grade coal (LGC) with high inorganic mineral content (Ahmaruzzaman, 2010). South Africa's power stations burn LGC in the production of electricity, which results in a large amount of waste in the form of unburnt minerals, called coal fly ash (CFA). CFA is one of the coal combustion by-products that cause environmental problems due to its composition. With the increase in population, the electricity demand in South Africa has increased proportionally, leading to an increase in the amount of CFA produced. CFA is composed of fine glass-like particles that are highly susceptible to distribution by wind, and thus may pollute the air and cause airborne diseases such as chronic bronchitis and asthma (Madzivire *et al*., 2010). CFA particles are mainly composed of Si, Al, O, Fe and Ca and traces of toxic elements such as As, Hg, B, Pb, Ni, Se, Sr, V and Zn (Musyoka *et al*., 2012, Inada *et al*., 2005, Querol *et al*., 2002). South African power stations generate approximately 40 Mt of fly ash (FA) per year and only 5.5% is reported to be utilised in construction industries, while the rest is being disposed of on land (Sibanda *et al*., 2016). With the huge quantities of CFA produced every year the current disposal strategy of this waste is becoming expensive, causing a severe strain on the electricity supplier, Eskom. Apart from the unavailability of land to dispose of this waste, the salts and the toxic elements present in the ash have a potential to leach into the soil, contaminating surface and ground waters (Heebink and Hassett, 2001). In order to address the environmental concerns posed by CFA, several studies have been conducted for its beneficiation with a view to addressing its management. CFA has found use in the synthesis of zeolites and geopolymers due to its high silica and alumina content (Muriithi *et al*., 2013, Musyoka *et al*., 2012, Mainganye, 2012, Álvarez-Ayuso *et al*., 2008, Querol *et al*., 2002, Swanepoel and Strydom, 2002). Zeolites are aluminosilicates characterised by a porous framework structure with aluminate (AlO_4) and silicate (SiO_4) tetrahedra connected to one another. The framework is negatively charged and is balanced by loosely-bound charge-balancing cations such as Ca^{2+}, Mg^{2+}, Na^{+} and K^{+}, and water molecules that are located within the pore space (Passaglia and Sheppard, 2001). Zeolites have unique properties which enable them to be used in various industrial applications. Their properties include high cation exchange capacity, the ability to act as an acid catalyst and their ability to sieve molecules of certain sizes due to their unique uniform pore sizes (Du Plessis, 2014, Musyoka *et al*., 2012, Querol *et al*., 2002).

On the other hand, geopolymers are heat-resistant coatings or adhesives formed from CFA during the geopolymerisation process. Scientifically, geopolymers can be defined as a mineral, chemical compound or mixture of compounds consisting of repeating units such as silico-oxide (-Si-O-Si-O-), silico-aluminate (-Si-O-Al-O-), ferro-silico-aluminate (-Fe-O-Si-O-Al-O-) or alumino-phosphate (-Al-O-P-O-) (Hardjito *et al*., 2004). Geopolymers can be used in construction industries as building materials (Nyale *et al*., 2014).

The synthesis of zeolites from CFA requires a pre-treatment to activate the CFA before synthesis, with fusion being the most commonly-used pre-treatment. In the fusion process, CFA is mixed with NaOH and the mixture is subjected to high temperatures ranging from 500 to 650˚C for 1.5 to 2 h (Musyoka, 2012, Querol *et al*., 2002). Fusion is mainly performed to liberate silica and alumina from CFA for the synthesis of zeolites. After fusion, the fused CFA is mixed with de-ionised water and there after the mixture is subjected to a hydrothermal process for crystallisation (Molina and Poole, 2004). Zeolites can either be synthesised from the clear solution or the bulk fused FA. Zeolites synthesised from the bulk fused FA are often mixed with other mineral phases, which compromise the quality of the zeolite, while zeolites synthesised from the clear solution are pure phase zeolites with lower yields. The synthesis of zeolites using the fusion method has been shown to generate a lot of liquid and solid waste, rendering the process not commercially viable. Du Plessis, (2014), examined the feasibility of recycling the liquid waste generated during the zeolite synthesis process in order to recover the Si and Al fed to the synthesis process and to make the process environmentally-friendly. In an attempt to solve the highlighted problems in the synthesis of zeolite using CFA, the literature had shown that silica and alumina have been extracted from CFA using alkaline and acid leaching methods respectively (Li *et al*., 2011,Font *et al*., 2009,Matjie *et al*., 2005). This study aims at using these methods to extract silica and alumina in a solid form and use these CFA extracts to synthesise pure phase zeolites, such as Zeolite ZSM-5 and faujasite, which have wide industrial application with acceptable yields, while the resulting solid residue will be used in the synthesis of geopolymers. Zeolite faujasite is an important catalyst in many chemical production processes, such as fluid catalytic cracking (FCC) of heavy petroleum distillates (Weitkamp, 2000), while the application of Zeolite ZSM-5 may include the conversion of methanol to gasoline, dewaxing of distillates, and the interconversion of aromatic compounds (Olson *et al*., 1981). Moreover, the geopolymer made from residuals can be used as concrete or bricks in the construction industry (Nyale *et al*., 2013, Aleem and Arumairaj, 2012).

1.2. Problem statement

Coal fly ash (CFA), which is a waste material produced from coal combustion during electricity generation, has been the focus area of interest in research over the years due to certain valuable elements contained in it. The disposal of CFA in the environment has caused huge environmental issues, posing severe dangers to human life in the areas surrounding disposal sites. The conversion of CFA into zeolites by treatment with alkaline solutions is a well-known process which, however, usually results in a zeolitic product with significant amounts of residual FA mineral phases, such as quartz and mullite, limiting its industrial application (Wdowin *et al*., 2014, Querol *et al*., 2002, Hollman *et al*., 1999). A significant amount of research has been conducted in the synthesis of zeolite by activating the CFA before the hydrothermal synthesis, with fusion being the most commonly-used activation step (Musyoka *et al*., 2013, Ojha *et al*., 2004, Molina and Poole, 2004, Chang and Shih, 2000). Pure phase zeolites have been synthesised from the bulk fused FA, but the synthesised zeolite products contain many of the toxic elements from CFA, limiting its value for industrial application. Mainganye (2012) showed that it is not only the hydrothermal synthesis conditions and the molar regime, but also the dissolution kinetics of the feedstock, that influence the outcome of the zeolite synthesis process. The literature has also shown that the clear solution from the fused FA mixture has been used to synthesise high purity valuable zeolites X, A and Na-P with fewer toxic fly ash elements (Musyoka *et al*., 2013, Fan *et al*., 2008, Machado and Miotto, 2005). However, this process leads to small yields of the synthesised zeolite products and enormous amounts of valueless fused FA solid residue waste, making the scalability of the process unfeasible. There are many disadvantages associated with the fusion method: Fusion consumes a lot of energy, requires the addition of silica or alumina source to adjust the Si/Al ratio depending on the desired zeolite to synthesise and when the unseparated fused fly ash is used in the synthesis of zeolite, the resultant zeolite product is often impure, thus limiting its industrial application. This is, however not the case when the filtrate from the fused fly ash is used in the zeolitisation process. The zeolites synthesised from the filtrate are often pure phase, with small yields, and the process generates additional waste which still needs to be disposed of, therefore limiting the scalability for zeolite production (Du Plessis, 2014, Mainganye, 2012, Medina *et al*., 2010). It is therefore important to develop a process which utilises CFA for zeolites and geopolymer production such that the resultant waste is eliminated or minimised.

1.3. Aim and Objectives and Research questions

In general terms, the main aim of this study is to develop a method of utilising CFA in the synthesis of Zeolite ZSM-5, faujasite and geopolymer, such that the resultant waste is minimised or completely eliminated. In specific terms, the objectives of the study include the following:

a. To investigate the extraction of alumina from CFA using concentrated sulphuric acid (H_2SO_4), with a view to using the alumina extract for zeolite synthesis.
b. To investigate the extraction of silica from CFA using sodium hydroxide (NaOH) and saturated oxalic acid solutions.
c. To synthesise zeolites ZSM-5 and/or faujasite using the alumina and silica extracted from (a) and (b) above.
d. To investigate the synthesis of geopolymers from the solid residues resulting from (a) and (b) above.
e. To determine the mass balances for the zeolite (ZSM-5 and faujasite) synthesis with a view to determining the fate of associated toxic elements for design purposes.

This study attempted to answer the following questions:

- What would be the optimum condition to extract silica and alumina from CFA?
- What would be the optimum conditions for the synthesis of zeolites ZSM-5 and faujasite from the CFA extracts?
- Could the chemical species that are present in the fly ash be monitored through the synthesis process using the engineering concept of mass balances?
- Could the solid residue after extraction of silica and alumina be used to synthesise the geopolymers?
- Would the strength of the synthesised geopolymers from the solid residues be sufficient for them to be used as construction materials?
- Would the yields of Zeolite ZSM-5 and faujasite be high enough for scale-up of the processes from the laboratory scale to the industrial scale?
- Would zero waste generation be achieved through this process?

1.4. Significance of investigation

This study aims at the synthesis of high purity zeolite products with acceptable yield.The solid residue remaining after acid and alkaline extraction of alumina and silica respectively will be used to synthesise geopolymers.The total use of CFA in the synthesis of zeolites and geopolymer may be a breakthrough in the synthesis of zeolites from CFA without further waste

generation. The synthesised products (zeolites and geopolymers) from CFA have the potential to create economic value, due to their potential application in the catalytic and construction industries respectively.

1.5. Delineations

Zeolites (ZSM-5 and faujasite) and geopolymers can be synthesised from different starting materials rich in silica and alumina. In this study, coal fly ash (CFA) from Matla power station is used as the sole source of alumina and silica. CFAs from other power stations in South Africa were not considered. In this study, alumina and silica were extracted using H_2SO_4 and NaOH respectively. The extraction process was investigated using two routes, Process 1 and Process 2. The silica extract obtained from Process 1 was used as the feedstock in the synthesis of Zeolite ZSM-5, while the resulting solid residue was used as the feedstock for the synthesis of a geopolymer. The synthesis of Zeolite ZSM-5 usually requires the addition of a structure directing agent, and tetrametylammonium hydroxide (TEAOH) was used as the structure directing agent for the synthesis of Zeolite ZSM-5 in this study. The alumina and silica extracts from Process 2 were used as the feedstock for the synthesis of zeolite faujasite, while the resulting solid residue was used as a feedstock for the synthesis of a geopolymer. Mass balance calculations were only performed for zeolite synthesis (ZSM-5 and FAU1) on a dry mass basis to determine the efficiency of the synthesis and determine the yields of the synthesised zeolite products. The strength tests of the synthesised geopolymer were not performed, since they fell outside the scope of this study.

1.6. Outline and structure of thesis

This thesis is divided into six chapters, including this chapter (Chapter One). Chapter Two presents the generic literature review of coal fly ash (CFA), zeolite (ZSM-5 and faujasite) and geopolymers. Previous work on the optimisation of zeolite synthesis from CFA to upscale its production to industrial scale has also been reviewed. The extraction of silica and alumina from CFA can stimulate the optimum conditions for the synthesis of Zeolite ZSM-5 and faujasite so as to increase its purity and yield. The literature also covers the use of CFA in the synthesis of geopolymers.

Chapter Three details the materials and the experimental methods used in this study. It provides background information on the sampling, storage conditions of the fresh fly ash and the lists of the chemicals and equipment used in this study. It highlights the experimental procedures used in the synthesis of Zeolite ZSM-5 and faujasite from CFA extracts. This

chapter also contains the methodological approach used in the synthesis of geopolymer. Finally, the analytical techniques used are presented. Chapter Four presents the characterisation of raw CFA, coal fly ash extracts, the Zeolite ZSM-5 or geopolymer synthesised from the CFA extracts or CFA solid residue respectively**.** The results of the characterisation of CFA extract (alumina and silica), zeolite faujasite and geopolymer synthesised from CFA are presented and discussed in Chapter Five. Lastly, Chapter Six summarises the important conclusions that were drawn from the results presented in this thesis and suggests future work based on the results obtained.

CHAPTER TWO

LITERATURE REVIEW

2.1. Introduction

This chapter highlights the review of literature that provides the foundation to this study. The reviewed topics include coal fly ash (CFA) formation and utilisation, the extraction of silica and alumina from CFA, the synthesis of Zeolite ZSM-5 and faujasite from CFA and the synthesis of geopolymers from CFA. This chapter reviews the synthesis of zeolite and geopolymer from CFA with a view to identifying the drawbacks of the existing zeolite synthesis methods that limit the feasibility of commercial production of zeolites from CFA. The literature identified the possibility of extracting silica and alumina from CFA separately, and the idea of this study is to use the extracts as direct feedstock in the synthesis of Zeolite ZSM-5 and faujasite, and further, to use the solid residue in the synthesis of geopolymers. The success of this project would promote zero waste generation during the production of zeolites and open up the possibility of upscaling the synthesis of fly ash-based zeolites and geopolymers.

2.2. Coal fly ash (CFA)

CFA is an incombustible waste material generated from the combustion of coal during electricity generation. CFA contains toxic heavy metals such as As, Hg, B, Pb, Ni, Se, Sr, V and Zn, and has therefore been classified as hazardous waste (Du Plessis, 2014, Musyoka *et al*., 2012). South African power plants generate about 40 million tons of CFA every year (Sibanda *et al*., 2016), and from this amount, only approximately 5.5% is being utilised effectively in the construction industry, while the rest is stockpiled and used as landfills (Petrik, 2004). The poor management of this waste material has resulted in serious environmental concerns, which include the potential contamination of soil, surface and ground water due to the presence of soluble metal species (Praharaj & Ray, 2001).

2.2.1. Properties of CFA

Several researchers are interested in CFA. CFA can be classified into two categories, namely Class F and Class C. The Class F fly ash is produced from burning of low grade coals (LGC) such as anthracite and bituminous coal, while the class C fly ash is produced from burning high grade coal (HGC) including lignite or subbituminous coal (Kruger, 1997, Naik, 1993). The American Society for Testing Materials (ASTM C618) requires that FA containing more than

70 wt% of SiO_2, Al_2O_3 and Fe_2O_3, and having a low CaO content (< 10%), be classified as Class F fly ash type. On the other hand, FA containing a total SiO_2, Al_2O_3 and Fe_2O_3 content ranged 50 and 70 wt%, and having a high CaO content of 10 to 40% is classified as class C fly ash type (Du Plessis, 2014, Mainganye, 2012, Musyoka *et al*., 2012, Ahmaruzzaman, 2010). Class C fly ash can also be categorised as cementitious and pozzolanic, while Class F fly ash is categorised as pozzolans used for making concrete (Kruger, 1997, Naik, 1993). South African power plants generate a class F fly ash type, due to burning of LGC (Du Plessis, 2014, Musyoka, 2012).

2.2.1.1 Chemical composition of CFA

The chemical composition of CFA varies depending on the type and the origin of coal used during the combustion process (Musyoka, 2012, Madzivire *et al*., 2010). CFA is mainly composed of SiO_2 (58.44%), Al_2O_3 (31.25%), CaO (3.21%), and Fe_2O_3 (3.09%) (Nyale *et al*., 2014). CFA may also contain some nutrients such as S, B, Ca, Mg, Fe, Cu, Zn, Mn, and P, which are beneficial for plant growth, as well as toxic metals such as As, Hg, Cr, Pb, Ni, Se, Sr, and V in trace amounts (Musyoka, 2012). According to Daniels *et al*., (2002), CFA is suitable for use as a liming material, due to the presence of CaO, MgO and other alkaline metal oxides that react with water to generate net alkalinity. Quartz, kaolite, ilite and mullite with trace amounts of magnetite and hematite phases are the dominant minerals in FA (Ahmaruzzaman, 2010, Moreno *et al*., 2001, Musyoka, 2009). Mullite and quarts are the major crystalline phases found in FA. The amorphous phase in CFA is responsible for its pozzolanic nature (Ahmaruzzaman, 2010, Querol *et al*., 2001, Fisher *et al*., 1978).

2.2.1.2 Physical appearance of CFA

The colour of CFA varies from light grey to dark grey, depending on the amount of unburned carbon after combustion (Madzivire *et al*., 2010). According to Mainganye, (2012), the tan and light colours of FA are characteristically associated with high lime content in the fly ash. CFA is abrasive, alkaline and refractory in nature (Madzivire *et al*., 2010). It consists of spherical micro-particles; these spherical particles are glassy and mostly transparent, indicating complete melting of silicate minerals (Madzivire *et al*., 2010, Fisher *et al*., 1978). The particle size of CFA ranges from 0.01 to 200 µm, with specific surface area and specific volume ranging from 21 to 3.0 m^2/kg and 170 to 100 m^3/K respectively (Ahmaruzzaman, 2010).

2.2.2. Formation of CFA

CFA is a by-product formed by non-combustible minerals during thermal production of energy through coal combustion. As the combustion products leave the combustion chamber, CFA is separated from the flue gas by means of electrostatic precipitators, bag houses and mechanical collection devices such as cyclones (Musyoka, 2012, Kuhn, 2005). The amount of non-combustible minerals depends on the type and the source of coal used (Ahmaruzzaman, 2010). The inorganic minerals that are incombustible materials, also known as coal combustion products (CCPs), may make up to 40% of coal, with FA being the main waste, amounting to 60% of all the CCPs (Musyoka *et al*., 2012). The use of LGC in the production of electricity in South Africa results in huge quantities of CFA waste, as the LGC contains high ash content (Oboirien, 2011).

2.2.3. Coal fly ash environmental problems

In South Africa, CFA has become one of the largest sources of industrial waste, due to increase in electricity demand (Zhang, 2013, Querol *et al*., 2002). Poor management of this waste constitutes a serious human and environmental problem. Eskom power generation stations produce about 40 Mt of CFA annually (Sibanda *et al*., 2016, Babajide *et al*., 2010), and only a small percentage of the ash is utilised efficiently in the building sector for production of cement and brick. Unused CFA is transported by pipes in a watery sludge and pumped into large ash dams (Ahmaruzzaman, 2010, Petrik, 2004, Van Hamburg *et al*., 2004). CFA is regarded as hazardous material because of the trace and toxic elements that it contains. These elements are concentrated on the surface of the CFA amorphous particles (Du Plessis, 2014, Musyoka *et al*., 2012, Madzivire *et al*., 2010, Bhanarkar *et al*., 2008, Sharma and Kalra, 2006). CFA is made of fine particles which have the capability to escape into the atmosphere, and threaten human health. CFA can severely damage the respiratory system. Literature reports have shown that fine CFA particles are enriched with toxic elements that can easily penetrate into the alveolar regions of lungs when inhaled (Bhanarkar *et al*., 2008, Goodarzi, 2006). The disposal of FA in landfills can cause the leaching of these toxic elements by rain, thus contaminating ground and surface water, thereby threatening humans, plants and aquatic life (Ahmaruzzaman, 2010, Carlson and Adriano, 1993). Although some elements found in CFA are deemed beneficial for the growth of plants, these benefits are outweighed by the considerable levels of environmental concerns associated with CFA, due to its constituent toxic elements.

2.2.4. Applications of CFA

The huge production of CFA coupled with the management challenges and the associated environmental concerns have resulted in many research studies aimed at developing different beneficial applications for CFA. Most of the studies are focused on optimisation for effective utilisation, beneficiation to increase value and subsequently ways to minimise environmental challenges associated with its disposal (Blissett and Rowson, 2012, Mainganye, 2012, Ferreira *et al*., 2003, Querol *et al*., 2002, Carlson and Adriano, 1993). A review report by Wang and Wu, (2006), summarises the applications of CFA in different sectors based on its chemical and physical properties, as shown in Figure 2.1.

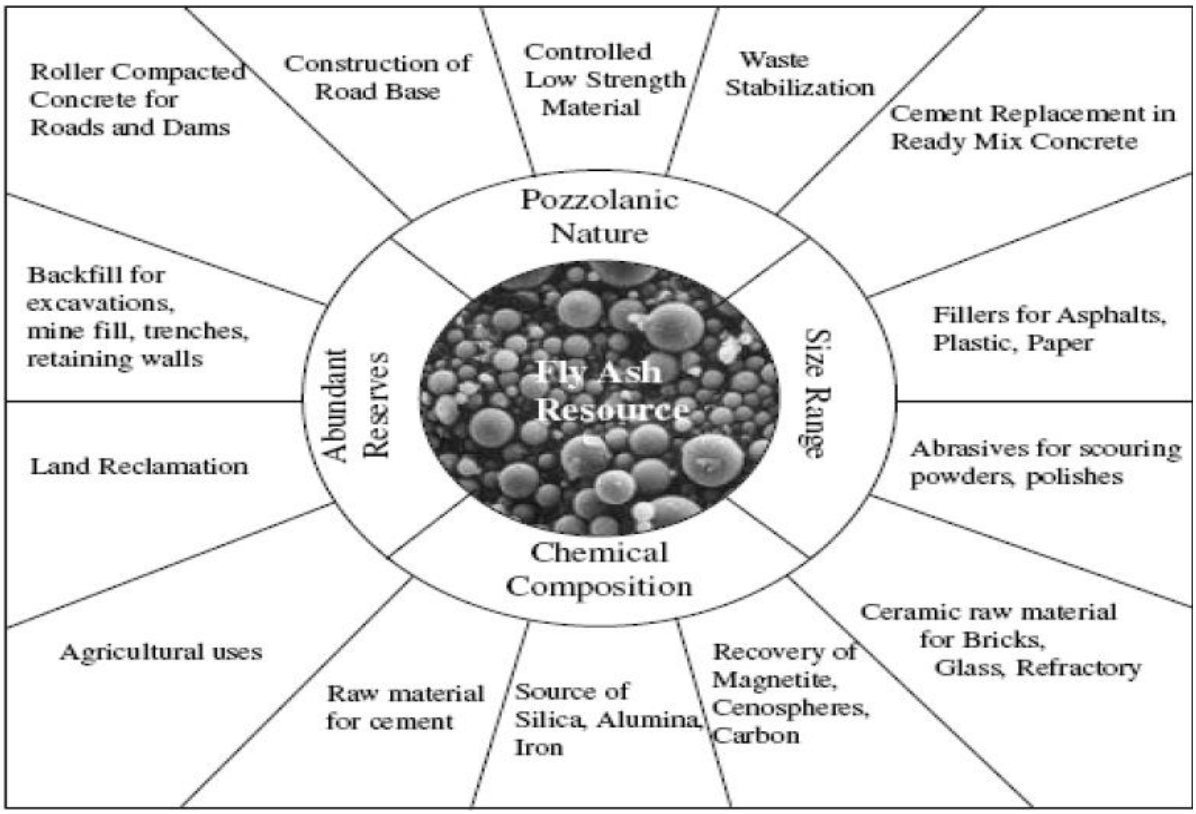

Figure 2.1: Summary of the applications of CFA depending on its chemical and physical properties

Source: (Wang & Wu, 2006)

CFA has found application in the synthesis of zeolites and geopolymers, due to its high SiO_2 and Al_2O_3 content (Querol *et al*., 2002). In recent times, the synthesis of zeolites using CFA has drawn more attention, due to the fact that CFA is an inexpensive source of silica and alumina and in addition, there are an increasing number of studies on CFA because zeolites have wide applications and they have several economic benefits (Musyoka, 2009).

Swanepoel and Strydom, (2002) stated that the similarity of FA to natural pozzolans has encouraged the use of CFA in the synthesis of geopolymers, a material which consists of a polymeric Si–O–Al framework (Nyale *et al*., 2013, Swanepoel and Strydom, 2002).

2.3 Extraction of alumina and silica from coal fly ash (CFA)

Although CFA is regarded as a hazardous waste of concern, it contains important substances such as Si and Al as major constituents. The chemical composition and desirable physical properties of CFA has attracted attention over the years. The possibility of transformation and extraction of the constituents for various economic uses are often attributed to its chemical and physical properties. A summative literature review on the extraction of these elements and their applications is presented in the subsections below.

2.3.1. Extraction of alumina from coal fly ash (CFA)

The main source of alumina for various industrial applications is bauxite, which is generally imported from China (Iyer, 2002). Nyale *et al*. (2014) reported that South African CFA from the Matla coal plant contains 31.25% of alumina. This unique characteristic of South African CFA makes it a potential good substitute for bauxite for the purposes of alumina extraction (Bai *et al*., 2011). Alumina extraction from CFA will save diminishing bauxite resources; it would contribute significantly to the strategic use of this waste and improve the waste management of CFA.

The first method used to recover alumina from CFA was initiated by an American researcher in the 1980's when there was a growing concern over the shortage of alumina (Iyer, 2002). The past decade has witnessed extensive interest and studies on extraction of alumina from CFA (Wu *et al*., 2012, Bai *et al*., 2011, Matjie *et al*., 2005, Iyer, 2002).

Extraction of alumina with acids has been one of the major technologies investigated for the recovery of alumina from CFA. The types of acid used to leach alumina from CFA include sulphuric acid, hydrochloric acid, hydrofluoric acid, and other organic acids (Bai *et al*., 2011, Singer *et al*., 1982). Harada *et al*, (1993) report that mullite powder was decomposed using sulphuric acid at a temperature of 230 °C for 16 h. The results reported showed that mullite powder was decomposed in a saturated sulphuric acid at high temperature to release silica and alumina. Seidel *et al*, (1999) reported the extraction of alumina from CFA using sulphuric acid, with an extraction efficiency of 30%. Bai *et al*, (2011) expressed the possibility of recovering alumina from CFA using a leaching temperature of 200−210 °C, leaching time of 80 min, and volumetric ratio of acid to CFA of 5:1 with an extraction efficiency yield of 87%.

The literature showed that it is possible to extract alumina from CFA using sulphuric acid, however the practical application was limited due to the excessive dosage of sulphuric acid as well as difficulty in separating aluminium sulphate from residual sulphuric acid solution (Bai *et al*., 2011). The main focus of the current study is to extract alumina from CFA using sulphuric acid and thereafter to extract silica from the resulting solid residue using NaOH. The extracted alumina and silica would be used in the synthesis of zeolite faujasite. The method proposed by Matjie *et al*., (2005) was employed for alumina extraction with slight modifications. The procedure is reported in Chapter Three, section 3.2.2.1 of this thesis.

2.3.2. Silica extraction from coal fly ash (CFA)

CFA is a potential source of silica. It has been established that silica is a major constituent of CFA and it constitutes approximately 58.44% by mass of CFA (Nyale *et al*., 2013). Silica is an important raw material which has various industrial applications (Misran *et al*., 2007). Research has shown that silica can be extracted from CFA using alkaline leaching methods (Font *et al*., 2009, El-Naggar *et al*., 2008, Moreno *et al*., 2002, Querol *et al*., 2002). Font *et al*, (2009) successfully extracted silica from CFA using 3 M NaOH, and alkaline solution/fly ash (NaOH/FA) ratio of 3 L/kg at 120 ^{0}C for 9 h. The authors report that a silica extraction efficiency of 120 g/kg of CFA was obtained under these specified conditions. Moreno *et al*, (2002) extracted silica from a European CFA, and an extraction efficiency of 190 g of SiO_2 per kg of CFA was obtained by employing a temperature of 120 °C for 6 h; a concentration of 2 M NaOH and a basic solution/fly ash ratio of 3 L/kg. Pure phases of 4A and X zeolites were synthesised from the extracted silica (Moreno *et al*., 2002). El-Naggar *et al*, (2008) detail the extraction of silica and alumina using fusion methods. Their procedure involved mixing 10 g of powdered FA with 10 g NaOH (99.9%), which was subsequently ground to obtain a fairly homogeneous mixture. The mixed material was then heated in air at 550 °C for 60 min. The author reported that the amount of silica extracted using the fusion method was 131.43 g/kg of CFA, while that of alumina was 41.72 g/kg of CFA. Based on extraction efficiencies and overall method efficacy, this project aims to employ alkaline leaching methods to extract silica from CFA and subsequently use the extracted silica as a feedstock in the synthesis of high pure phase Zeolite ZSM-5.

2.4 Zeolites

Zeolites have been known for about 250 years and identified as aluminosilicate materials. This class of materials is characterised by a porous framework structure with aluminate (AlO_4) and silicate (SiO_4) tetrahedral networks connected to one another (Weitkamp, 2000). There are

about 45 naturally-occurring zeolite minerals, of which mordenite, clinoptilolite, chabazite, erionite, phillipsite, laumontite, ferrierite, and analcite are generally exploited commercially (Hanson, 1995).

Natural zeolites are formed when volcanic rocks and ash layers react with alkaline water. They are produced in post-depositional environments over thousands to millions of years in shallow marine basins. Naturally-occurring zeolites are rarely pure and their contamination may vary in degree. These forms of impure natural zeolites may contain other minerals, metals, quartz, or other zeolites (Musyoka *et al*., 2012, Weitkamp, 2000). For this reason, naturally-occurring zeolites are excluded from many important commercial applications where homogeneity and purity of zeolites are essential (Ramesh *et al*., 2011).

Zeolites can also be synthesised in the laboratory and these types of zeolites are known as synthetic or artificial zeolites. Efforts to synthesize zeolites artificially have been attempted as far back as 1848, but it was only in the 1940s that a zeolite was successfully synthesised. The early synthetic zeolite did not have a matching counterpart comparable with the natural zeolites. The first synthesis of zeolites followed the pioneering work performed by Barrer and Milton (Weitkamp, 2000, Barrer, 1948). To date, there are over 300 different types of synthetic zeolites (Auerbach *et al*., 2003). Zeolite materials have unique properties, and as a result they are used for various industrial applications.

2.4.1. Chemistry of zeolites

The major components of zeolites are SiO_4 and AlO_4. Zeolites are made of adjacent tetrahedral networks of Si and Al, which are linked by means of a common oxygen atom, and this creates an inorganic macromolecule with a structure composed of a three-dimensional framework (Musyoka, 2012, Weitkamp, 2000). The composition of zeolite frameworks mainly depends on the synthesis conditions (Du Plessis, 2014, Musyoka, 2012, Weitkamp, 2000). The chemical composition of zeolite can be expressed by the following molecular formula:

$$M^{n+}_{x/n}\ Al_x\ Si_{1-X}\ O_2 \cdot yH_2O$$

Where x varies from 0 to 0.5 and M^{n+} represents extra-framework cations (Passaglia and Sheppard, 2001) The primary structural framework of a typical zeolite material is presented in Figure 2.2.

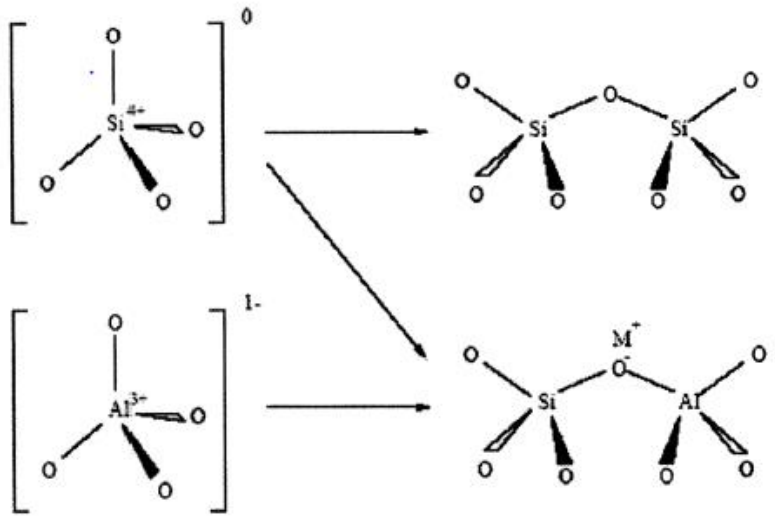

Figure 2.2: Primary structure of zeolite

Source: (Zhao *et al*., 1997)

A zeolite framework contains channels or interconnected pores of voids of distinct sizes, in the range of 0.3-20 Å (Georgiev *et al*., 2009) which are occupied by charge balancing cations and water molecules (Weitkamp, 2000). Typically, these cations are elements belonging to the group IA and IIA of the periodic table. The counter ions can be exchanged reversibly with other ions possessing the same charge. This type of reversible exchange is possible when an aqueous solution containing the substitute ions is passed through the channels and voids. This replacement results in the reduction of the diameter of the zeolite channels, depending on the size of the ion replaced (Georgiev *et al*., 2009). Water and organic non-framework cations present during the synthesis of zeolites can be desorbed by thermal treatment or oxidation processes. The property of retaining their structural integrity during thermal treatment or oxidation distinguishes them from other porous hydrated materials (Byrappa and Yoshimura, 2001).

2.4.2. Mechanism of zeolite synthesis

The science of zeolite synthesis was first developed by Barrer and Milton in the early 1940s (Cundy and Cox, 2003). Richard Barrer synthesised the first zeolite material in 1948 using an earlier investigated approach where he studied the conversion of known mineral phases in a strong salt solution at temperatures of 170 and 270ºC. In 1949, Robert Milton was able to synthesise zeolite A, Na-P, hydroxysodalite and the crystalline impurity designated as zeolite X, using freshly-precipitated aluminosilicate gels under mild conditions. However, in 1950 the author perfected his work by synthesising a pure phase zeolite X (isostructural with the naturally-occurring mineral faujasite) and a synthetic chabazite. The pioneering work of Barrer

and Milton recommended further investigation and brought improvements in the field of zeolite synthesis (Venuto & Habib Jr, 1979).

Synthetic zeolites have been shown to offer great advantages over natural zeolites. Natural zeolites are formed under uncontrolled conditions, hence they incorporate various impurities into the zeolite structure. The presence of impurities in the natural zeolites is a major limitation on their industrial applications (Du Plessis, 2014). Synthetic zeolites are made under specific controlled conditions, and often the reaction conditions for the synthesis influence the type of zeolite synthesised. The mechanism of zeolite synthesis is not a mathematically modelled subject, but rather has been proposed based on findings from different experimental observations (Mainganye, 2012). Zeolites have been synthesised from different sources of alumina and silica. Figure 2.3 presents a schematic of zeolite formation.

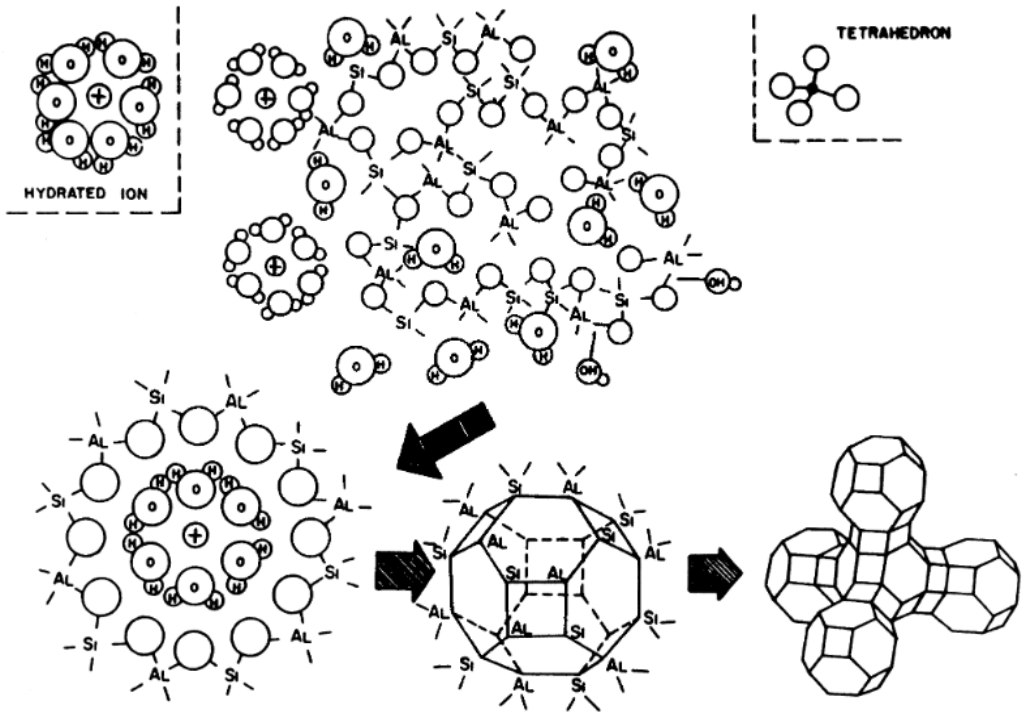

Figure 2.3: Schematic representation of the formation of zeolite crystal nuclei in a hydrous gel

Source: (Cundy & Cox, 2003).

The composition of any typical zeolite framework mainly depends on the synthesis conditions (Musyoka *et al*., 2012). In the mechanistic formation of zeolites, the aluminosilicate gel structure is depolymerised by hydroxide ions, and then the aluminosilicate and silicate species

present in the hydrous gel are rearranged around the hydrated cations present. The tetrahedral networks of atoms regroup around hydrated sodium ions to form the basic polyhedral units (24-hedra).

These polyhedral units are then linked to form the massive, ordered crystal structure of the zeolite (Cundy and Cox, 2003). The mechanisms of zeolite formation are complex, due to the diversity of chemical reactions, equilibriums, and solubility variations that occur throughout the heterogeneous synthesis mixture during the crystallisation process (Davis and Lobo, 1992). The formation of zeolites can be summarised as a series of steps involving dissolution of silica and alumina species from the feedstock to form monomeric species of mostly TO_4 tetrahedran; condensation of TO_4 polyhedral building blocks around hydrated cations to form simple secondary building blocks of up to double 6-ring polyhedral units; and networking of building blocks to create zeolite structural groups and large zeolite crystals with arrays of pores and channels (Du Plessis, 2014, Cundy and Cox, 2003, Auerbach *et al*., 2003, Murayama *et al*., 2002). As mentioned earlier, aluminosilicate zeolites have been synthesised from different silicon and aluminium sources, but this study will focus on the synthesis of Zeolite ZSM-5 and faujasite from silica and alumina extracts of South African CFA.

2.4.3. Synthesis of zeolites from coal fly ash

CFA has been successfully employed as a feedstock in the synthesis of zeolites, due to its high silicon and aluminium content (Du Plessis, 2014, Wdowin *et al*., 2014, Musyoka, 2012, Mainganye, 2012, Belviso *et al*., 2009, Querol Carceller *et al*., 2007, Ojha *et al*., 2004, Murayama *et al*., 2002, Querol *et al*., 2002, Moreno *et al*., 2001). The synthesis of zeolites from CFA can be achieved in three sequential steps:

- Dissolution of Al_2O_3 and SiO_2 from CFA using a mineralising agent. The most commonly-used mineralising agent is the hydroxyl anion (OH^-), which increases the solubility of silicon and aluminium from CFA and effects the formation of silicate and aluminate gel (Mainganye *et al*., 2013),
- Separation of the aluminosilicate gel from the unreacted CFA, depending on the desired type of zeolite,
- Hydrothermal synthesis, which may be defined as the zeolite crystal growth stage (Mainganye, 2012, Moliner *et al*., 2012, Inada *et al*., 2005).

Different types of zeolites can be synthesised by varying the physical synthesis parameters, such as pressure, temperature and activation time, as well as the chemical composition of the hydrothermal gel (Moreno *et al*., 2001).

The first attempt to convert CFA into zeolites was achieved by (Holler and Wirsching, 1985). Berkgaut and Singer (1996), reported that the yields of zeolite synthesised from CFA could not be improved above ±50%. The reported low yield of zeolites synthesised from CFA is assumed to be strongly influenced by the difficulty to dissolve all the silicon and aluminium from CFA during the zeolitisation process, which often requires longer contact time or high energy, as well as the inconsistency of the CFA chemical composition that varies from one source of CFA to the next (Musyoka, 2012). The inadequacy of the conventional method limits the potential application of CFA for the synthesis of zeolites on a commercial scale. Although the synthesis of zeolite from CFA is not a new field of research, current interests involve several attempts at modifying and improving the conventional methods for the synthesis of zeolites from CFA with the aim of achieving improved purity and overall yield of the final product. Some of the existing methods used to achieve better results are discussed in the subsections below.

2.4.3.1. Microwave assisted synthesis of coal fly ash-based zeolites

Microwave energy is a powerful heating source which has not been studied extensively in the synthesis of zeolites (Chandrasekhar and Pramada, 2008, Li and Yang, 2008). The microwave-assisted method has been used to synthesise zeolites from pure sources of Si, Al and CFA (Querol *et al*., 1997, Arafat *et al*., 1993). The microwave process is based on the application of electromagnetic radiation with wavelengths ranging from 1 m to 1 mm, with corresponding frequencies ranging between 300 MHz to 300 GHz (Musyoka, 2012). The use of microwaves in the synthesis of zeolites has proven to reduce the synthesis time from 24 or 48 hours to 30 minutes (Querol *et al*., 1997). It was also shown that crystallisation rate could be increased and the crystal size of zeolite product can be reduced significantly in a microwave system (Du Plessis, 2014, Musyoka *et al*., 2012). Even though the reaction time for zeolite synthesis can be reduced in a microwave system, the technique mostly results in zeolite products with a small pore size, scientifically known as microporous zeolites. Microporous zeolites exhibit pore diameter of less than 2 nm. These types of materials have limited industrial application, since the small pores impose diffusional limitations on rates of reaction (Jacobsen *et al*., 2000).

2.4.3.2. Fusion-assisted synthesis

Another existing method which has been widely studied for the synthesis of zeolites is the fusion-assisted method (Du Plessis, 2014, Moliner *et al*., 2012, Mainganye, 2012, Musyoka *et al*., 2012, Inada *et al*., 2005, Molina and Poole, 2004, Ojha *et al*., 2004, Querol *et al*., 1997, Shigemoto *et al*., 1993). This method requires an activation step of CFA in order to increase the dissolution of silicon and aluminium prior to the zeolite synthesis. During fusion, CFA is

mixed with NaOH and fused at temperatures between 500-600 ^{o}C (Musyoka *et al*., 2012, Shigemoto *et al*., 1993). The crystalline and amorphous Si- and Al-bearing phases in CFA are converted into sodium silicate and aluminosilicate species respectively, which promotes the dissolution of Si and Al in the solution. Zeolite synthesis relies mostly on the Si/Al ratio. Once the Si and Al species are dissolved in the solution, the Si/Al ratio can be adjusted depending on the target form of zeolite (Chareonpanich *et al*., 2011). Despite the fact that fusion is the most commonly-used method for activation of CFA, the method has several disadvantages which limit its applicability to the commercial production of zeolites. The limitations of the fusion method include: high energy consumption, generation of excessive liquid and solid waste during zeolite synthesis, and low yield of the synthesised zeolite product, thus making the scaling up of the process not commercially feasible. However, several attempts were made to improve the scalability of the synthesis of zeolites from CFA. Du Plessis, (2014) reported that liquid waste could be recycled into the zeolite synthesis system in order to increase the percentage yield of the zeolite product and also minimise water consumption and reduce the amount of waste generated during the process. In another study, Mainganye, (2012) investigated the effect of impeller design and agitation rates during the aging step, using three different impellers at three agitation speeds. The author also looked at the effect of CFA composition and water sources on the phase purity of zeolites, as well as the effect of hydrothermal reaction time during the synthesis of zeolite. According to the findings of the studies, Mainganye proved that the phase purity of zeolite NaP1 was strongly affected by agitation and the type of impeller used during the aging step of the synthesis process. The author also showed that the variation in the mineralogy of CFA affected the quality of zeolite produced significantly. This indicates that each batch of CFA would require a separate optimisation process of the synthesis conditions. To an extent, it is not clear whether the finding from this study is realistic for an industrial scale set-up.

2.4.3.3. Ultrasound-assisted synthesis

The ultrasound-assisted method has also been used in the synthesis of various zeolites from CFA. The starring role of the ultrasound method in enhancing zeolite formation in different heterogeneous and homogeneous processes is as recognised as its general contribution to the crystallisation of distinct mineralogical phases (Run and Wu, 2004). The most important mechanism enhancing crystallisation is ultrasonic cavitation, a phenomenon that can be defined as the growth and explosive collapse of microscopic bubbles (Belviso *et al*., 2011), which may result in hot spots or local temperatures greater than 5000 K and cooling rates greater than 10^{7} °C/s (Ensminger and Bond, 2011). Musyoka *et al*. (2011), used the ultrasound method to sonicate the filtrate (clear solution) which was obtained after the fusion process, but prior to the hydrothermal synthesis. The author reported a significant reduction in the

crystallisation time for the synthesis of Zeolite A. A similar study by Bukhari *et al*. (2015), showed that Zeolite A was attained at a lower synthesis temperature than those applied by Musyoka *et al*. (2011). Furthermore, Ojumu *et al*., (2016), investigated the possibility of replacing the fusion step, which consumes a lot of energy with a high intensity ultrasonic process during the synthesis of Zeolite A from South African coal fly ash. The author reported that during sonication only amorphous phases from the ash were dissolved, and a total of 24% of Si from the coal fly ash was extracted, which is not far from the 32% obtained through the fusion processes. It was also reported that the ultrasound was successful in reducing the conversional 90 min energy intensive fusion step to 10 min of high intensity through ultrasound irradiation (Ojumu *et al*., 2016). Even though Ojumu *et al*., (2016) has shown a novel and economically viable approach to the synthesis of Zeolite A from South African coal fly ash, scalability of this process remains a subject that requires further investigation.

2.4.4. Synthesis of zeolite faujasite and ZSM-5 from coal fly ash (CFA)

This section presents a summative literature review on the methods for the synthesis of zeolite faujasite and ZSM5-5 from CFA, and their industrial applications.

2.4.4.1. Synthesis of Zeolite faujasite from coal fly ash

Since the discovery of synthetic zeolites, zeolite faujasite (X/Y) has gained special interest in industrial spheres, due to its application in fluid catalytic cracking (FCC) of heavy petroleum distillates, which is one of the most important chemical processes globally (Weitkamp, 2000).

Zeolite Y is preferable to Zeolite X in the FCC application because the latter is less active and less stable at high temperatures, due to the lower Si/Al ratio compared to that of the former. Zeolite Y is also used in the hydrocracking units as a platinum/palladium support to increase aromatic content of reformulated refinery products. On the other hand, Zeolite X can be used to selectively adsorb CO_2 from gas streams and can also be used in the pre-purification of air for industrial air separation (Golden *et al*., 2000).

The use of CFA in the synthesis of zeolites generally produces mixed mineral phases in the synthesised zeolite product. Therefore, extensive research has been carried out to find alternative ways to selectively synthesise the desired zeolite product using CFA as feedstock.

The chemistry of zeolite faujasite is well understood and it was first studied by Bergerhoff *et al*., (1958). The method for the synthesis of zeolite faujasite was developed by Baur, (1964). The synthesis of zeolite material from CFA generally requires the dissolution of Si and Al from CFA using either fusion or other dissolution methods. The synthesis of zeolite faujasite from CFA has been studied by Musyoka (2012), Thuadaij and Nuntiya (2011), Ojha *et al*. (2004), and Mondragon *et al*., (1990). The molar regime used to synthesise zeolite faujasite in this

study was adopted, with some modifications, from the method suggested by Htun *et al*. (2012). The author synthesised zeolite faujasite from pure aluminium and silica sources using a molar regime of $4.2Na_2O$: $1Al_2O_3$: $3SiO_2$:$180H_2O$, at 100 °C for 6 h. The modified method used in this study to synthesise zeolite faujasite is presented in Chapter Three, Section 3.3.2.4.

2.4.5. Zeolite ZSM-5

Zeolite ZSM-5 is a high silica content crystalline zeolite which was originally discovered by Mobil Oil Corporation. In 1972, a patent was filed for this invention (US 3702886 A) claiming the discovery of an ultra-stable synthetic siliceous crystalline Zeolite ZSM-5 material and methods to prepare this type of zeolite (Argauer and Landolt, 1972). The patent showed that the composition of Zeolite ZSM-5 can be identified in terms of mole ratio of oxides 0.9 ± 0.2 $M_{2/n}O : W_2O_3 : 5\text{-}100YO_2 : zH_2O$, wherein M is at least one cation, n is the valence thereof, W is selected from the group consisting of aluminium and gallium, Y is selected from the group consisting of silicon and germanium, and z is a factor ranging from 0 to 40 (Argauer and Landolt, 1972). Zeolite ZSM-5 possesses an interconnected two-pore system, one consisting of zig-zag channels and another of straight channels, slightly elliptical (García *et al*., 2013). This form of zeolite with a high silica content can be synthesised from a hydrothermal gel containing a Si/Al ratio of greater than 10 (Singh and Dutta, 2003).

The synthesis of Zeolite ZSM-5 occurs by a hydrothermal process, with silica and alumina being the reagents, and as with other types of zeolites, OH^- or F^- is used as a mineralising agent. Moreover, in most cases an organic molecule is used as a structure directing agent (Singh *et al*., 2008). A number of papers and patents have been published on the synthesis of Zeolite ZSM-5 (Chareonpanich *et al*., 2011, Fouad *et al*., 2006, Singh *et al*., 2008, Dwyer and Chu, 1985, Pelrine, 1978, Argauer and Landolt, 1972). The pioneering work by Argauer and Landolt (1972), opened up opportunities to improve the chemical structure of Zeolite ZSM-5 in order to increase potential applications for catalytic reactions. Pelrine (1978) investigated a novel method of synthesising a new form of Zeolite ZSM-5 which could be used in certain chemical conversion reactions.

The crystals of Zeolite ZSM-5 synthesised from conventional methods are coffin-shaped with some twinning and range in size from 3 × 3 microns to 8 × 8 microns. Pelrine (1978) was able to increase the crystal size of the synthesised zeolite to a crystalline product which consisted of highly twinned rectangular prismatic crystals exhibiting extreme uniformity in sizes from 5 × 10 microns to about 10 × 20 microns. The crystalline size can enhance the catalytic activity for certain chemical reactions. This high-silica-content zeolite can be used in catalytic processes such as alkylation of aromatics with olefins, aromatisation of normally gaseous olefins and paraffins, aromatisation of normally liquid low molecular weight paraffins and

olefins, isomerisation of aromatics, paraffins and olefins, disproportionation of aromatics, transalkylation of aromatics, oligomerisation of olefins and cracking and hydrocracking (Pelrine, 1978).

2.4.6. Applications of zeolite

There are three major industrial applications of zeolite materials, namely adsorption, catalysts, and ion exchange. The applications of zeolites mainly depend on the surface area, acidity and pore size of the synthesised zeolite product. Zeolites can be classified into three categories based on silica composition: low silica, intermediate and high silica zeolites. Table 2.1 shows the classification of zeolites according to their Si/Al ratio. The industrial applications of zeolites are presented in the subsections below.

Table 2.1: Grade of zeolites

Zeolite grade	Si/Al ratio	Common mineral names, and their framework codes
Low silica	<2	Analcime (ANA), Cancrinite (CAN), Na-X (FAU), Natrolite (NAT), Phillipsite (PHI), Sodalite (SOD)
Intermediate	2 to 5	Chabazite (CHA), Faujasite (FAU), Mordenite (MOR), Na-Y (FAU)
High silica	>5	ZSM-5 (MFI), Zeolite – β (BEA)

Source: (Jha & Singh, 2011)

2.4.6.1. Adsorption

Zeolites are porous materials. This unique property enables them to reversibly absorb large volumes of vapour, and as a result enables the practical application of zeolites for large-scale purification and separation of industrial process streams. The most familiar examples of such a process is the removal of undesirable impurities such as H_2S and mercaptans from natural gasses, and also the removal of organic pollutants from water (Ruthven, 1984). The adsorption property of zeolites originates as a result of their molecular-sieving property and the presence

of regular pores with definite aperture sizes (Musyoka *et al*., 2012). Zeolites have been used as absorbents to remove volatile organic compounds from air (Charles and Ho, 2013), as absorbents for removal of metallic contaminants from water and also for dye removal (Crini, 2006, Oliveira *et al*., 2004).

2.4.6.2. Catalysts

Synthetic zeolites have been used for organic compound conversions due to their high thermal stability, porosity and high ion exchange properties. These exclusive materials are widely used as catalysts in fluid catalytic cracking (FCC) of heavy petroleum distillates. The most commonly-used form of zeolites for this application are zeolites X and Y (Weitkamp, 2000). Weitkamp (2000) reported that the use of these synthetic zeolites in catalytic reactions has brought about a momentous increase in yields of gasoline, which is a valuable product of the FCC plants. Zeolites Y (FAU) and ZSM-5 (MFI) are consumed in large quantities in the FCC units on oil refineries, and have been used in the conversion of methanol to hydrocarbon molecules (Marchi and Froment, 1991, Lunsford, 1990). The use of synthetic zeolites in catalytic industries has been reported on extensively in articles and books (Corma, 2003, Weitkamp, 2000, Young, 1982, Anderson *et al*., 1979, Gates *et al*., 1979).

2.4.6.3. Ion exchange

The ability of zeolites to exchange their extra-framework ions has provided an opportunity for zeolites to be used in ion exchange applications (Pfenninger, 1999). Zeolites A and X are often used as ion exchange agents due to their extra-framework cation content (Auerbach *et al*., 2003). Ion exchange is one of the most important properties of microporous materials (Musyoka, 2012). Due to their ion exchange properties, applications of zeolites include wastewater treatment and binders for detergents (Petrik *et al*., 2003a, Chang and Shih, 2000, Ouki and Kavannagh, 1999). Hui and Chao, (2006) report that zeolites can be used to remove calcium ions in water and from their investigations they have proven that the synthetic zeolite 4A could be used as a builder in detergents because of its purity, crystallinity, morphology, particle size and ion exchange capacity.

2.5. Geopolymers

Geopolymers, known as inorganic polymers, were first developed by Davidovitbis in 1978. These materials have drawn the world's attention because of their unusual properties. This section provides a literature review on the formation and the synthesis of geopolymers.

2.5.1. Formation of geopolymers

Geopolymers are a class of three-dimensionally networked inorganic polymers, similar to natural zeolites. This class of inorganic polymers is based on three different monomeric units

characterised based on the ratio of silica and alumina, (–Si–O–Al–O–) polysialate, (–Si–O–Al–O–Si–O–) polysialatesiloxo and (–Si–O–Al–O–Si–O–Si–O–) polysialatedisiloxo with a SiO_2/Al_2O_3 ratio of 2, 4 and 6 respectively (Andini *et al*., 2008).

Unlike other materials such as organic polymers, glasses or ceramics, geopolymers are non-combustible, heat-resistant, and acid-resistant (Duxson *et al*., 2007). The mechanism of geopolymer formation has not been fully understood, but is nonetheless believed to be a two-step process which involves the dissolution of aluminium and silica from the starting material using an alkali mineralising agent, followed by the polymerisation of active surface groups and soluble species to form a gel, and subsequently a hardened geopolymer structure (Nyale *et al*., 2013, Andini *et al*., 2008, Swanepoel and Strydom, 2002, Purdon, 1940). According to Davidovits (1994), the mechanism of geopolymer hardening mainly includes the poly-condensation reaction of geopolymeric precursors, usually alumina-silicate oxides, with alkali polysilicates yielding polymeric Si-O-Al bonds. The framework structure of geopolymers consists of tetrahedral aluminosilicate units of varying Si/Al ratio linked together by the sharing of oxygen atoms (Nyale *et al*., 2013). Aluminium is four-coordinated with respect to oxygen. As a result, this creates a negative charge imbalance and consequently necessitates the presence of cations such as K^+ and Na^+ to maintain electric neutrality in the matrix. Davidovits (1994) proposed a new terminology to better explain the three dimensional geopolymeric structures. The three dimensional geopolymeric structures can be summarised as follows (Van Jaarsveld *et al*., 1997).

- Poly (sialate) with [-Si-O-Al-O-] as repeating unit
- Poly(sialate-siloxo) with [-Si-O-Al-O-Si-O-] as repeating unit
- Poly(sialate- disiloxo) with [-Si-O-AI-O-Si-O-Si-O-]as repeating unit

The chemical structure of geopolymers differs according to the Si/Al ratio (Davidovits and Davidovics, 1991). The Si/Al molar ratio of geopolymers greatly affects their properties and thus their industrial applications (Nyale *et al*., 2013). The formation of the geopolymeric structure is explained by the chemical structure in Figure 2.4.

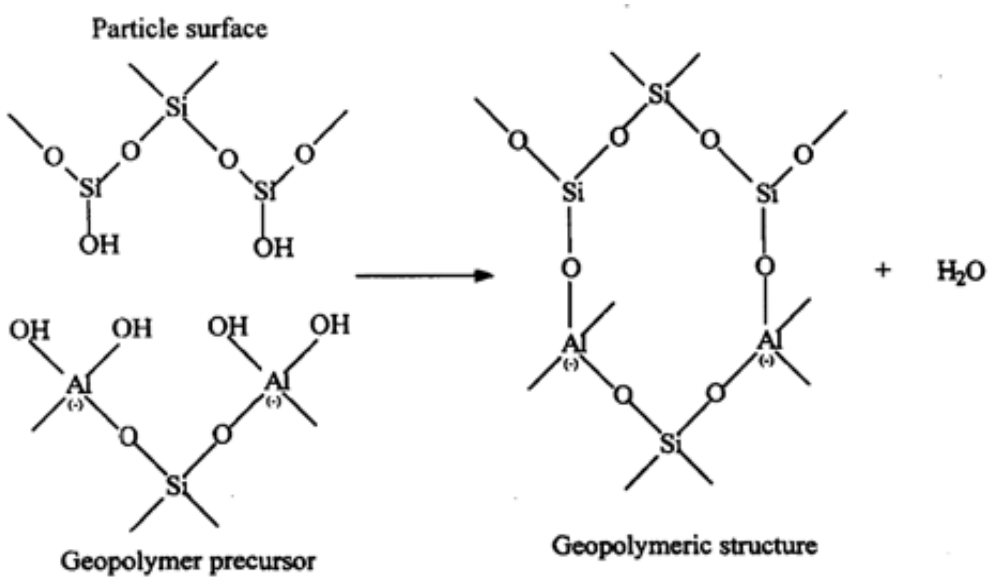

Figure 2.4: Formation of a geopolymeric structure

Source: (Van Jaarsveld *et al*., 1997)

2.5.2. Synthesis of geopolymers

Glukhovsky (1994) developed an alkali-activated cement using alkali-activated slags containing large amounts of calcium, whereas Davidovits and Davidovics, (1991) initiated the use of calcium-free systems based upon calcined clay. Alkali activation of aluminosilicates can produce X-ray amorphous aluminosilicate gels, or geopolymers, with excellent mechanical and chemical properties (Saravanan *et al*., 2013). As part of developing sustainable disposal strategies for CFA to reduce its environmental impact and disposal cost, CFA has found utility in the synthesis of geopolymers, because of their similarities to natural pozzolans (Saravanan *et al*., 2013, Nyale *et al*., 2013, Swanepoel and Strydom, 2002). Bhandari *et al*, (2013) synthesised geopolymers from CFA using KOH and Na_2SiO_3 as activators. A fly ash based geopolymer was synthesised by mixing 8 kg of fly ash, 8 kg of NaOH and 40 litres of H_2O in a jet-loop reactor. The mixture was mixed for 180 min in a jet-loop reactor and thereafter underwent a hydrothermal treatment at 80ºC for 5 days (Nyale *et al*., 2014). Böke *et al*, (2015) investigated the effect of NaOH/FA on the formation of foamed geopolymers.

The authors report that a mixture of NaOH/FA improved geopolymerisation up to a ratio of 0.20 and porosity up to a ratio of 0.22, after which geopolymerisation and porosity declines. Andini *et al*, (2008), synthesised geopolymer from CFA by mixing CFA with an alkali metal silicate solution and the mixture was poured in a prism of 4 × 4 × 16 cm^3 which was sealed using polyethylene bags and cured at 85°C for 6 h. Rattanasak and Chindaprasirt, (2009) mixed CFA with sodium silicate solution and 10 M NaOH for 1 min, and the resulting paste

was moulded in 25 mm diameter × 25 mm height plastic containers. Thereafter the sample was wrapped with Clingfilm and cured at 65°C for 48 h.

The chemical and physical properties of a geopolymer product are influenced by feedstock materials and processing conditions during the synthesis. Properties of geopolymers may include high compressive strength, low shrinkage, fast or slow setting, acid resistance, fire resistance and low thermal conductivity (Duxson *et al*., 2007). Geopolymeric material can be used for various industrial applications such as ceramics, cements, and matrices for hazardous waste, due to their fire resistance, durability and excellent mechanical properties. The research on geopolymer synthesis from CFA has increased in the past years due to these excellent physical and chemical properties, thus creating a valuable material for use in the construction industry. As mentioned previously, CFA can be used as a source of alumina and silica. Synthesis of geopolymer from CFA may provide an option of using this feedstock with resultant zero emission.

2.5.3. Uses of geopolymers

In order to reduce the carbon footprint of concrete, most geopolymers are synthesised from low-calcium CFA. Geopolymers may be used in construction materials as an alternative to Portland-based calcium silicate (Alomayri *et al*., 2014). The applications and properties of geopolymers depend significantly on the Si/Al ratio. A low Si/Al atomic ratio of 1, 2 or 3 initiates a 3D-Network that is very rigid, whereas a Si/Al atomic ratio higher than 15 produces geopolymeric materials exhibiting polymeric character which makes these types of geopolymers resistant to both heat and fire. (Nyale *et al*., 2013, Abdullah *et al*., 2011, Van Jaarsveld *et al*., 1997).

2.6. Chapter summary

This chapter presents the literature concerning the use of South African CFA, a waste material used in the synthesis of zeolites and geopolymers. The synthesis of zeolites and geopolymers from CFA stands out as one of the most attractive ways to beneficiate CFA. The current methods used in the synthesis of zeolites have shown some disadvantages, which limit the industrial application of CFA-based zeolites. Fusion is one of the most commonly-used methods in the synthesis of zeolites. The unseparated (unfiltered) alkaline slurry obtainable from fusion methods or the clear filtrates can be used in the synthesis of zeolites. The literature has shown that zeolites synthesised from unseparated CFA alkaline slurry result in impure zeolite products, thus limiting their industrial application. Although zeolites synthesised from the clear filtrate were pure phase zeolites, the yields of the synthesised zeolite products are

very low. The process also often generates a lot of solid waste, which makes the synthesis of CFA based zeolite not economically viable.

Another identified limitation of the preferred and commonly-used method (fusion) for the synthesis of zeolite is the co-extraction of silica and alumina and other elements into the same final solution. Attempts to separate components of this solution have proven difficult. In addition, there is the need to synthesise zeolites immediately after extraction as the chemical composition of the extracted solution changes over time. The method also requires the addition of aluminosilicate to adjust the Si/Al ratio for the synthesis of desired zeolites.

In view of the gaps identified from previous work carried out on the use of CFA in the synthesis of zeolites, this study seeks to find alternative methods for the synthesis of zeolite to improve the yield of zeolite and minimise the waste generated.

This study aims at using acid and alkaline leaching methods to extract alumina and silica respectively from CFA. The proposed method is divided into two processes (Process 1 and Process 2). Process 1 involves the extraction of silica from CFA using NaOH and the silica extracted from this process will be used in the synthesis of high silica zeolites ZSM-5 without the addition of other silica sources. On the other hand, Process 2 involves the extraction of alumina and silica using sulphuric acid and sodium hydroxide respectively from the same CFA sample. The extracted alumina and silica from Process 2 would be used in the synthesis of zeolite faujasite without the addition of an aluminosilicate source. The solid residue resulting from Process 1 and 2 will be used to synthesise a geopolymeric material, thus creating a zero waste zeolite synthesis process. The success of this study would provide a breakthrough process for the commercialisation of CFA-based zeolites.

CHAPTER THREE

MATERIALS AND EXPERIMENTAL METHODS

3.1. Introduction

This chapter details the materials and chemicals used in this study, including the sampling and storage procedures of raw materials. It also presents the experimental procedures that were followed for the extraction of coal fly ash alumina extract (CFAAE) and coal fly ash silica extracts after oxalic acid treatment (CFASE-AAT). Furthermore, this chapter outlines the experimental procedures used in the synthesis of zeolites (Faujasite and ZSM-5) and geopolymers, as well as the analytical techniques used to analyse the starting material coal fly ash (CFA) and final products (CFAAE and CFASE-AAT, zeolites faujasite and ZSM-5 and geopolymers).

3.2. Experimental approach

The experimental procedures were designed to achieve the objective established in Chapter One of this thesis. The schematic block flow diagram (BFD) presented in Figure 3.1 highlights the different experimental steps followed in this study. This study is divided into two processes. Process 1 comprises the extraction of silica from coal fly ash using sodium hydroxide (CFASE1-BAT), treatment of silica extract with oxalic acid treatment (CFASE1-AAT), synthesis of Zeolite ZSM-5 using the extracted CFASE1-AAT as a feedstock and, lastly, the synthesis of geopolymer from the solid waste resulting from the extraction of CFASE1-AAT. Process 2 comprises the extraction of alumina from coal fly ash (CFAAEs) using sulphuric acid, extraction of silica from coal fly ash using sodium hydroxide (CFASE2-BAT), treatment of silica extract using oxalic acid treatment (CFASE2-AAT), synthesis of zeolite faujasite using CFAAE and CFASE2-AAT as a feedstock, and lastly the synthesis of geopolymer from the solid waste resulting from the extraction of CFAAE and CFASE2-AAT respectively.

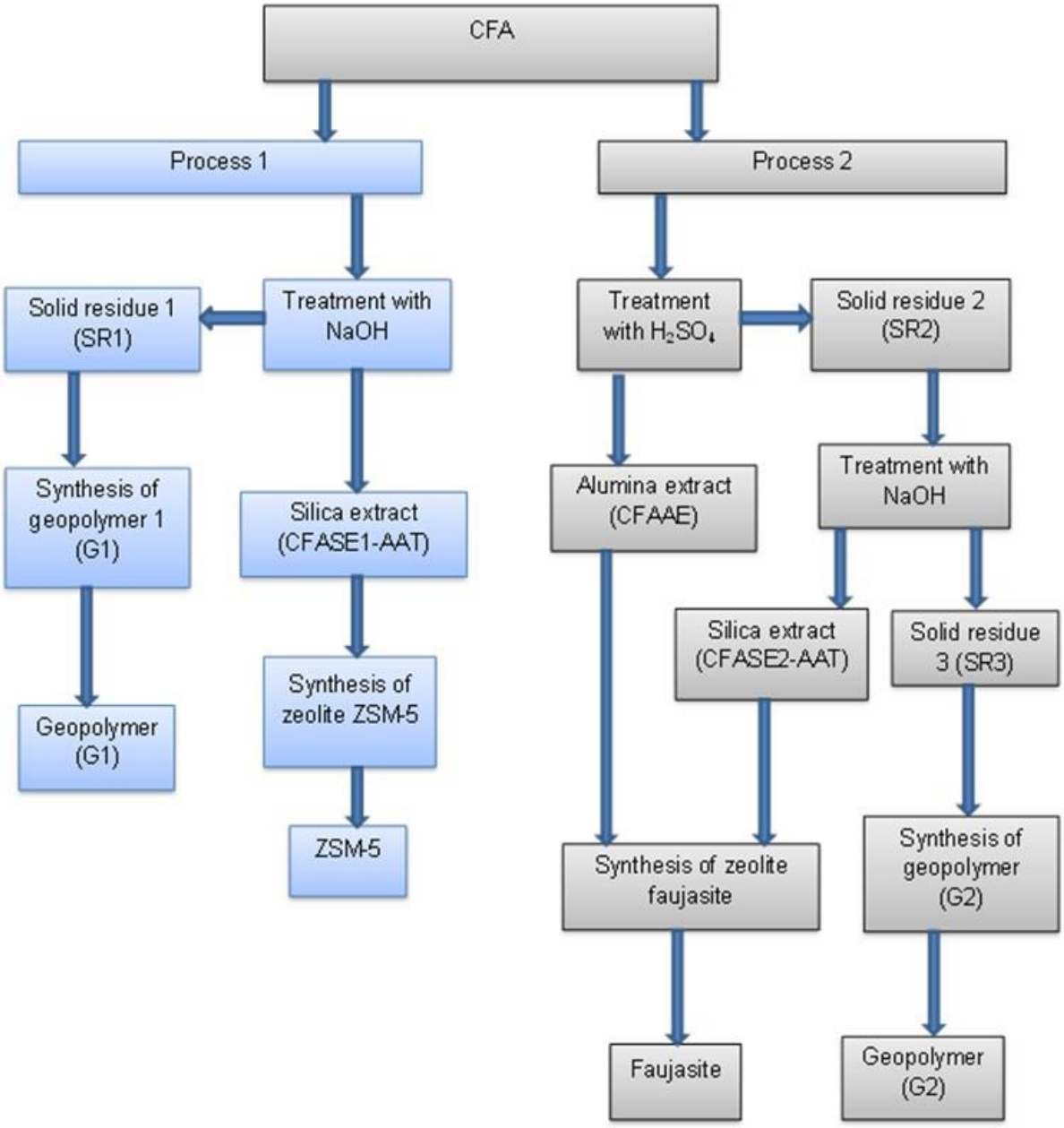

Figure 3.1: Block flow diagram (BFD) for the extraction of coal fly ash silica extracts (CFASE1-AAT and CFASE2-AAT), coal fly ash alumina extract (CFAAE), synthesis of Zeolite ZSM-5 and Faujasite, synthesis of geopolymers following Processes 1 and 2

3.3. Materials and chemicals

This section details the sampling and storage of the raw materials (CFA) as well as the list of chemicals used in this study.

3.2.1. Sampling and storage procedures of the raw material

The CFA used in this study was collected from Matla power station, located in Mpumalanga province, South Africa (Figure 3.2). The CFA was sampled, stored in a sealed container and kept at room temperature in a dark place to avoid any change in composition. The same batch of CFA was used throughout the project to minimise variations in quality and quantity of the final products.

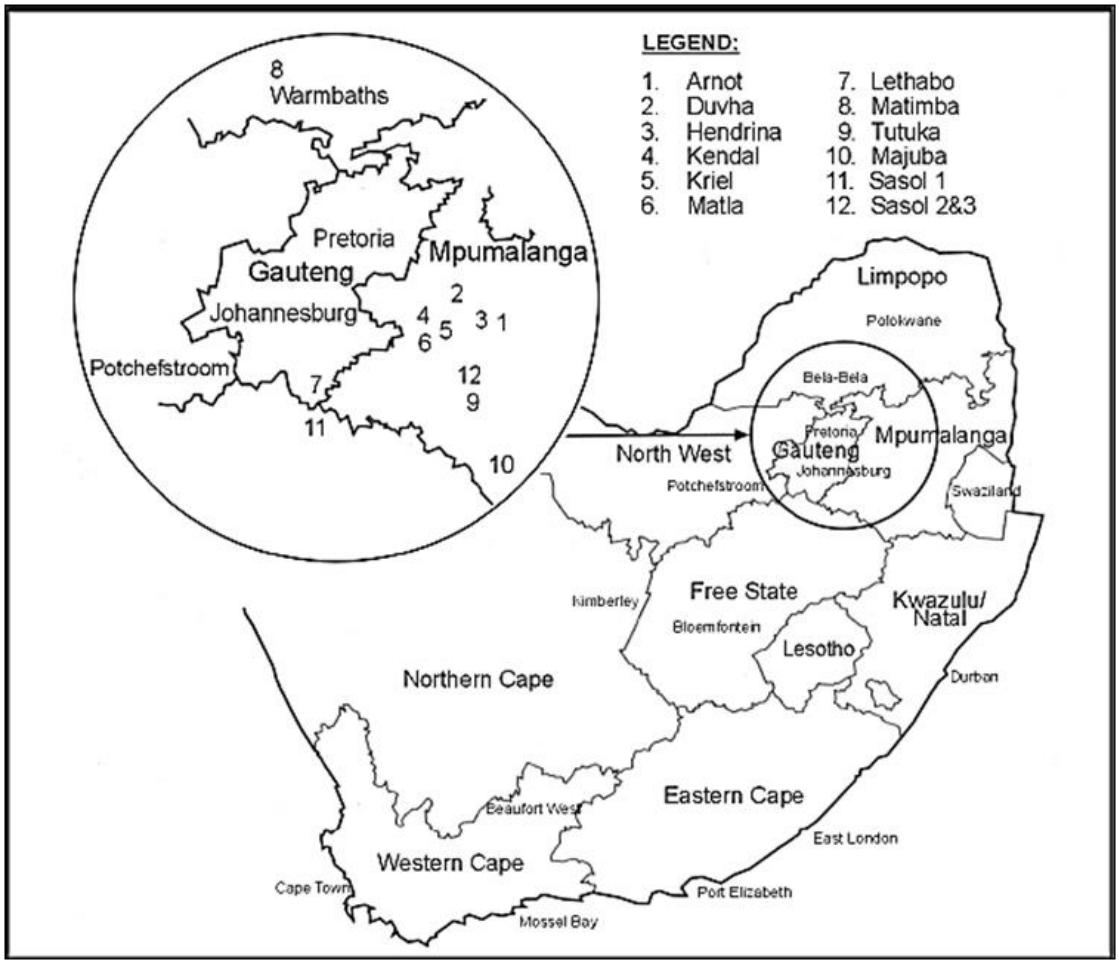

Figure 3.2: Coal power plants in South Africa (Kruger, 1997).

3.2.2. Chemicals

The list of chemicals, chemical purity and the name of the suppliers are listed in Table 3.1.

Table 3.1: List of chemicals used in this study

Name of chemicals	Supplier	Purity (%)
Sulphuric Acid (H_2SO_4)	Kimix	95-99
Tetra ethyl ammonium hydroxide (TEAOH)	Merck	20
Sodium hydroxide (NaOH) pellets	Kimix	min 98
Oxalic acid	Kimix	99.80
Hydrochloric acid (HCl)	Merck	min 37
Hydrofluoric acid (HF)	Scienceworld	40
Nitric Acid (HNO_3)	Kimix	50
Boric acid	Kimix	99.5
Ammonium nitrate (NHO_4NO_3)	Sigma-Aldrich	>98

3.3. Methods

The experimental procedure was divided into two processes (Process 1 and Process 2).

3.3.1. Process 1

Process 1 involves three main stages. The process involves the extraction of coal fly ash silica extract (CFASE1-AAT), synthesis of Zeolite ZSM-5 from the extracted CFASE1-AAT, and synthesis of geopolymers. The steps are detailed as follows:

3.3.1.1. Extraction of CFASE1-AAT from CFA using NaOH

Figure 3.3 represents a block flow diagram (BFD) for the extraction of CFASE1-AAT from CFA. The extraction procedure employed in this study to extract CFASE1-AAT from CFA was adopted and modified from the methods suggested by (Font *et al*., 2009, Schlomach and Kind, 2004).

In order to extract CFASE1-AAT from CFA, CFA (250 g) was mixed with 500 mL of de-ionised water and stirred for 24 h at room temperature to reduce the iron content in CFA. A magnetic

stirrer was used to extract and recover the magnetic fraction from the slurry. The recovered magnetic fraction was dried overnight at 70°C, digested as shown in Section 3.3.1.4 and analysed by inductively-coupled plasma atomic emission spectrometry (ICP-AES). Thereafter, the remaining CFA (slurry) was filtered, and the filtrate (liquid waste) was analysed by ICP-AES. The Solid Residue 1 (herein coded as SR1) was dried, a portion was digested, as described in Section 3.3.1.4, and analysed by ICP-EOS. Subsequently, a weighed sample (100 g) of the dried SR1 was mixed with 500 mL of 8, 4 or 2 M NaOH solutions respectively in a round bottom flask and heated at 150˚C under reflux conditions for 24 h. The mixture was allowed to cool down and filtered. An amount of concentrated H_2SO_4 (95-99%) was added drop wise into the obtained filtrate while stirring, until a pH of 10 was reached. A white precipitate, coal fly ash silica extract before oxalic acid treatment (coded herein as CFASE1-BAT) was formed, filtered and the recovered CFASE1-BAT was dried overnight at 70°C. A portion was digested as described in Section 3.3.1.4 and analysed by ICP-AES.

A dried sample of CFASE1-BAT weighing 30 g was mixed with 300 mL of saturated oxalic acid solution in a 500 mL round bottom flask. The mixture was heated at 80°C for 6 h under reflux condition. Thereafter, the mixture was allowed to cool to room temperature, filtered, dried and a portion was digested, as shown in Section 3.3.1.4, and analysed by ICP-AES. The treated CFASE1-BAT with oxalic acid was then coded coal fly ash silica extract after oxalic acid treatment (CFASE1-AAT).

The obtained CFASE1-AAT was then used as the source of silicon and aluminium in the synthesis of Zeolite ZSM-5. The solid residue (SR1) obtained after the extraction of CFASE1-AAT was used as the feedstock in the synthesis of the geopolymer (G1).

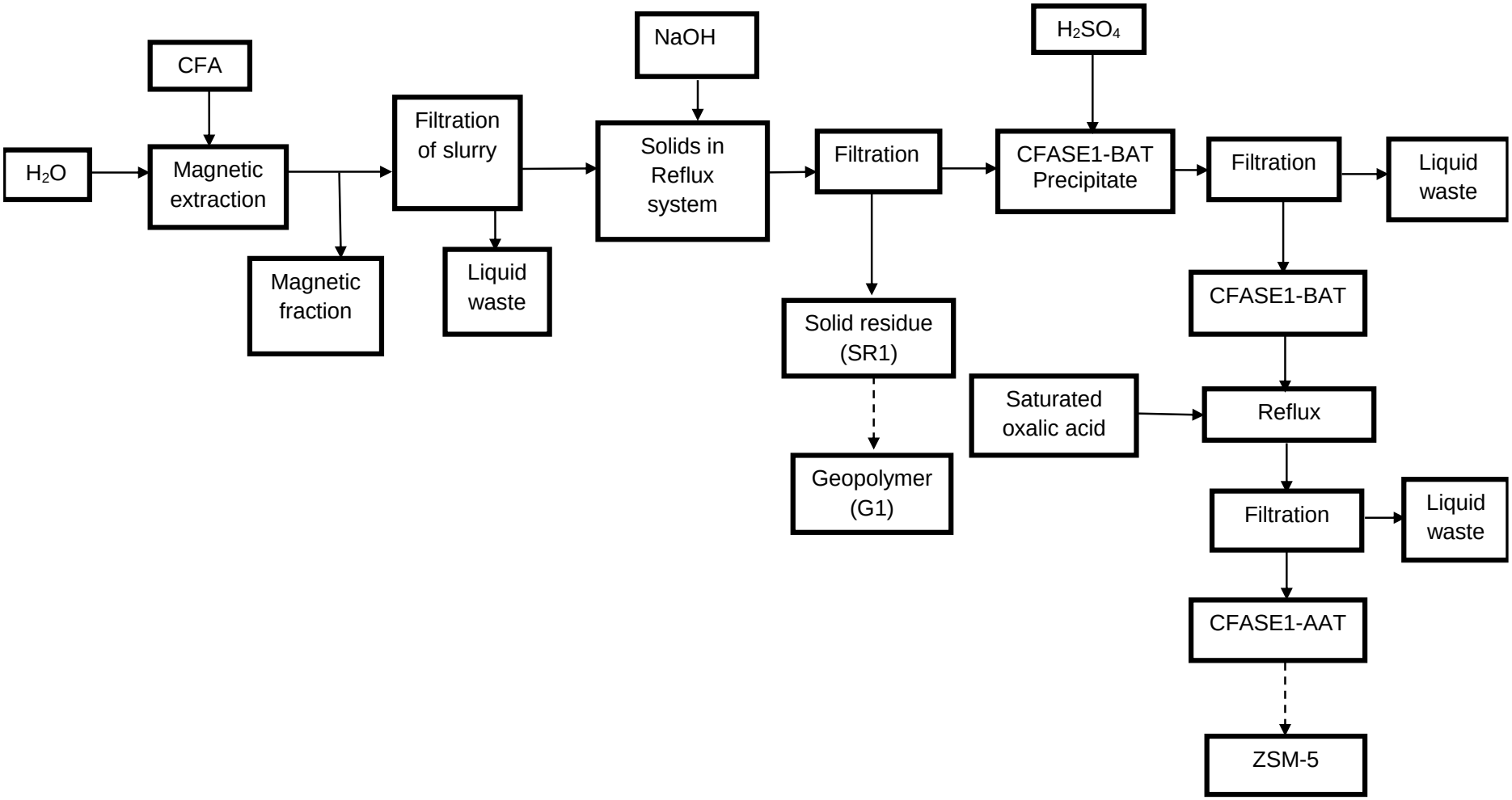

Figure 3.3: Block flow diagram (BFD) for the extraction of silica, coal fly ash silica extract before oxalic acid treatment (CFASE1-BAT), coal fly ash silica extract after oxalic acid treatment.

3.3.1.2. Synthesis of Zeolite ZSM-5

The dried CFASE1-AAT silica extract obtained from the procedure detailed in Section 3.2.1.1 contained enough residual alumina to initiate the synthesis of Zeolite ZSM-5. Figure 3.4 shows the block flow diagram (BFD) for the synthesis of Zeolite ZSM-5 from CFASE1-AAT.

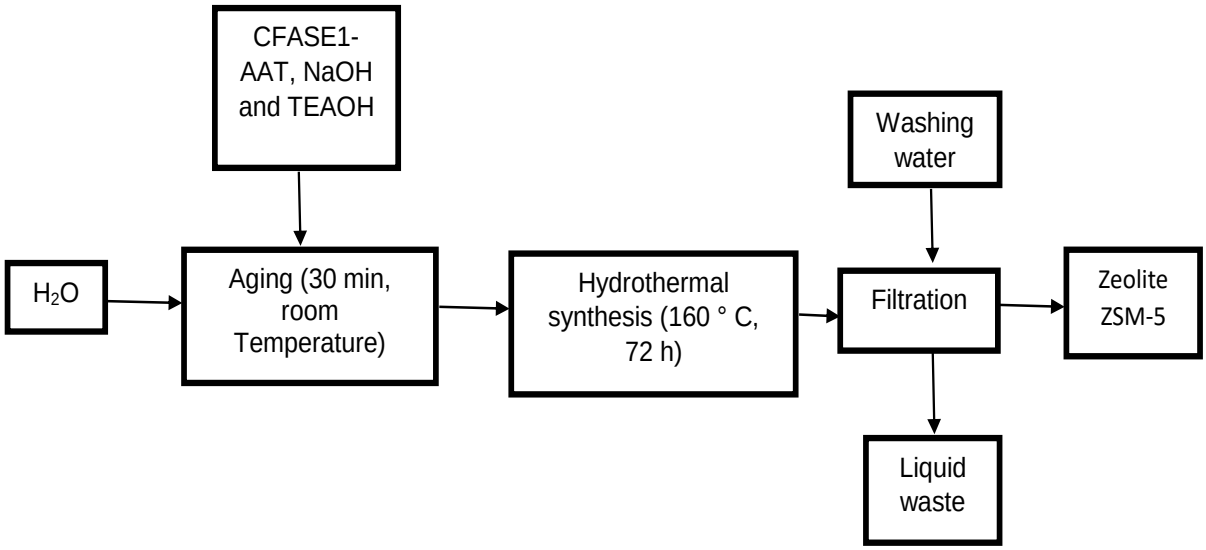

Figure 3.4: BFD for the synthesis of Zeolite ZSM-5, coal fly ash silica extract after oxalic acid treatment.

CFAESE1-AAT (2 g), 0.4 g of NaOH, 1 g of tetraethyl ammonium hydroxide (TEAOH) and 50 mL of H_2O were mixed in a 100 mL beaker and aged for 30 min at room temperature. The resultant mixture was then poured into a 100 mL digestion vessel and the mixture underwent hydrothermal synthesis in a pre-heated oven at 160°C for 72 h. Afterwards, the digestion vessel was allowed to cool to room temperature and the obtained product (Zeolite ZSM-5) was filtered, washed with de-ionised water, and dried overnight at 70°C. The obtained Zeolite ZSM-5 (Na-ZSM-5) was calcined at 550°C for 3 h. The zeolite product (Na-ZMS-5) was transformed to the H-form using a method proposed by Narayanan *et al*. (1995). In order to achieve the protonation, zeolite ZMS-5 was treated with 0.5 M NH_4NO_3 solution at a zeolite/NH_4NO_3 ratio of 1:10 at 80°C for 1 h and the treatment was repeated four times using a fresh aliquot of NH_4NO_3 each time. After the ion exchange was complete, the mixture was filtered and the filtrate was analysed using ICP-AES in order to determine the type and amount of extra-framework cations that were substituted by NH_4^+. The solid product (NH_4-ZSM-5) obtained after filtration was dried overnight at 70°C and was calcined at 550°C, with a ramping rate of 15°C/min and a holding time of 3 h in order to transform NH_4-ZSM-5 to H-ZSM-5. The obtained zeolite product was characterised by ICP-AES, SEM, FTIR, XRD and NMR.

3.3.1.3. Synthesis of geopolymer (G1) following Process 1

Figure 3.5 illustrates the block flow diagram (BFD) for the synthesis of geopolymer (G1) using the solid residue (SR1) obtained after the extraction of CFASE1-AAT.

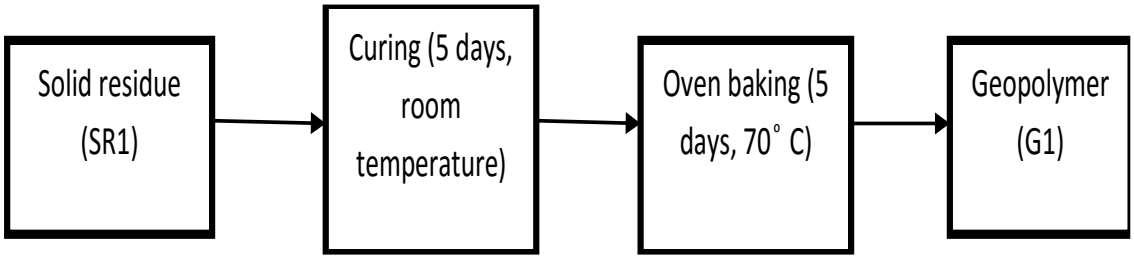

Figure 3.5: BFD for the synthesis of the geopolymer (G1)

The wet solid residue (SR1) obtained after the extraction of CFASE1-AAT was thoroughly mixed to obtain a homogenous mixture and then poured into a heat-resistant plastic mould. The mould was sealed and left to cure for five days at room temperature. Afterwards, the plastic mould was placed in a pre-heated oven at 70°C for five days. After five days in the pre-heated oven, the seal on the mould was removed and left to stand for three days to allow for total dryness of G1. The obtained geopolymer product was analysed by ICP-AES (after digestion following the method detailed in section 3.3.1.4). Characterisation was performed using SEM, FTIR, XRD, NMR, and BET. A compressive strength test was also performed using compressive strength test methods (Nazari and Riahi, 2011).

3.3.1.4. Total digestion of solid samples

All solid samples obtained in this study were digested in order to determine their chemical composition, using ICP. The total digestion method investigated by Nham and Bombelka (1991) was adopted in this study to digest solid samples prior to ICP analysis. For digestion procedures, a solid sample (0.25 g) was mixed with 2 mL of concentrated hydrofluoric acid (HF) and 5 mL of aqua regia (HNO_3/HCl, 1:3) in a digestion vessel that was placed in a pre-heated oven at 100°C for 2 h.

Thereafter, the mixture was allowed to cool and the excess HF in the digestate was neutralised by adding 25 mL of saturated boric acid (H_3BO_3) solution. The digestate was filtered through a 45-µm pore filter paper; and the effluent diluted to 50 mL with de-ionised water. The chemical composition of each sample was determined using ICP-AES. The atomic percentage in 0.25 g of each sample was then calculated.

3.3.2. Process 2

Process 2, (see Figure 3.1) involved four major steps: extraction of alumina (CFAAE), extraction of silica (CFASE2-AAT), synthesis of zeolite faujasite and the synthesis of geopolymers.

3.3.2.1. Extraction of CFAAE from CFA using sulphuric acid (H_2SO_4)

The method used to extract CFAAE in this study was adapted and modified from the methodology suggested by (Matjie *et al*., 2005). Figure 3.6 illustrates the extraction of CFAAE from CFA using concentrated H_2SO_4 (95-99%).

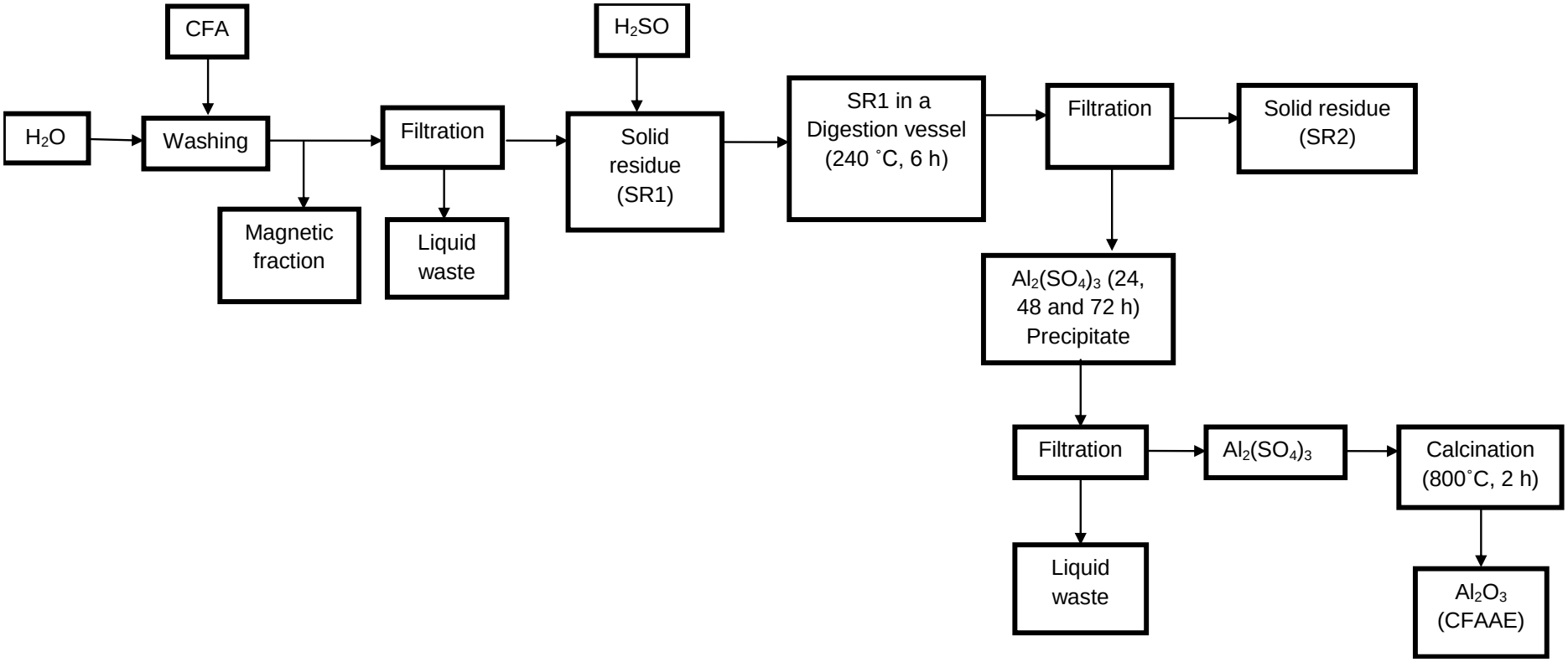

Figure 3.6: BFD for the extraction of coal fly ash alumina extract from CFA using concentrated H_2SO_4 (95-99%).

Iron was magnetically extracted from CFA with de-ionised water prior to the extraction of CFAAE. The magnetic procedure was the same as the one presented in 3.2.1.1. A mass of 30 g of the dried CFA retained after removing the magnetic fraction was mixed with 60 mL of concentrated H_2SO_4 (95-99%) in a 100 mL digestion vessel. The digestion vessel was placed in a pre-heated oven at 240˚C for 6 h. After the reaction time was complete, the digestion vessel was allowed to cool. The mixture was poured into a 250 mL beaker, 180 mL of de-ionised water was added and heated to 85˚C for 30 minutes with continuous stirring. Afterwards, the mixture was filtered while still hot. The obtained Solid Residue 2 (SR2) was dried overnight at 70˚C and weighed while the filtrate was slowly boiled to evaporate some of the water content. The solution was not evaporated to dryness. The remaining pre-concentrated solution obtained after evaporation was allowed to cool to room temperature and left overnight to allow for the precipitation of $Al_2(SO_4)_3$. The precipitation process was repeated four times. The crystals of $Al_2(SO_4)$ were recovered each time by filtration after 24 h. The recovered crystals were oxidised by calcination at 800°C for 2 h at a ramping temperature of 30°C/min. The obtained CFAAE were coded CFAAE 1, CFAAE 2, CFAAE 3 and CFAAE 4 respectively. A portion of each of CFAAE 1, CFAAE 2, CFAAE 3 and CFAAE 4 were digested following the method detailed in Section 3.3.1.4 and analysed using ICP-OES. The H_2SO_4 filtrate recovered after the precipitation of $Al_2(SO_4)_3$ crystals was recycled for the next extraction of CFAAE.

3.3.2.2. Extraction of CFASE2-AAT from the solid residue 2 (SR2) obtained after the extraction of CFAAEs.

The solid residue (SR2) obtained after the extraction of CFAAEs was further used as starting material for the extraction of CFASE-AAT using NaOH, as illustrated in figure 3.7.

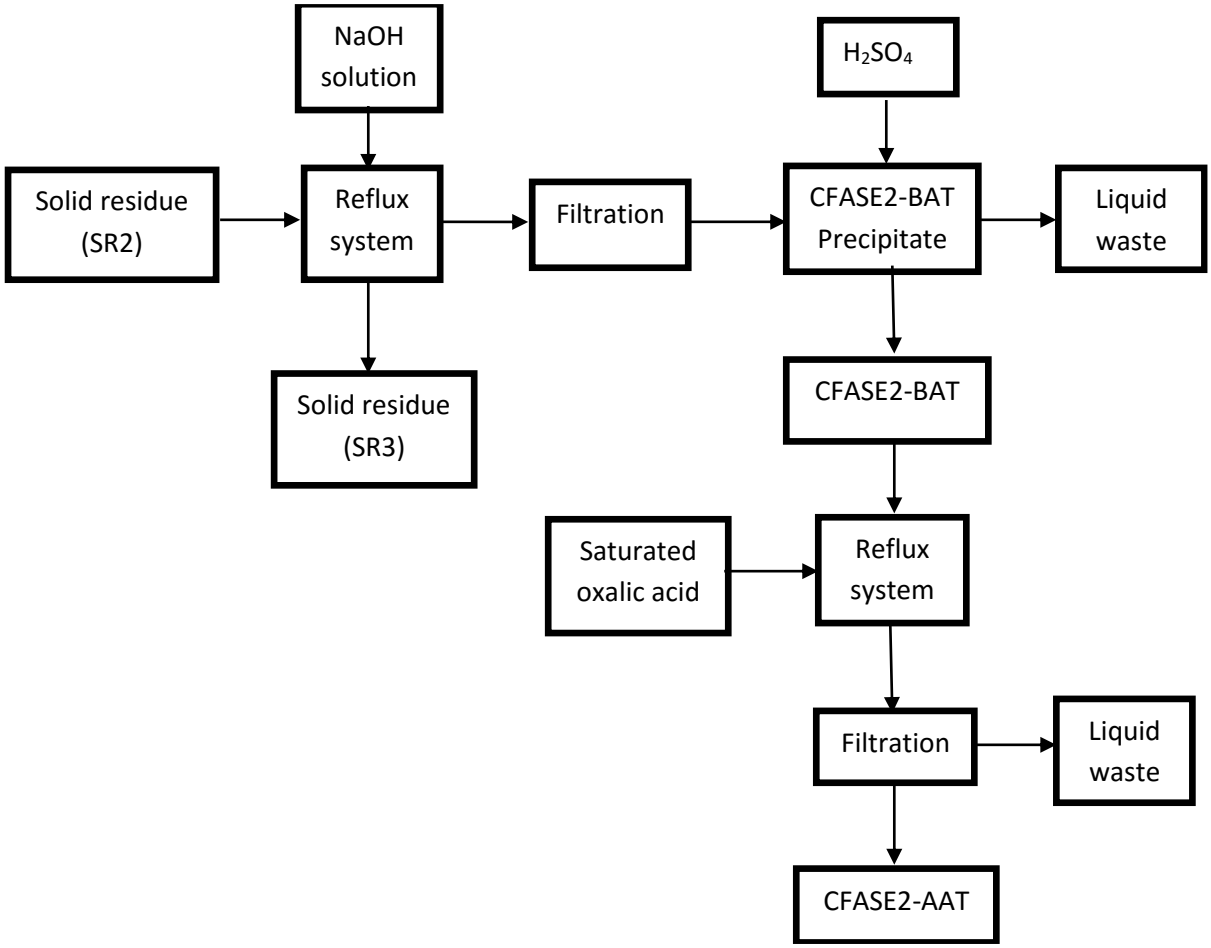

Figure 3.7: BFD for the extraction of CFASE2-AAT from the SR2 obtained after the extraction of CFAAEs.

A portion of SR2 was digested, as presented in Section 3.3.1.4, and analysed by ICP-AES. The rest of the dried SR2 was mixed with 500 mL of 8 M NaOH solution in a round bottom flask and heated at 150˚C under reflux condition for 24 h. The mixture was allowed to cool and then filtered. Concentrated H_2SO_4 (95-99%) was added drop wise to the obtained filtrate while stirring until pH 10 was achieved. A white silica-rich precipitate (CFASE2-BAT) was formed after pH adjustment. The precipitate was filtered, dried overnight at 70°C, digested and analysed by ICP-AES. From the dried CFASE2-BAT extract, 30 g was weighed and mixed with 300 mL of saturated oxalic acid solution in a 500 mL round bottom flask. The mixture was heated at 80°C for 6 h under reflux conditions. Thereafter, the mixture was allowed to cool and the new silica precipitate (coded CFASE2-AAT) was filtered, dried, and a portion digested, as detailed in Section 3.3.1.4, and analysed using ICP-AES.

3.3.2.4. Synthesis of zeolite faujasite from CFAAEs (CFAAE 1, CFAAE 2, CFAAE 3 or CFAAE 4) and CFASE2-AAT

The CFAAEs (CFAAE 1, CFAAE 2, CFAAE 3 or CFAAE 4) and CFASE2-AAT extracts were used as feedstock in the synthesis of zeolite faujasite. The molar regimes and code names of the synthesised zeolites are presented in Table 3.2.

Table 3.2: Mass of CFASE2-AAT, CFAAE, and NaOH, volume of H_2O and molar regimes used for the synthesis of zeolite faujasite

Zeolite code name	Silica extract		Al extract		Mass of NaOH (g)	Volume of H_2O	Molar regimes
	Code name	Mass (g)	Code name	Mass (g)			
FAU1	CFASE2-AAT	1	CFAAE1	1.2	2	19.3	1Si : 1.1Al : 8.6Na : 102.7H_2O
FAU2			CFAAE2	1.1	2	19.3	1Si : 1.1Al : 8.2Na : 101.1H_2O
FAU3			CFAAE3	2.1	2.2	21.3	1Si : 1.1Al : 7.9Na : 96.2H_2O
FAU4			CFAAE4	2.4	2.1	20.9	1Si : 1.1Al : 7.9Na : 97.4H_2O

The silica and alumina extracts (CFAAE and CFASE2-AAT) were used as the feed stock in the synthesis of zeolite faujasite. Figure 3.8 shows the block flow diagram for the synthesis of zeolite faujasite.

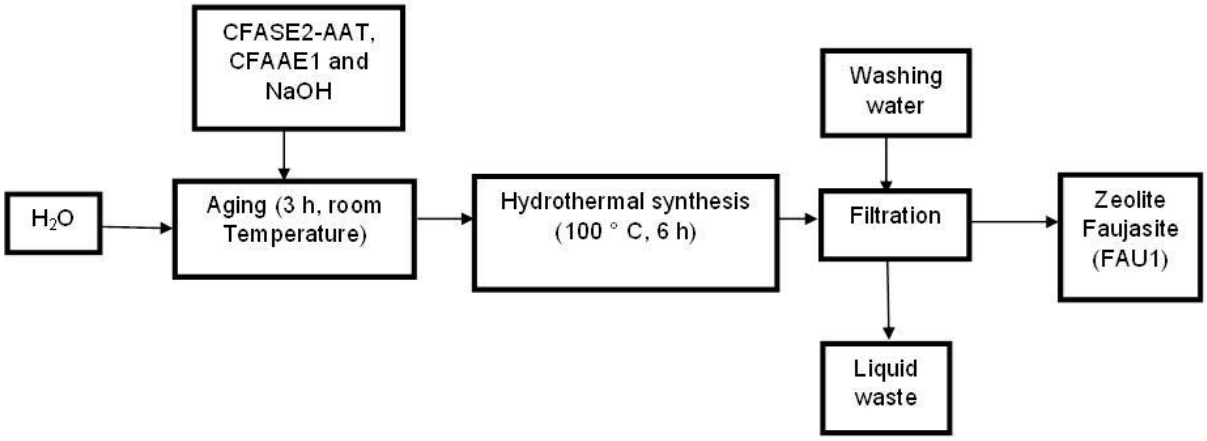

Figure 3.8: BFD for the synthesis of zeolite faujasite 1 (FAU1) from the CFA extracts, silica (CFASE2-AAT) and alumina (CFAAE1)

The molar regime and the synthesis conditions were adapted from the work carried out by Htun *et al*. (2012) with slight modifications. The CFAAE (CFAAE 1, CFAAE 2, CFAAE 3 or CFAAE 4) and CFASE2-AAT extracts from CFA, which were extracted as presented in Sections 3.2.2.1 and 3.2.2.2, were used as starting materials for the synthesis of zeolite faujasite. A mixture of CFAAE 1, CFAAE 2, CFAAE 3 or CFAAE 4, CFASE2-AAT, NaOH and de-ionised H_2O was prepared to get different molar regimes, as presented in Table 2. The prepared aluminosilicate gel was aged at room temperature for three hours and then subjected to hydrothermal treatment at 80, 90 or 100°C respectively for 6 h in an oil bath with continuous stirring. The product was left to cool, filtered, washed, dried overnight at 70°C and analysed using SEM, FTIR, XRD and NMR.

3.3.2.5. Synthesis of geopolymer 2 (G2)

A geopolymeric material was synthesised from Solid Residue 3 (SR 3), obtained after the extraction of CFASE2-AAT in Process 2, (Section 3.3.2.2). Figure 3.9 gives an illustration of the synthesis process.

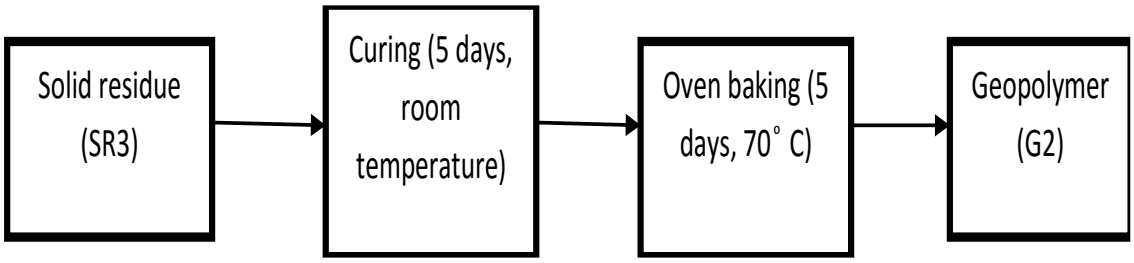

Figure 3.9: Block flow diagram for the synthesis of geopolymer from solid residue 3

Geopolymer 2 (G2) was synthesised from SR 3, which was obtained after the extraction of CFASE2-AAT from CFA in Process 2. The solid residue, SR 3, was thoroughly mixed to obtain a homogenous mixture and poured in a heat-resistant plastic mould. The mould was sealed and left to cure for five days at room temperature. Afterwards, the sealed plastic mould was placed in a pre-heated oven at 70°C for five days. After the five days, curing was completed, the seal on the mould was removed, and the content of the mould was left for three days to allow total dryness of the formed geopolymer (G2). The obtained geopolymer (G2) product was analysed using ICP-AES (after digestion following the method presented in Section 3.3.1.4). Characterisation was carried out using SEM, FTIR, XRD and NMR.

3.4. Analytical techniques

The different analytical techniques used to analyse solid and liquid samples in this study are presented in the following sub-sections.

3.4.1. Inductively coupled plasma atomic emission spectrometry (ICP-AES)

Inductively coupled plasma atomic emission spectrometry (ICP-AES) analysis was performed for liquid and solid samples obtained in this study, following the digestion method presented in Section 3.3.1.4. Where relevant, the ICP-AES technique was used to measure trace and major elements in a sample. The presence and concentration of elements in CFA, CFAAE and CFASE2-AAT, zeolites (ZSM-5 and Faujasite), geopolymers, liquid wastes and solid wastes were identified and quantified using ICP-AES. Each liquid sample was diluted 10 times and 100 times in 2% HNO_3 solution. Prior to the operation of the instrument, calibrations were performed daily and accuracy was checked by analysing quality control standards for all the elements analysed. Analysis was carried out in triplicate for each sample.

3.4.2. Scanning Electron Microscopy (SEM)

Scanning Electron Microscopy (SEM) is an analytical technique used to determine the morphology and crystalline structure of the sample. The samples were analysed using a Hitachi X-650 Scanning Electron Micro-analyser equipped with a CDU-lead detector at 25 kV, and a tungsten filament. The samples were prepared by placing a carbon adhesive tape onto an aluminium stub. A small amount of each sample was applied onto the carbon adhesive tape, which was coated with carbon in an Emitech K950X carbon Evaporator for 6 sec to render it conductive. The samples were placed in the column of the SEM and then specimens were observed under different magnifications. Micrographs of each sample were captured and displayed on an LCD computer.

3.4.3. Fourier Transform Infrared spectroscopy (FT-IR)

Fourier Transform Infrared spectroscopy (FTIR) was used to identify the surface functionalities and structural configurations of the starting material (CFA), CFASE2-AAT and CFAAEs, zeolite (ZSM-5 and Faujasite) and the synthesised geopolymers. In this study, the Perkin Elmer spectrum 100 FT-IR spectrometer was used for the FTIR analysis. Approximately 15 mg of each sample was placed on the Attenuated Total Reflectance (ATR) sample holder of the spectrometer and an equal force was applied to the sample. Infrared (IR) spectra were obtained within a range of 4000-400 cm^{-1} to identify the structural configurations of the sample. Baselines were corrected for background noise, which was subtracted from the spectra before data collection.

3.4.4. X-ray diffraction

X-ray diffraction (XRD) analysis was performed on the solid samples (coal fly ash, coal fly ash extracts, zeolites and geopolymers). The XRD analysis was carried out to determine the mineral phases of the identified samples. The utilised instrument was a Philips X-pert pro MPD X-ray diffractometer with Cu-K radiation at 40 KV and 40 mA. In order to carry out XRD analysis, approximately 0.5 g of the sample was prepared and placed onto a glass substrate inside a hollow sample holder. The sample height was levelled up with respect to the edge of the sample holder and inserted into the XRD instrument. The analysis was performed between 0° and 60° 2Θ and the obtained mineral phases were identified using HighScore Xpert software. The spectra obtained were compared with standard patterns from the powder diffraction database supplied by the International Centre for Diffraction Data (ICDD).

3.4.5. Nuclear magnetic resonance (NMR) spectroscopy

Solid state nuclear magnetic resonance (NMR) spectroscopy (^{27}Al NMR) was used to determine the percentage of framework and extra-framework Al in the starting materials and synthesised zeolites and geopolymers. Approximately 50 mg of the sample was compressed in a NMR rotor that had an inner diameter of 7 mm. Thereafter; the rotor was closed and inserted in the NMR instrument. The analysis was performed using a Bruker UltraShield 600 MHz/54 mm spectrometer.

CHAPTER FOUR

CHARACTERISATION OF FLY ASH, SYNTHESISED ZEOLITE ZSM-5 AND THE GEOPOLYMER.

4.1. Introduction

This chapter details the characterisation of coal fly ash (CFA), CFASE1-AAT and SR1 used as feedstock in the synthesis of Zeolite ZSM-5 and geopolymer respectively. Further, the elemental composition of the alkaline extraction of silica from CFA before (CFASE1-BAT) and after oxalic acid treatment (CFASE2-AAT) are presented and duly discussed. Lastly, the chapter highlights the characterisation of the final products (Zeolite ZSM-5 and geopolymer) of the process, as well as the mass balance of the zeolite synthesis process, in the following sub-sections.

4.2. Characterisation of coal fly ash (CFA)

The CFA was characterised using various analytical techniques in order to determine the chemical composition, morphology, and the physical or crystalline structure of the material prior to its application in producing the silica extract used in the synthesis of Zeolite ZSM-5. The solid residue (SR1) was used for preparing the geopolymer (as detailed in Chapter Three, Section 3.3.1.2 and 3.3.1.3). The analyses were carried out in triplicate to verify the reproducibility of the results. XRD was used to determine the mineralogy of the CFA sample. XRF and ICP techniques were used to determine its chemical composition. FTIR was used to determine the structural bands of the final products, while the morphological characterisation was performed using SEM.

4.2.1. Mineralogical analysis of CFA using X-ray diffraction (XRD)

The XRD analysis was performed as described in Chapter Three, Section 3.4.4, in order to determine the mineralogical phases present in CFA. The result (Figure 4.1) showed that mullite and quartz were the major mineral phases present in CFA, with traces of hematite mineral phase. This observation has been confirmed elsewhere (Du Plessis, 2014, Nyale *et al*., 2013, Musyoka *et al*., 2012, Mainganye, 2012).

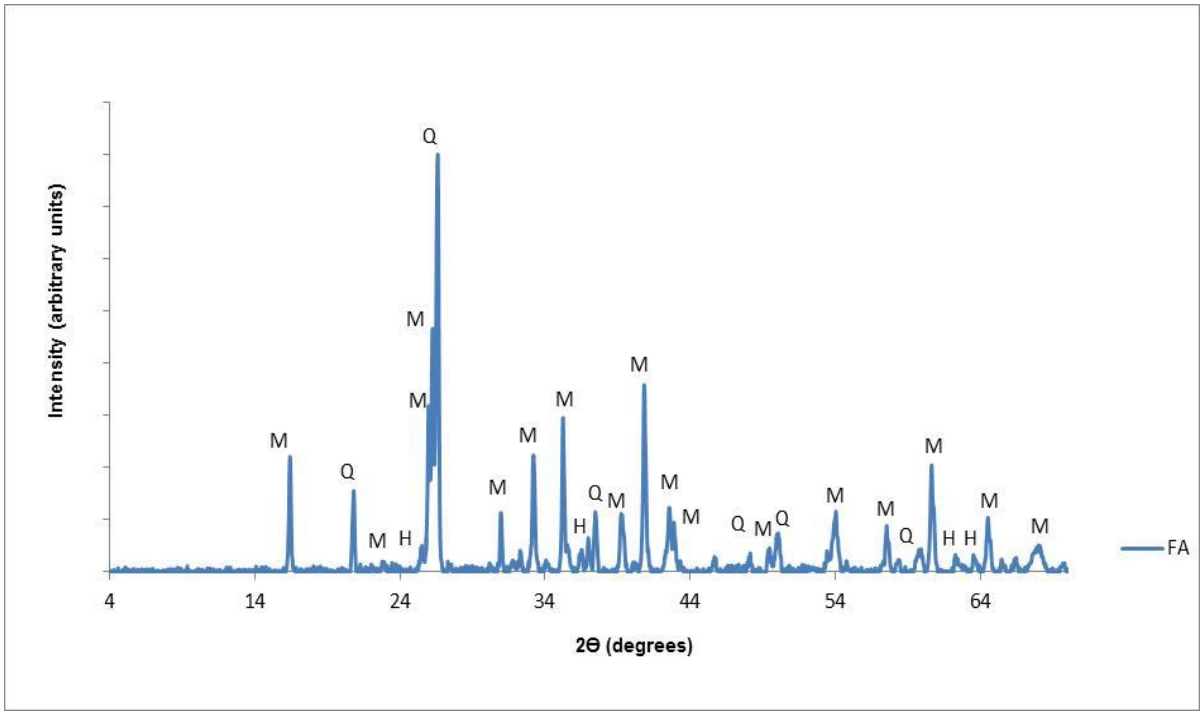

Figure 4.1: XRD pattern for coal fly ash (CFA). Where M = mullite, Q = quartz, H = hematite.

4.2.2. Morphological analysis of CFA using SEM

Scanning electron microscopy (SEM) was used to analyse the surface morphology of the CFA. The SEM micrograph of CFA is presented in Figure 4.2. It can be seen that the different sizes of CFA particles were all roughly spherical. The spherical particles are also known as aluminosilicate cenospheres, which are formed as a result of the chemical transformation of mineral particles due to the high temperatures created during the combustion of coal (Nyale *et al*., 2013).

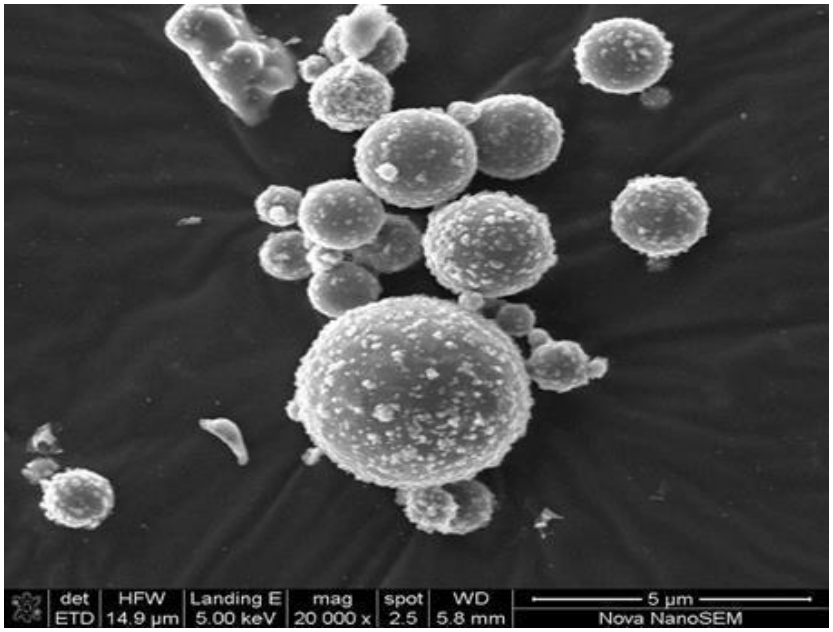

Figure 4.2: SEM image for the coal fly ash (CFA)

4.2.3. Structural analysis of CFA using Fourier Transform Infrared (FTIR)

FTIR spectroscopic analysis was performed for the structural analysis of CFA, following the procedure described in Chapter Three, Section 3.4.3. The FTIR spectrum of CFA (Figure 4.3) revealed four bands (463, 556, 780 and 1084 cm^{-1}) characteristic of aluminosilicates. The band appearing at 463 cm^{-1} was associated with the T-O bending vibration (Fernández-Jiménez and Palomo, 2005), while the band appearing at 556 cm^{-1} was assigned to octahedral aluminium of mullite phase present in CFA (Criado *et al*., 2007).The bands appearing at 780 cm^{-1} and 1084 cm^{-1} were associated with symmetric stretching vibrations of Si-O-Si and asymmetric stretching vibrations of Si-O-T respectively (Nyale *et al*., 2013, Flanigen *et al*., 1971).

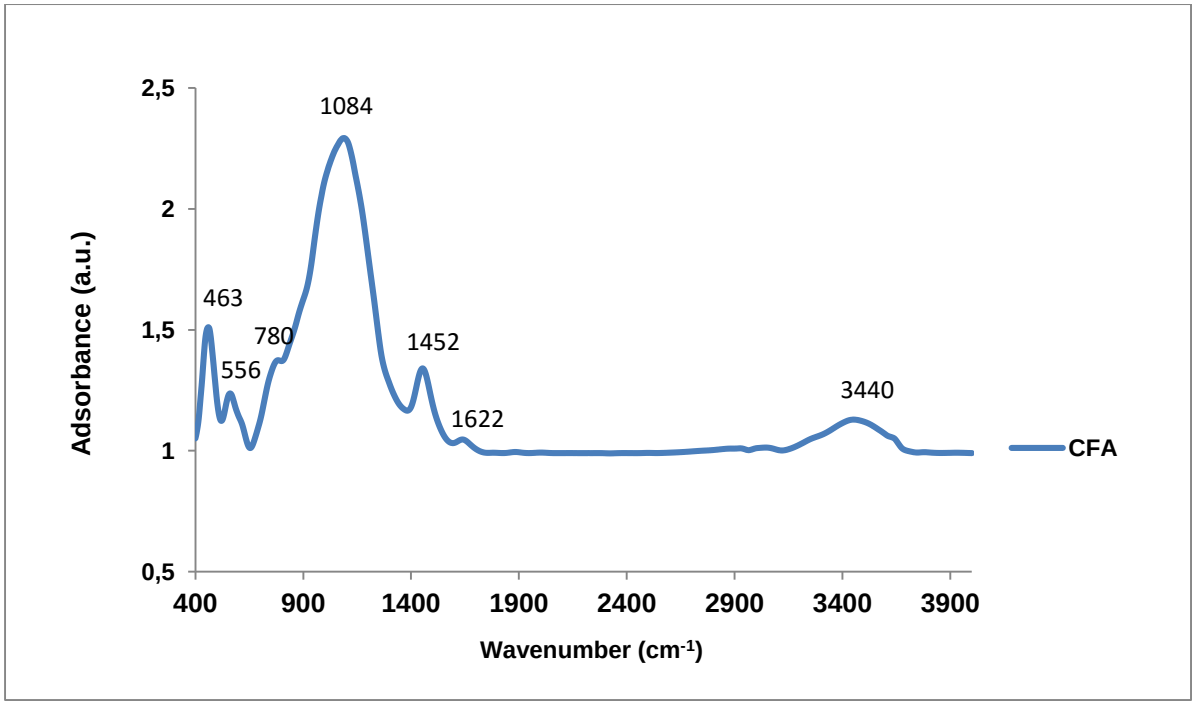

Figure 4.3: FTIR spectrum of CFA

The bands appearing at 1452 cm^{-1} and 1622 cm^{-1} were characteristic of carbonate and sulphate respectively, while the band appearing at 3440 cm^{-1} was associated with the characteristic of a H-O-H stretching, and is indicative of the fact that the CFA sample contained or absorbed a small content of water (Saikia and Parthasarathy, 2010).

4.2.4. XRF and ICP analysis of CFA

The elemental composition of CFA used as feedstock in this study is presented in Table 4.1. The values reported are the mean of triplicate analysis and the standard deviations. The XRF results indicated that SiO_2 and Al_2O_3 were the major oxides present in the Matla CFA with a percentage composition of 52.3±0.24 and 28.6±0.10% respectively, followed by CaO (7.78±0.06%) and Fe_2O_3 (3.12±0.03).

Table 4.1: Elemental composition of major elements present in CFA (n = 3)

Species	XRF of MCFA (% w/w)	Element (%)	CFA (XRF)	CFA (ICP)
SiO_2	53.1 ± 0.24	Si	53.11	47.83
Al_2O_3	29.1 ± 0.10	Al	29.06	29.63
CaO	7.9 ± 0.06	Ca	7.90	10.88
Fe_2O_3	3.17 ± 0.03	Fe	3.17	4.27
TiO_2	2.12 ± 0.02	Ti	2.12	2.44
MgO	2.08 ± 0.04	Mg	2.08	2.42
P_2O_5	0.88 ± 0.00	P	0.89	0.37
K_2O	0.67 ± 0.01	K	0.67	1.08
SO_3	0.56 ± 0.01	S	0.56	0.43
Na_2O	0.38 ± 0.01	Na	0.38	0.55
MnO	0.04 ± 0.00	Mn	0.04	0.06
Cr_2O_3	0.02 ± 0.01	Cr	0.02	0.03
Total	100 ± 0.53	Total	100.00	100.00

The SiO_2 and Al_2O_3 are regarded as the oxides of interest in the synthesis of zeolites and geopolymers, and both oxides accounted for more than 80% of the total elements present in the ash sample, with a SiO_2/Al_2O_3 ratio of 1.82. It can be seen from the results that the elemental composition of CFA analysed by ICP showed that Si and Al were the main dominant elements in CFA, with a percentage composition of 53.11 and 29.06% respectively. The Si/Al ratio calculated from the ICP results was 1.61. Matla CFA can be classified as class F fly ash (FA) because the total amount of SiO_2, Al_2O_3 and, Fe_2O_3 is greater than 70 wt% at 88.65%. According to the American Society for Testing Materials (ASTM C618), FA with a total amount of SiO_2, Al_2O_3 and, Fe_2O_3 above 70 wt% are classified as class F FA. This observation is in agreement with published results on the composition of Matla CFA (Nyale *et al*., 2013, Madzivire, 2009, Petrik *et al*., 2003b). The composition of South African FA varies depending on the place of origin (Musyoka, 2012, Madzivire *et al*., 2010). It can be seen from these results that the composition of CFA analysed from XRF and ICP gave similar results, with a SI/Al ratio of 1.82 and 1.61 respectively.

4.3. Elemental composition of coal fly ash silica extracts

This section details the elemental composition of coal fly ash silica extracts before oxalic acid treatment (CFASE1-BAT) that were obtained following Process 1, as detailed in Section 3.3.1.1. For the extraction of silica, CFA was mixed with 8, 4, and 2 M of NaOH solution respectively under reflux conditions for 24 h at 160ºC. The recovered silica extracts were coded CFASE1-BAT (8 M), CFASE1-BAT (4 M) and CFASE1-BAT (2 M) respectively. These extracts were digested and analysed for elemental composition using ICP, as detailed in Section 3.4.1. The CFASE1-BAT extracts were further treated with oxalic acid in order to reduce the concentration of undesired elements prior to the synthesis of Zeolite ZSM-5. The oxalic acid treated silica extract was coded coal fly ash silica extract after oxalic acid treatment (CFASE1-AAT). These results are presented in the sub-sections below.

4.3.1. Elemental composition of coal fly ash silica extracts before oxalic acid treatment (CFASE1-BAT) using ICP

The dried silica extracts were coded, coal fly ash silica extract before oxalic acid treatment CFASE1-BAT (8 M), CFAE1-BAT (4 M) and CFASE1-BAT (2 M). The elemental compositions of CFA, CFASE1-BAT (8 M), CFASE1-BAT (4 M) and CFASE1-BAT (2 M) are presented in Figure 4.4.

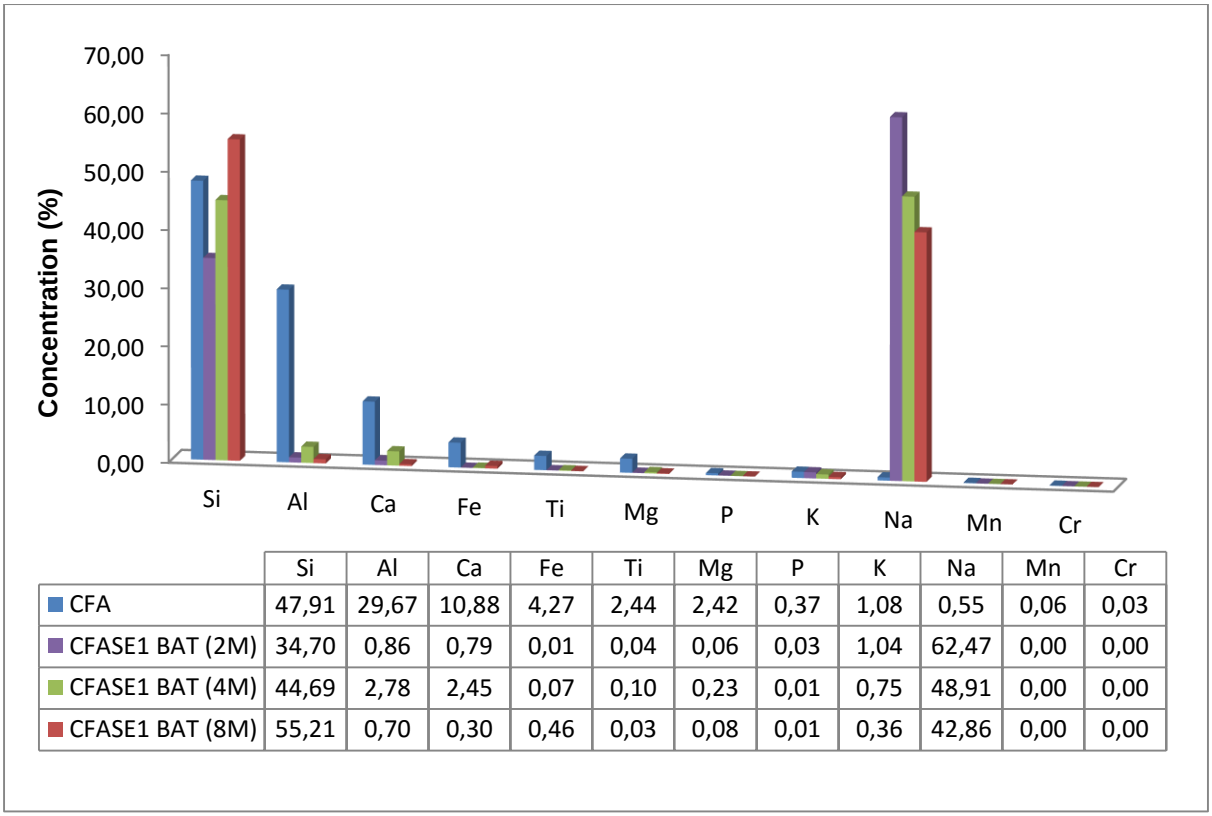

	Si	Al	Ca	Fe	Ti	Mg	P	K	Na	Mn	Cr
CFA	47,91	29,67	10,88	4,27	2,44	2,42	0,37	1,08	0,55	0,06	0,03
CFASE1 BAT (2M)	34,70	0,86	0,79	0,01	0,04	0,06	0,03	1,04	62,47	0,00	0,00
CFASE1 BAT (4M)	44,69	2,78	2,45	0,07	0,10	0,23	0,01	0,75	48,91	0,00	0,00
CFASE1 BAT (8M)	55,21	0,70	0,30	0,46	0,03	0,08	0,01	0,36	42,86	0,00	0,00

Figure 4.4: Elemental composition of CFA and coal fly ash silica extracts before oxalic acid treatment (CFASE1-BAT) obtained using 8, 4, and 2 M NaOH solution

Figure 4.4 shows the percentage of the elements present in the CFA and the CFASE1-BAT (8, 4 and 2 M). The ICP analysis for CFA and CFASE1-BAT (8,4 and 2M) was performed to assess the concentration of Si, Al, Ca, Fe, Ti, Mg, P, K, Na, Mn, and Cr in the starting material used for the extraction of silica. The technique was also used to analyse the presence and concentration of these elements in the extracted coal fly ash silica extract before oxalic acid treatment CFASE1-BAT (8, 4 and 2 M). It can be seen from Figure 4.4 that CFASE1-BAT (8 M), CFASE1-BAT (4 M) and CFASE1-BAT (2 M) contained all the elements identified in the starting material (CFA) in trace amounts. The mass percentages of Si and Al in CFA were 47.91 and 29.71 respectively. It can be seen from the CFA ICP that the Si/Al ratio is 1.61. The mass percentage of Si in CFASE1-BAT (8 M), CFASE1-BAT (4 M) and CFASE1-BAT (2 M) was 55.21, 44.69 and 34.70% respectively, while that of Al was 0.7, 2.78 and 0.86% respectively, thus the Si/Al ratios were 78, 16 and 40 respectively. Moreover, the Na content increased significantly after NaOH treatment with CFA, CFASE1-BAT (8 M), CFASE1-BAT (4 M) and CFASE1-BAT (2 M) at 0.59, 42.86, 48.91 and 62.47% respectively.

The increase in the amount of Na in the silica extracts is due to the addition of NaOH solution during the precipitation of silica. It is evident from these results that Si was the most extracted

element from CFA during the alkaline leaching process. It can be seen that CFASE1-BAT (8 M) resulted in the highest Si extraction at 55.21%, thus, the use of 8 M NaOH in the extraction of CFASE2-BAT from CFA was effective when compared to 4 M and 2 M NaOH respectively, but could have an inappropriate Na content for zeolite synthesis.

According to literature, it is necessary to reduce the concentration of Na in the extract in order to increase the concentration of Si. Hattori and Yashima, (1994) investigated the effect of Na_2O/SiO_2 ratio on the synthesis of Zeolite ZSM-5. The authors reported that below a Na_2O/SiO_2 ratio of 0.008, the zeolite synthesised was mixed with an amorphous phase. However a pure phase of Zeolite ZSM-5 was formed when the Na_2O/SiO_2 ratio was between 0.008 and 0.2, and the increase in Na_2O/SiO_2 ratio to 0.2 was accompanied by formation of Zeolite ZSM-5 and α-SiO_2. Therefore, it could be predicted that the high Na content in CFASE1-BAT could affect the nature of the final product during the synthesis of Zeolite ZSM-5. Consequently, a saturated oxalic acid solution was used to remove Na from CFASEs, as detailed in Section 3.3.2.2.

The CFASE1-BAT silica extract obtained at the optimum condition of 8 M NaOH was used for further work in this study, and was treated with a saturated oxalic acid solution in order to reduce the Na content, as well as some undesirable elements such as K and Fe in the CFASE1-BAT and to increase the Na_2O/SiO_2 ratio prior to the synthesis of Zeolite ZSM-5.

4.3.2. Elemental composition of CFASE1-BAT and CFASE1-AAT

The ICP analysis for CFASE1-BAT and CFASE1-AAT was performed following the procedure detailed in Section 3.4.1. Figure 4.5 showed the mass percentage of elements present in CFA, CFASE1-BAT and CFASE1-AAT. The ICP result of CFA was discussed in Section 4.3.1.

It can be seen from the ICP results that the Si content in CFASE1-BAT and CFASE1-AAT was 55.21 and 86.84% respectively, while the concentration of Al remains at 0.7% even after the treatment of CFASE1-BAT with saturated oxalic acid. It is important to note that the concentration of Na decreased from 42.86% in CFASE1-BAT to 11.62% in CFASE1-AAT. It can also be observed that the concentration of Si in CFASE1-AAT increased due to the significant decrease in Na content after treatment with oxalic acid. This result showed that the treatment of CFASE1-BAT with saturated oxalic acid was successful. The Na/Si ratio of the CFASE1-AAT was found to be 0.13.

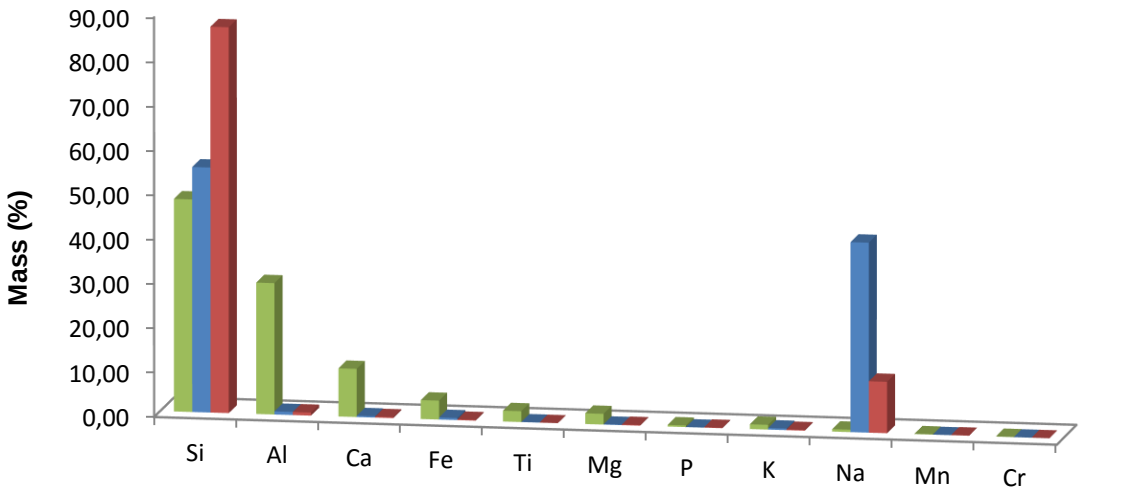

	Si	Al	Ca	Fe	Ti	Mg	P	K	Na	Mn	Cr
CFA	47,91	29,67	10,88	4,27	2,44	2,42	0,37	1,08	0,55	0,06	0,03
CFASE1-BAT	55,21	0,70	0,30	0,46	0,03	0,08	0,01	0,36	42,86	0,00	0,00
CFASE1-AAT	86,84	0,70	0,21	0,16	0,01	0,15	0,09	0,16	11,62	0,05	0,00

Figure 4.5: Elemental composition of CFASE1-BAT and CFASE1- AAT

This value is close to the Na_2O/SiO_2 ratio of 0.2 recommended for the synthesis of Zeolite ZSM-5 (Hattori and Yashima, 1994). The treated CFASE1-AAT was then used as the feedstock in the synthesis of Zeolite ZSM-5. Based on the ICP results the extraction efficiency of extracted Si was calculated using the following formula:

$$\eta = \frac{Mass(si)_{CFASE1-AAT}}{Mass(Si)_{CFA}} * 100$$

Where ŋ is the extraction efficiency.

The efficiency was found to be 91.92%. Font *et al*., (2009) reported the Si extraction efficiency of 34.13 and 20.55% from two Spanish CFAs using 3 M NaOH at 120ºC for 9 h. The extraction efficiency of Si in the current study was much higher than those reported by Font *et al*. (2009) and Moreno *et al*. (2002), due to the drastic conditions applied (8 M NaOH at 150ºC for 24 h). This result showed that the extraction of Si using these conditions was successful.

4.3.4. XRD analysis for CFASE1-BAT in comparison with CFASE1-AAT

XRD was used, as described in Chapter Three, Section 3.4.4, to analyse the mineral phases of CFASE1-BAT and CFASE1-AAT. Figure 4.6 present the XRD for CFASE1-BAT and CFASE1-AAT.

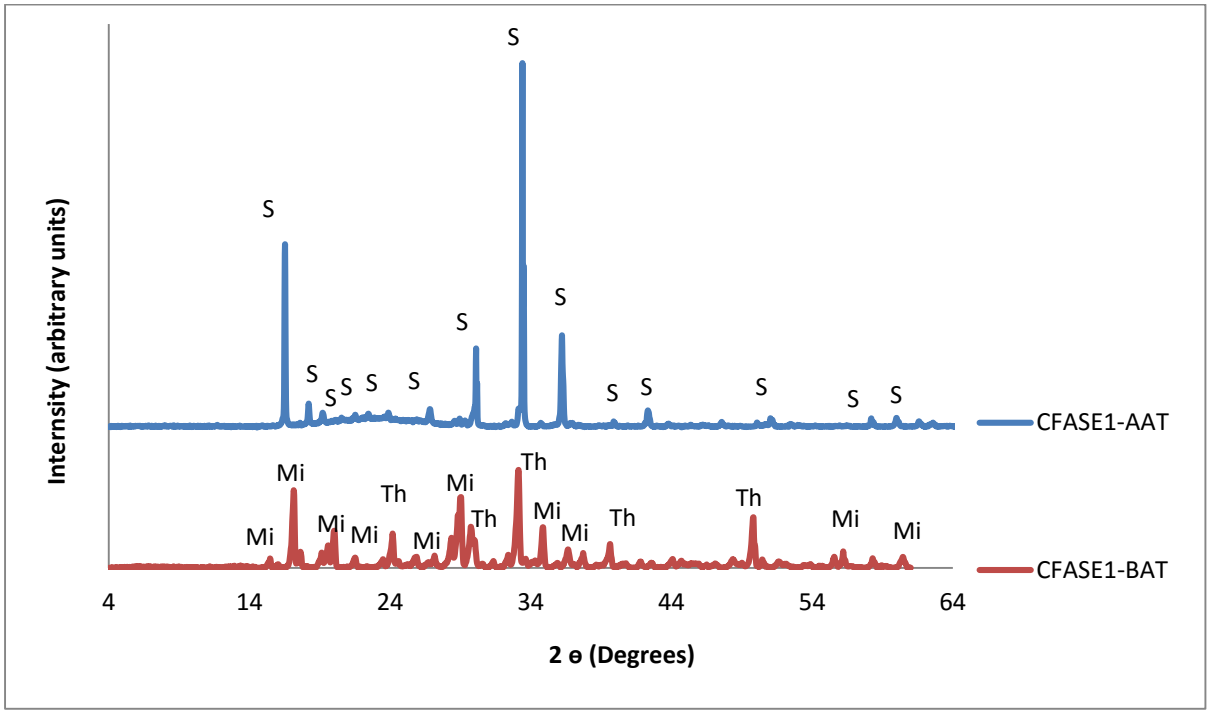

Figure 4.6: XRD pattern for CFASE1-BAT and CFASE1-AAT. Where Mi = Mirabilite ($Na_2SO_4 \cdot 10H_2O$), Th = Thenardite (Na_2SO_4) and S = Sodium Hydrogen Oxalate Hydrate ($C_2HNaO_4 \cdot H_2O$).

The XRD patterns of CFASE1-BAT and CFASE1-AAT presented in Figure 4.6 showed that there are mirabilite and thenardite peaks in the CFASE1-BAT sample. The mirabilite and thernardite peaks in CFASE1-BAT are assumed to be caused by the use of NaOH during the extraction of silica.

It can be seen from these results that most of the Na from NaOH precipitated with the silica extract. This result confirms the ICP result, where Na accounted for 42.86 mass% in the CFASE1-BAT. The XRD pattern of CFASE1-AAT showed high intensity peaks of sodium hydrogen oxalate hydrate. It can be seen that a broad hump characteristic of amorphous silica appeared at 16 to 25 2Ɵ. This observation was also reported by other researchers (Xu and Khor, 2007, Inada *et al*., 2005, Kalapathy *et al*., 2000). The sodium hydrogen oxalate hydrate peaks appearing on the CFASE1-AAT XRD pattern can be associated with the use of oxalic acid during the treatment of CFASE1-AAT. The characteristic hump of amorphous silica

ranging between 16 to 25 2Θ was also reported in previous studies (Xu and Khor, 2007, Inada *et al*., 2005, Kalapathy *et al*., 2000). It can be seen from these results that oxalic acid was successfully used to treat CFASE1-BAT to remove the excess Na content in the extract. The treated silica extract (CFASE1-AAT) would be used as a feedstock in the synthesis of Zeolite ZSM-5.

4.3.5. FTIR analysis for CFASE1-BAT and CFASE2-AAT

The FTIR analysis of CFASE1-BAT and CFASE1-AAT was performed following the procedure detailed in Chapter Three, Section 3.4.3. The FTIR results for both samples are presented and compared in Figure 4.7.

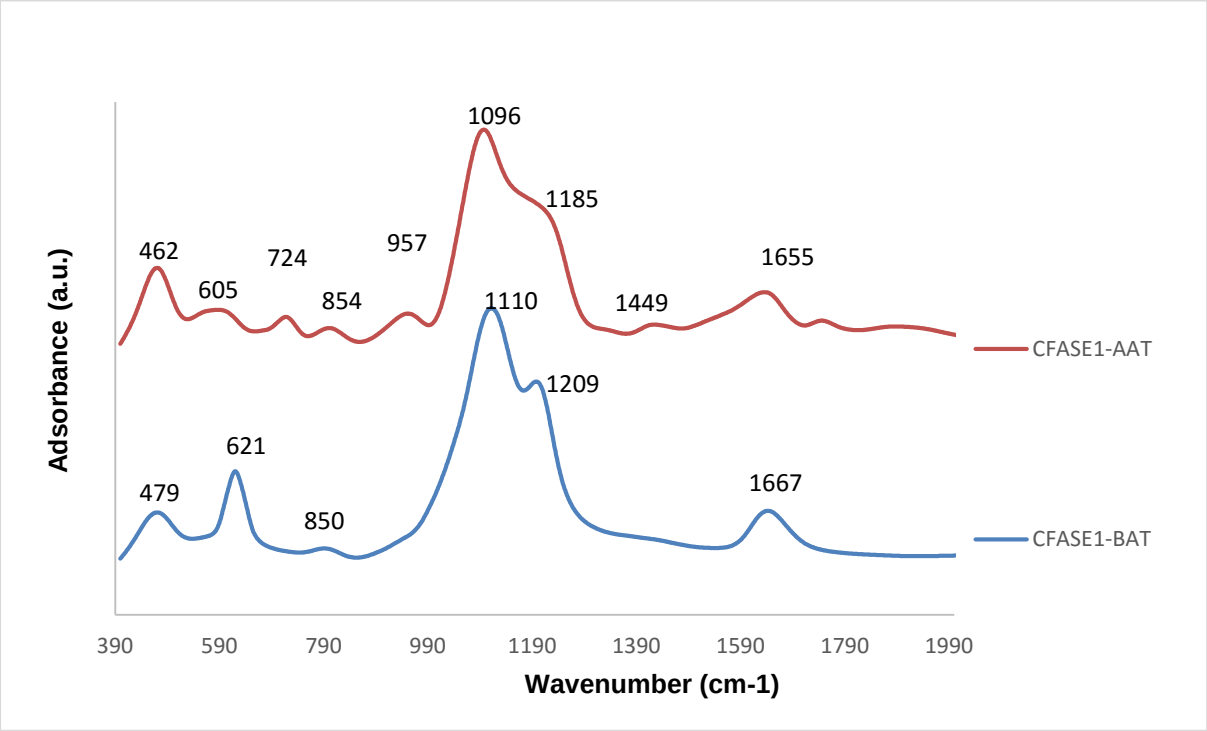

Figure 4.7: FTIR spectra for CFASE1-BAT in comparison with CFASE1-AAT

Figure 4.7 showed that the FTIR spectrum of CFASE1-BAT had five bands correlating to those of amorphous silica. The absorption band appearing at 479 cm^{-1} was attributed to the T-O bend vibration (Saikia and Parthasarathy, 2010). The band at 621 cm^{-1} was assigned to the stretching vibration of the Al-O bands with aluminium ions in four-fold co-ordinated (Aronne *et al*., 1997) and the band at 850 cm^{-1} was assigned to monomeric or dimeric silicate species (Böke *et al*., 2015). Two broad bands appearing at 1110 and 1209 cm^{-1} were also observed, which could be associated with a silicon centre that is bonded to four other T atoms through oxo-bridges, as shown in Figure 4.8 (Böke *et al*., 2015). Furthermore, two peaks which are not associated with the aluminosilicates were also identified in the CFASE1-BAT spectra. The

identified peaks are 1667 cm^{-1} and 3493 cm^{-1}, the identified peak at 1667 cm^{-1} is related to the O-H deformation of water (Attia *et al*., 2013). The FTIR spectra of CFASE1-AAT have shown seven aluminosilicate bands. The band at 462 cm^{-1} can be assigned to Si-O, and the bands at 605, 724 and 854 cm^{-1} can be assigned to the stretching vibration of the Al-O bands with aluminium ions in four-fold co-ordinated (Aronne *et al*., 1997). The bands at 957 and 1096 cm^{-1} can be associated with a silicon centre that is bonded to two and three other T atoms through oxo-bridges respectively, while the band appearing at 1185 cm^{-1} can be associated with a silicon centre that is bonded to four other T atoms through oxo-bridges (Böke *et al*., 2015). The bands appearing at 1449 and 1655 can be associated with the carbonate and O-H deformation of water respectively (Attia *et al*., 2013, Miller and Wilkins, 1952). The infrared result showed that the treatment of silica extract with oxalic acid was effective, since CFASE1-AAT showed more bands of aluminosilica, which confirms the ICP and the XRD result. Figure 4.8 shows a more detailed assignment of the asymmetric stretching of T-O bands to silicate species, as well as the depolymerisation and condensation processes involving silicate species.

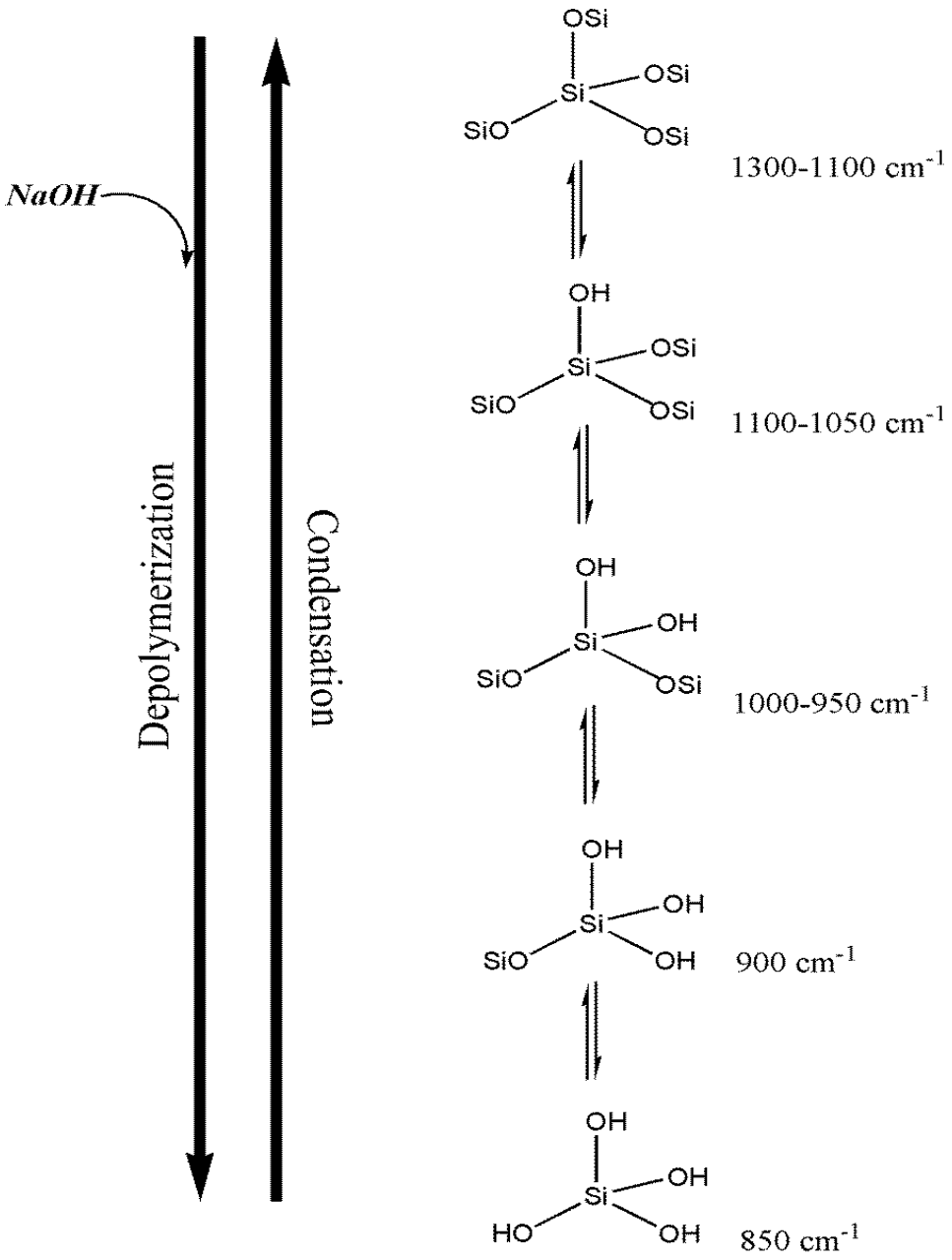

Figure 4.810: The depolymerisation and condensation process involving silicate species, including the corresponding wavenumbers for each species

Source: (Böke *et al*., 2015)

4.4. Characterisation of Zeolite ZSM-5 synthesised from CFASE1-AAT

This section discuses and compares the characteristics of extracted coal fly ash silica extract after oxalic acid treatment (CFASE1-AAT) to that of the synthesised Zeolite ZSM-5 using different analytical techniques (SEM, FTIR, XRD and solid state NMR). The results are presented in the following subsections.

4.4.1. Mineralogical analysis of Zeolite ZSM-5 and CFASE1-AAT using XRD

The extract of CFASE1-AAT (oxalic acid treated sample) was used as the feedstock in the synthesis of Zeolite ZSM-5. CFASE1-AAT was mixed with NaOH, TEAOH and water in mass ratio of 2, 0.4, 1 and 50 g respectively. Thereafter the resultant mixture was subjected to hydrothermal synthesis in a pre-heated oven at 160ºC for 72 h. After the reaction time was complete, the mixture was filtered and the recovered product was dried at 70ºC for 24 h. The synthesis procedure for Zeolite ZSM-5 has been reported previously in Section 3.3.1.2. The mineralogical analysis for the dried product and CFASE1-AAT was performed using XRD. Figure 4.9 shows the XRD pattern for CFASE1-AAT and the synthesised product.

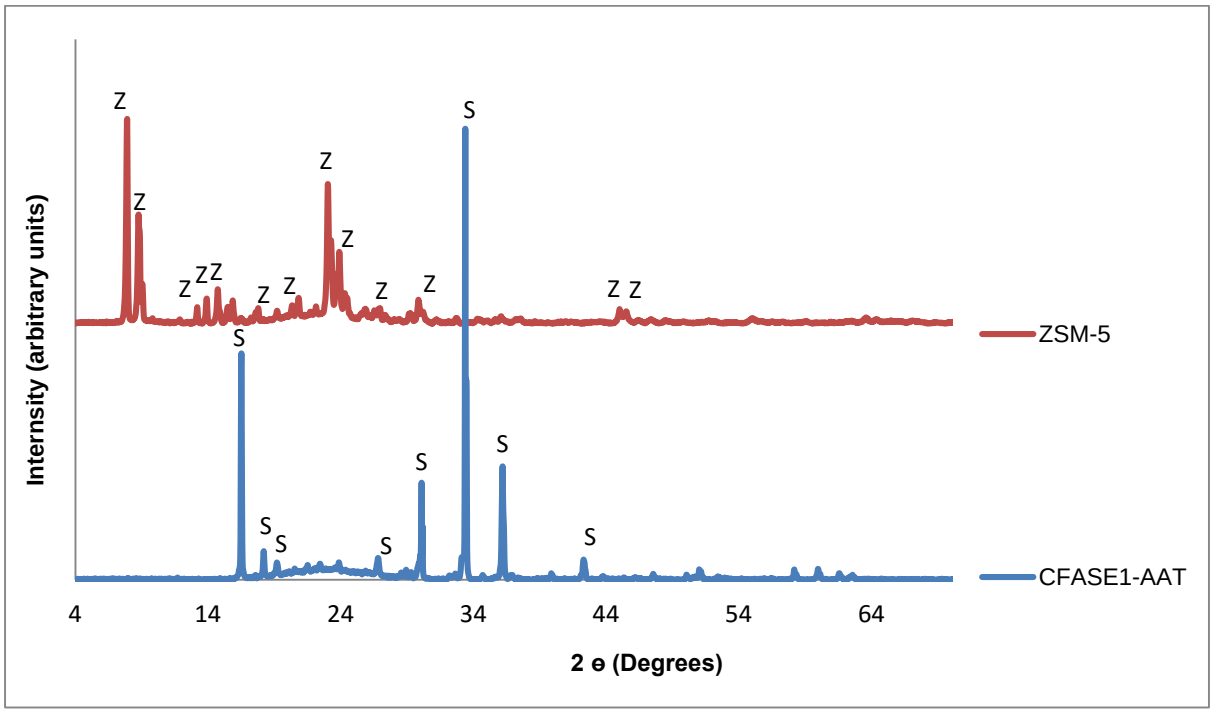

Figure 4.9: XRD patterns for CFASE1-AAT and the synthesised Zeolite ZSM-5. Where Z = ZSM-5 and S = Sodium Hydrogen Oxalate Hydrate.

The XRD patterns of CFASE1-AAT and Zeolite ZSM-5 are presented in Figure 4.9. The XRD pattern of CFASE1-AAT was discussed in Section 4.3.4. The XRD pattern of Zeolite ZSM-5 revealed the presence of a pure phase Zeolite ZSM-5. The observable peaks of the Zeolite ZSM-5 that was synthesised in this study were similar to those in the collection of simulated XRD power patterns for zeolites (Treacy and Higgins, 2001).In the literature, it was stated that SiO_2/Al_2O_3 mole ratio found in fly ashes is not sufficient to initiate the synthesis of Zeolite ZSM-5, as Zeolite ZSM-5 is a high silica zeolite. In order to obtain mole ratio required for Zeolite

ZSM-5 synthesis, a sodium silicate solution is usually added to adjust the mole ratio of these compounds in raw fly ash (Chareonpanich *et al*., 2004). On the However, the results of this study showed that Zeolite ZSM-5 can be synthesised successfully without the addition of sodium silicate solution using CFASE1-AAT (Si/Al of 124.1).

4.4.2. Morphology analysis of CFASE1-AAT and Zeolite ZSM-5 using SEM

SEM was used as described in Section 3.4.2 to analyse the surface morphology of CFASE1-AAT and Zeolite ZSM-5. Figure 4.10 presents the SEM image of CFASE1-AAT and Zeolite ZSM-5 products.

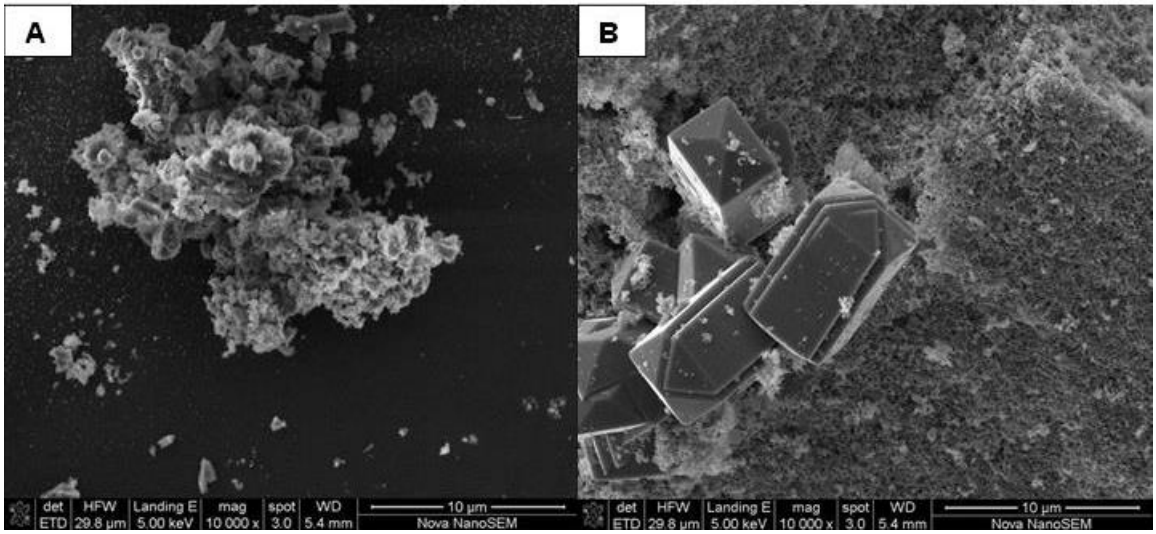

Figure 4.10: SEM images for CFASE1-AAT (A) and ZSM-5 (B)

The SEM micrographs presented in Figure 4.10 show that the amorphous silica CFAE1-AAT was transformed into characteristic lath-shaped crystals of Zeolite ZSM-5, as described by Petrik *et al*. (1995). However it can be seen in micrograph B that most of the amorphous silica was not converted into Zeolite ZSM-5.

This could be as a result of an incomplete synthesis reaction. Sang *et al*., (2004) reported the synthesis of lath-shaped ZSM-5 crystals using water glass and aluminium sulphate as source of silicon and aluminium, and ethylamine and isopropylamine as templates. However, Fouad *et al*., (2006) synthesised Zeolite ZSM-5 from sodium aluminate, fumed silica and sodium hydroxide, using tetraethylammonium hydroxide (TEAOH) as the directing template. The authors report that the synthesised Zeolite ZSM-5 crystallised into rod-like and sphere-like crystals. Based on the results found in the literature, it can be concluded that the use of a template does not predict the morphology of the synthesised zeolite, but directs the formation

of the desired zeolite structure. The SEM result showed that CFASE1-AAT was successfully used in the synthesis of Zeolite ZSM-5 without the addition of a silica source to adjust the Si/Al ratio, but the synthesis conditions should be optimised in order to allow total conversion of the amorphous silica into Zeolite ZSM-5.

4.4.3. Structural analysis of CFASE1-AAT and Zeolite ZSM-5 using FTIR

The FTIR analysis of CFASE1-AAT and Zeolite ZSM-5 were performed following the procedure detailed in Section 3.4.3. The FTIR results for both samples are presented and compared in Figure 4.11.

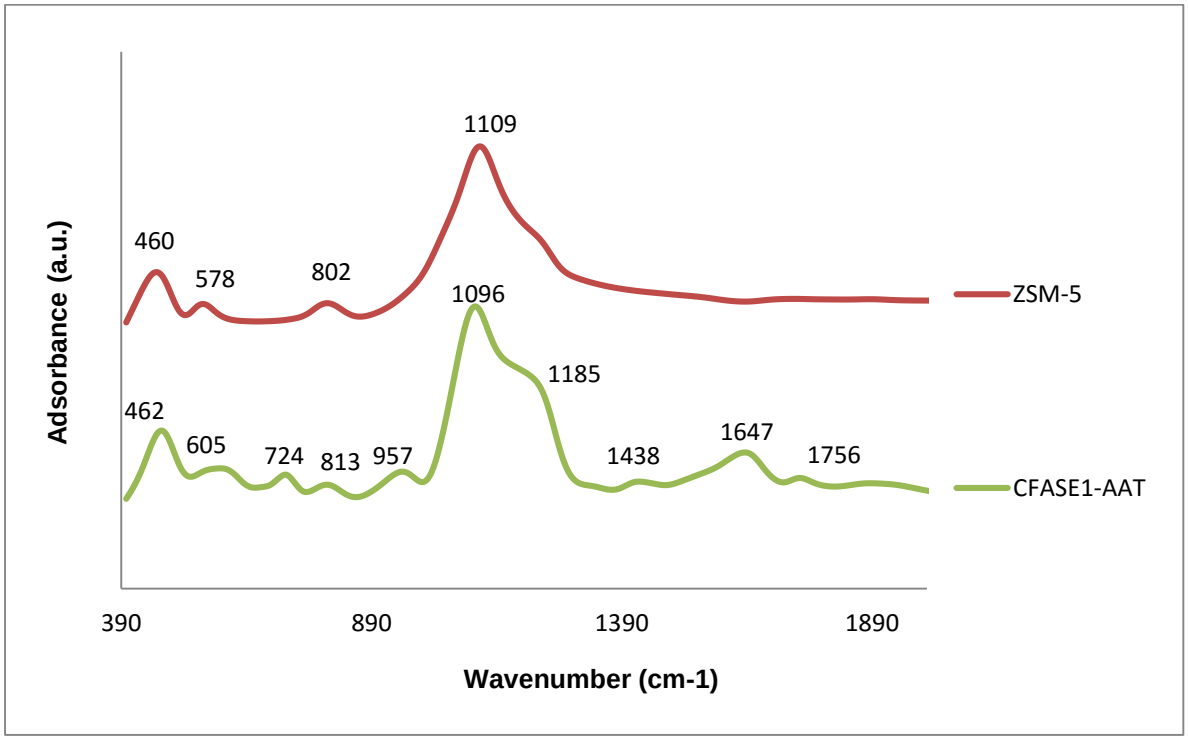

Figure 4.11: FTIR spectra for coal fly ash silica extract (CFASE-1-AAT) in comparison with synthesised Zeolite ZSM-5

The FTIR spectra of CFASE-AAT and ZSM-5 are presented in Figure 4.11. The FTIR spectrum of CFASE1-AAT is discussed in Section 4.3.5. The FTIR spectrum of Zeolite ZSM-5 showed bands characteristic of Zeolite ZSM-5. The bands at 460 cm^{-1} and 578 cm^{-1} are attributed to T-O bend vibration and double ring vibration respectively (Lee and Van Deventer, 2003). The bands at 802 cm^{-1} and 1109 cm^{-1} were assigned to the symmetric stretch vibration band and asymmetric vibration bands respectively (Flanigen *et al*., 1971). The infrared result of ZSM-5 confirms the XRD and the SEM results presented in Sections 4.4.1 and 4.4.2 respectively.

4.4.4. Nuclear magnetic resonance (NMR) spectroscopy analysis of CFASE1-AAT and Zeolite ZSM-5

This section compares the ^{27}Al and ^{29}Si NMR spectra for CFASE1-AAT and Zeolite ZSM-5. The procedure for the NMR analysis is detailed in Section 3.4.6. The results for the ^{27}Al and ^{29}Si NMR analysis for both CFASE1-AAT and Zeolite ZSM-5 are discussed as follows.

The framework and extra-framework Al in CFASE1-AAT and Zeolite ZSM-5 were investigated by solid state ^{27}Al NMR spectroscopy, as presented in Figure 4.12. The ^{27}Al NMR spectrum of CFASE1-AAT revealed a peak at about 0 ppm that corresponded to a hexa-coordinated extra-framework Al, while the ^{27}Al NMR spectrum of ZSM-5 showed a peak at about 55 ppm that characterised a tetra-coordinated framework Al.

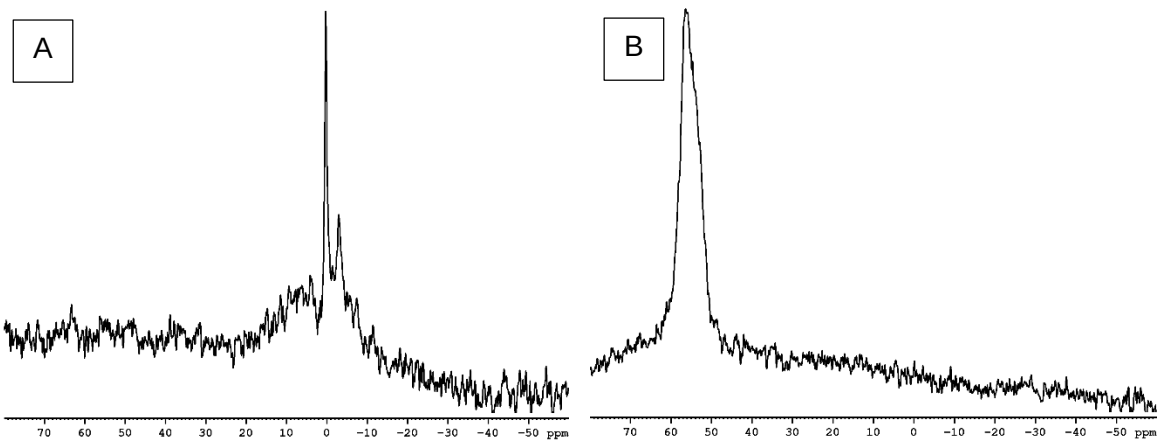

Figure 4.12: Solid state ^{27}Al NMR spectra for CFASE1-AAT (A) and Zeolite ZSM-5 (B)

The ^{27}Al NMR spectrum of CFASE1-AAT revealed a peak at about 0 ppm that corresponded to a hexa-coordinated extra-framework Al, while the ^{27}Al NMR spectrum of ZSM-5 showed a peak at about 55 ppm that characterised a tetra-coordinated framework Al.

These results show that all extra-framework Al in CFASE1-AAT were transformed into framework Al in Zeolite ZSM-5 and also, these NMR results corroborated the SEM, FTIR and XRD results where it was shown that the amorphous CFASE1-AAT was successfully transformed into crystallised Zeolite ZSM-5. Rodríguez-González *et al*., (2007) studied the acidic properties of zeolites ZSM-5 obtained from Zeolyst by ^{27}Al-MAS-NMR and the authors also associated the peaks at about 0 and 55 ppm to hexa-coordinated extra-framework Al and tetra-coordinated framework Al respectively. This result confirms that the alumina content of CFASE1-AAT was completely converted into a Zeolite ZSM-5 framework during the

hydrothermal synthesis and that very little amorphous phase remained. These results were confirmed by the XRD, SEM and FTIR result, as shown in Section 4.3.1, 4.3.2 and 4.3.3 respectively.

Figure 4.13 compares the solid state ^{29}Si NMR spectra of CFASE1-AAT and Zeolite ZSM-5. The ^{29}Si NMR spectra for CFASE1-AAT (A) and Zeolite ZSM-5 (B) are presented in Figure 4.13. From the ^{29}Si NMR spectrum of CFASE1-AAT (86.84% Si), two signals were identified at -100 and -110 ppm, corresponding to Si(2Al) and Si(1Al) units respectively. Thus, the alumina in the CFASE1-AAT extract (0.7%) occurred as small monomer or dimeric species in the extract. The ^{29}Si NMR spectrum of Zeolite ZSM-5 revealed one signal at -110 ppm which corresponds to the Si(1Al) unit. These results showed that there was no extra framework Al, and that the alumina content in the CFASE1-AAT was converted into the Zeolite ZSM-5 structure. These results are similar to those reported in work carried out by (Triantafyllidis *et al*., 2004, Byrappa and Yoshimura, 2001).

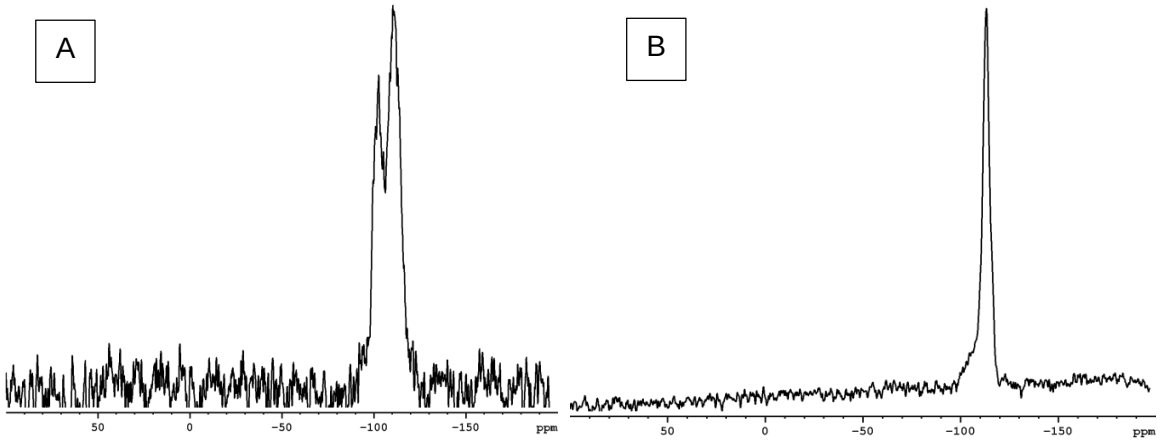

Figure 4.13: ^{29}Si NMR spectra for CFASE1-AAT (A) in comparison with ZSM-5 (B)

4.4.5. Mass balance for the synthesis of Zeolite ZSM-5 from CFASE1-AAT

This section presents the mass balances for the proposed method for synthesis of Zeolite ZSM-5 from CFASE1-AAT. The mass balance calculations were based on a dry mass of the samples. The CFASE1-AAT extract was obtained after the leaching of CFA with NaOH. Figure 4.14 illustrates the mass balance block flow diagram (BFD) for the synthesis of Zeolite ZSM-5 from the CFASE1-AAT. CFASE1-AAT was used as the feed stock in the synthesis of Zeolite ZSM-5. The CFASE1-AAT extract was mixed with NaOH, tetra ethyl ammonium hydroxide (TEAOH) and water in masses of 2, 0.4, 1 and 50 g respectively. The resulting mixture was aged for 30 min and thereafter subjected to hydrothermal synthesis in a pre-heated oven at

160°C for 72 h. When the reaction was complete, the product was filtered and dried, as discussed in Section 3.3.2.3.

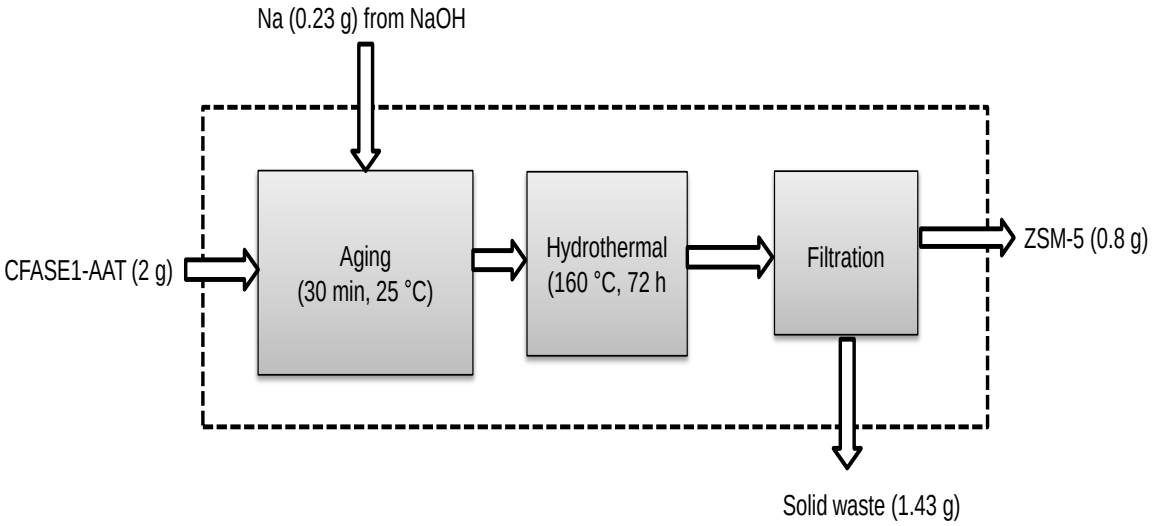

Figure 4.14: BFD for illustrating the mass balances for the synthesis of Zeolite ZSM-5

Figure 4.14 shows the mass distribution of the zeolite synthesis process. CFASE1-AAT (2 g) was mixed with 0.23 g of Na to obtain 0.8 g Zeolite ZSM-5 product and a solid waste which amounted to 1.43 g. The mass of Na was calculated based on the mass of NaOH added to the system. The OH was not considered, since it does not participate in the formation of zeolite structure. It can be seen from the BFD that most of the feed stock (CFASE1-AAT and Na) was not converted into Zeolite ZSM-5 during the hydrothermal process and as a result, these masses were accounted for in the waste stream. It is therefore recommended that the process should be optimised in order to recover the Si and Al lost into the waste stream, in order to increase the yield of the synthesised zeolite product and to make the process economically feasible.

Table 4.2: Material balance on the synthesis of Zeolite ZSM-5

Elements (%)	Feed stock			Products		
	CFASE1-AAT	NaOH	Total feed stream	ZSM-5	Solid waste	Total Product stream
Si	100	0	100	44.49	55.51	100.00
Al	100	0	100	46.99	53.01	100.00
Ca	100	0	100	40.14	59.86	100.00
Fe	100	0	100	38.21	61.79	100.00
Ti	100	0	100	35.90	64.10	100.00
Mg	100	0	100	25.05	74.95	100.00
P	100	0	100	25.52	74.48	100.00
K	100	0	100	20.93	79.07	100.00
S	100	0	100	0.00	0.00	0.00
Na	50.27	49.73	100	3.38	96.62	100.00
Mn	100	0	100	24.44	75.56	100.00
Cr	100	0	100	0.00	100.00	100.00

Table 4.2 illustrates the weight% distribution of the elements from the feedstock to the final products of the process. Only 44.49 and 46.99% out of the 100% Si and Al fed into the process corresponded to the zeolite product respectively, whereas 55.51 and 53.01% of Si and Al reported to the solid waste stream (in the filtrate) respectively. It can be seen that out of the 100% of Na feed in the process, only 3.38% contributed to the formation of zeolite structure and the rest reported to the waste stream. This reflects a high level of wastage of the Si, Al and Na fed into the process and as a result, this could be a determinant in the poor yield of the final zeolite product obtained (0.8 g) as shown in Figure 4.13. It was found that 20.93% of K reported to the zeolite products while the rest reported to the solid waste stream. The amount of K (20.93%) which reported to the zeolite product is assumed to be a competing charge stabilising ion (Querol *et al*., 1995). The synthesised Zeolite ZSM-5 also contained the other elements that were initially present in CFASE1-AAT such as Ca, Fe, Ti, Mg, P, Mn and the amounts were 40.14, 38.21, 35.9, 25.05, 25.52 and 24.44% respectively. It can also be seen that the Ca content in the zeolite product amounted to 40.14%. The presence of Ca in the zeolite structure can be useful as a charge balancing cation to maintain electrical neutrality in the zeolite framework (Breck, 1964).

4.5. Characterisation of geopolymer synthesised from the solid residue (SR1) remaining from the extraction of CFASE1-AAT

This section details the characteristics of geopolymer synthesised from the solid residue remaining after the extraction of CFASE1-AAT from CFA using 8 M NaOH solution, as detailed in Chapter Three, Section 3.3.1.1. The method employed to synthesise the geopolymer was presented in Section 3.3.1.3. The synthesised geopolymer was analysed using the following analytical techniques: SEM, FTIR, XRD and NMR and the results are presented in the following subsections.

4.5.1. Mineralogical analysis of geopolymer and CFA using XRD

The geopolymer (G1) was synthesised from the SR1 obtained after the extraction of CFASE2-AAT. The SR1 was poured in a 50 by 50 cm cubic mould, sealed and left to cure for five days at room temperature, the mould was further cured in an oven and heated at 70ºC for five days. Thereafter, the recovered geopolymer product was analysed using XRD. The mineral phase of the synthesised geopolymer in comparison with CFA is presented in Figure 4.15.

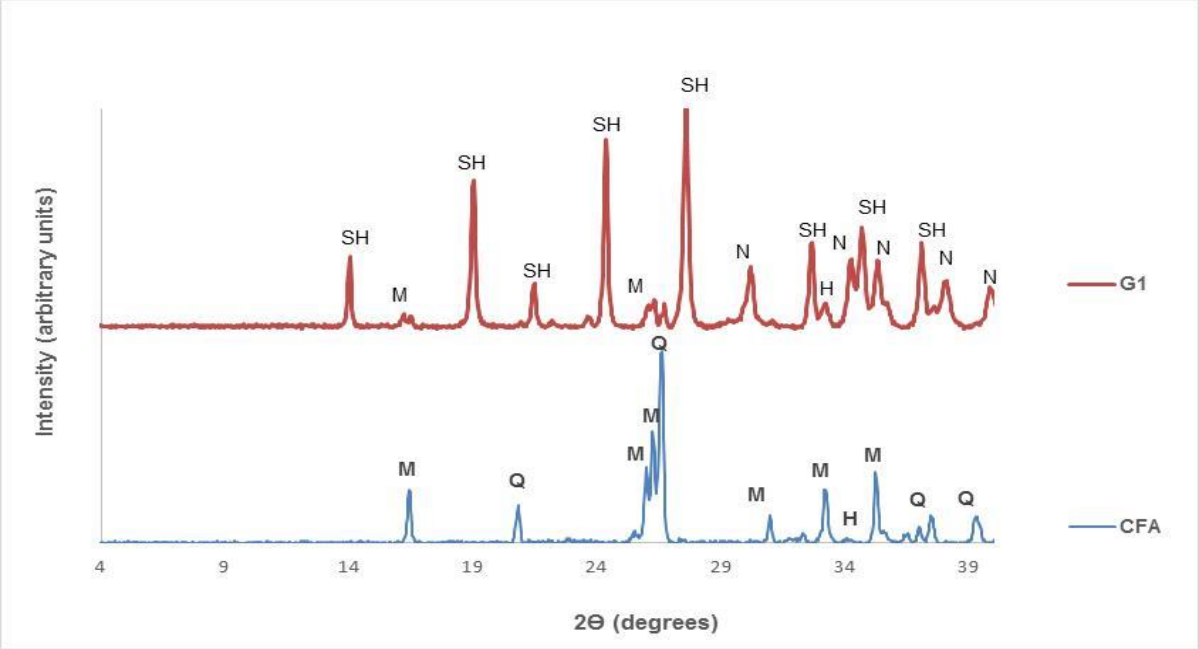

Figure 4.15: XRD of CFA and geopolymer (G1). Where SH = sodium aluminium silicate hydroxide hydrate ($Na_8(AlSiO_4)_6(OH)_2{\cdot}4H_2O$), M = mullite ($Al_6Si_2O_{13}$), N = natrite ($Na_2CO_3$), H = hematite ($Fe_2O_3$) and Q = quarts ($SiO_2$).

The XRD spectra presented in Figure 4.15 showed the mineral phases present in CFA and the synthesised G1. It can be seen from the XRD patterns that CFA was mainly dominated by mullite and quartz phases, whereas G1 revealed the presence of sodium aluminium silicate hydroxide hydrate and natrite mineral phases, with some trace of unreacted mullite and hematite from CFA. The presence of mullite in G1 indicated that not all SiO_2 and Al_2O_3 participated in the geopolymerisation reaction. However, it is noteworthy that most of the mullite and quartz was converted into sodium aluminium silicate hydroxide hydrate to form a geopolymer. The formed G1 was not strong, due to the presence of sodium hydroxide species, thus making G1 a form of hydroscopic material. Nyale *et al*., (2013) also synthesised a geopolymer from CFA using FA: NaOH: NaOCl: H_2O mass ratio of 3.03: 1.00: 1.14: 1.00 respectively, and the synthesised geopolymer contained quartz, mullite, sodalite and halite as mineral phases. These results indicate that the geopolymerisation process was not complete due to the mineral phases identified in the solid waste.

4.5.2. Morphology analysis of CFA and G1 using SEM

SEM analysis was carried out as described in Section 3.4.2 to determine the surface morphology of the CFA and synthesised G1. The SEM micrographs of CFA and G1 are presented in Figure 4.16.

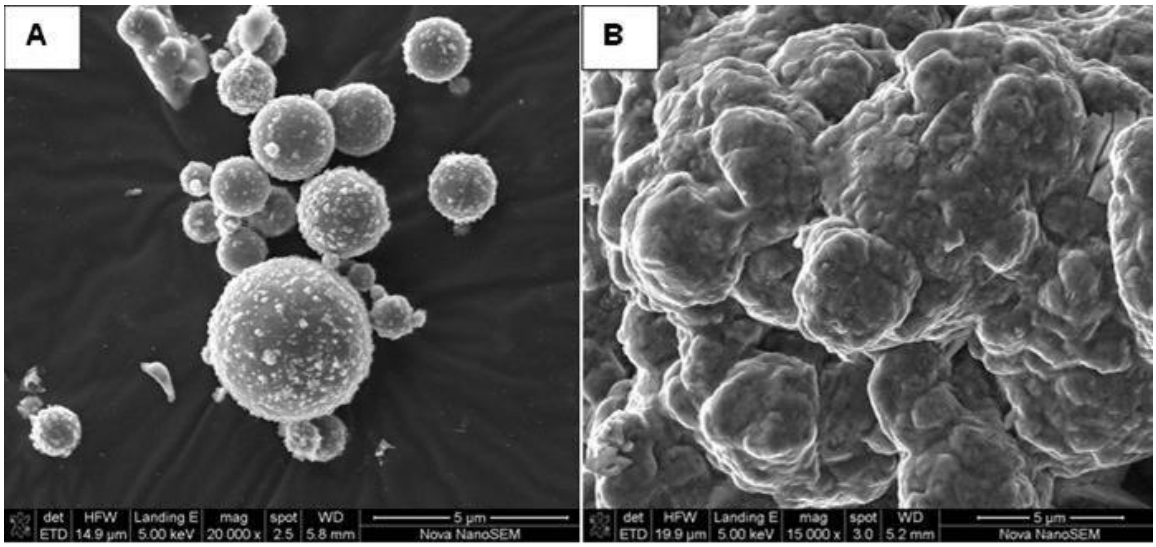

Figure 4.16: SEM images of CFA (A) in comparison with G1 (B) synthesised from the solid waste obtained after extraction of CFASE1-AAT

Figure 4.16 shows the SEM images of CFA (A) and G1 (B). From these micrographs, it was observed that the spherical particles of CFA (A) were polymerised into a bulky mass in G1 (B) under the influence of NaOH at 70 °C for 5 days. However, it can be seen that G1 was not completely polymerised, since small spherical particles of CFA were particularly visible, as shown in the SEM image of G1.

4.5.3. Structural analysis CFA and synthesised G1 using FTIR

The FTIR spectra results for CFA and G1 are presented in Figure 4.17. The FTIR spectrum of CFA was discussed in section 4.4. The spectrum shown in Figure 4.17 reveals that CFA and G1 have some similar bands. The FTIR spectrum of G1 shows bands at 454 cm^{-1}, 562 cm^{-1} and these bands can be assigned to the T-O vibration band and octahedral aluminium of the mullite phase respectively (Saikia and Parthasarathy, 2010).

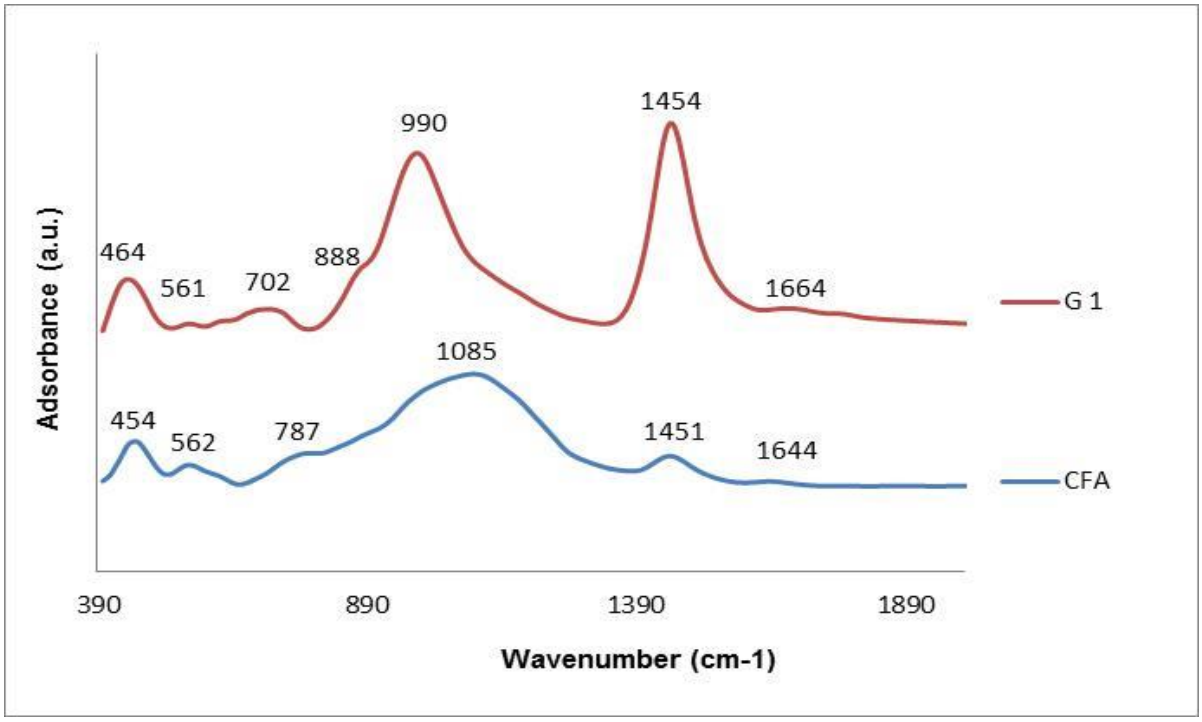

Figure 4.17: FTIR spectra for coal fly ash (CFA) in comparison with geopolymer (G1)

The FTIR spectrum of CFA was discussed in section 4.4. The spectrum shown in Figure 4.17 reveals that CFA and G1 have some similar bands. The FTIR spectrum of G1 shows bands at 454 cm^{-1}, 562 cm^{-1} and these bands can be assigned to the T-O vibration band and octahedral aluminium of the mullite phase respectively (Saikia and Parthasarathy, 2010). The bands at 702 cm^{-1} and 888 cm^{-1} are identified as the analytical wavenumber bands for silica (SiO_2) which represent the bending vibrational mode of the –Si–O–Si– bonds in the polymeric $(SiO_2)n$ molecule (Schiavon, 2007). The band appearing at 990 cm^{-1} can be assigned to the asymmetric stretching vibration Si-O-Al in Q_2 silicon site (Külaviir, 2014, Flanigen *et al*., 1971). Furthermore, a shift in absorption of the band from 1085 cm^{-1} in CFA spectrum to 990 cm^{-1} for G1 was observed.

The same observation was reported by (Nyale *et al*., 2013). The strong band around 1454 cm^{-1} indicates the presence of sodium carbonate (Na_2CO_3) (Tchadjié *et al*., 2016). The absorption band observed at 1664 cm^{-1} can be assigned to the –OH stretching and bending vibration of water molecules, which indicates the presence of weak H_2O bonds present in the solid waste (Tchadjié *et al*., 2016, Palomo *et al*., 1999).

4.5.4. NMR spectroscopy analysis for CFA and G1

This section presents the results of ^{27}Al and ^{29}Si NMR analysis performed for CFA and the synthesised G1.

Figure 4.18 shows the ^{27}Al NMR spectra of CFA and G1. The ^{27}Al NMR of CFA presented in Figure 4.18A shows a major peak of extra-framework aluminium at about 58 ppm and a small hump-like peak of hexacoordinated Al at 0 ppm. The broad peak could indicate various states of Al in amorphous glassy phases of CFA. It can also be seen that an undefined peak at -35 ppm was present in the CFA spectra. The peak at 58 ppm with a broad baseline can be assigned to various tetra-coordinated aluminium (Singh *et al*., 2005). The G2 spectra identified two peaks at 60 ppm and -30 ppm respectively. The resonance shift at 60 ppm is attributed to the fourfold oxygen coordinated aluminium remaining in the framework of the geopolymer (Freude *et al*., 1983). The peak at -30 was unidentified.

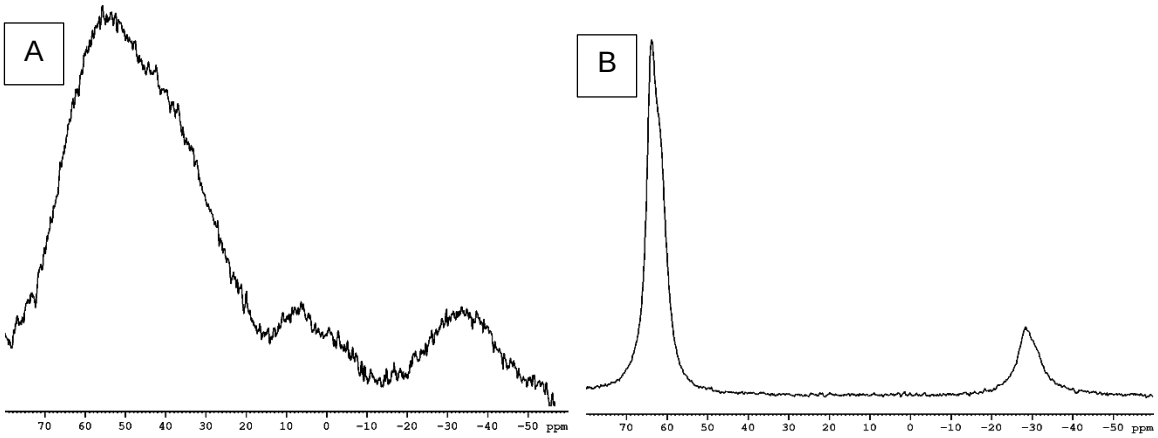

Figure 4.18: ^{27}Al NMR spectra for CFA (A) in comparison with G2 (B)

The ^{29}Si NMR of CFA and G1 is presented in Figure 4.19. The figure shows that the ^{29}Si NMR spectrum of CFA (A) contained a peak at about -110 ppm and this peak corresponds to the Si(1Al) units. The NMR spectra for G1 showed a peak at -90 ppm which correspond to the Si(3Al) units and a peak at -140 ppm that could be associated to the Si(0Al) units (Byrappa and Yoshimura, 2001). The Si(3Al) units identified in the G1 NMR spectra are assumed to be influenced by the extraction silica from CFA, as detailed in Section 3.3.1.1.

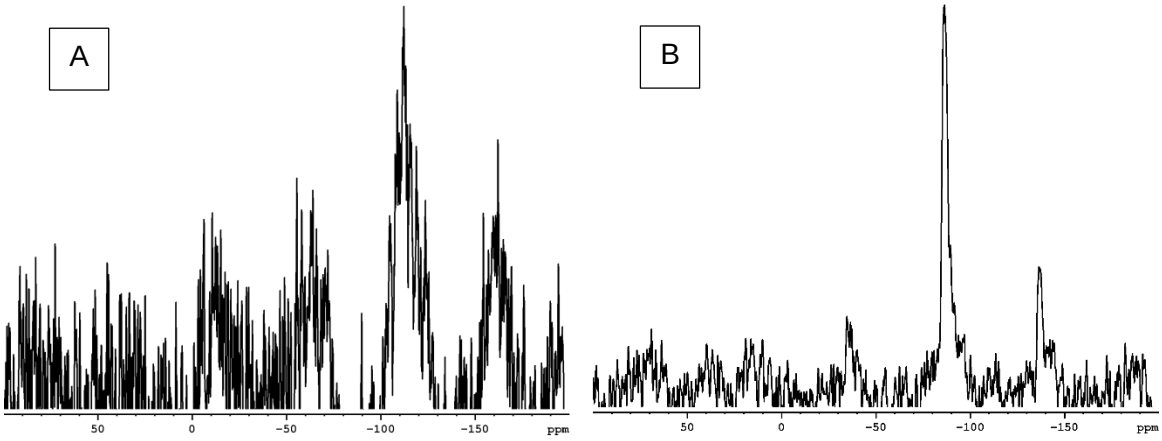

Figure 4.19: ^{29}Si NMR spectra for CFA (A) n comparison with G1 (B)

4.5.5. Mass balance of the geopolymerisation process.

Table 4.3 presents the elemental compositions of geopolymer (G1) that was synthesised from the solid waste obtained after the extraction of CFASE1-AAT from CFA. The G1 was synthesised following the procedure detailed in Section 3.3.1.3.

Table 4.3: Elemental composition of the geopolymer synthesised from the solid waste resulting after the extraction of CFASE1-AAT

Elements (%)	G1
Si	62.31
Al	6.66
Ca	1.87
Fe	6.31
Ti	1.67
Mg	1.05
P	0.33
K	1.49
Na	17.27
Mn	0.17
Cr	0.86
Total	**100.00**

The elemental composition of G1 is presented in Table 4.3. It can be seen from the results that the G1 mainly contains Si which accounted for 62.31% of the total elements in the sample and Na, which accounted for 17.27%. It can also be seen that Al and Fe content were 6.66 and 6.31% in the formed G1 respectively. The Si/Al ratio of the synthesised G1 was 9.4. According to Giannopoulou and Panias (2007), the applications of geopolymers are dependent on the geopolymer structure and the Si/Al ratio. The application of a geopolymer with a Si/Al ratio of 9.4 has not been reported. However, the synthesised G1 was not strong, as some fractures were observed in the final material, and this might be attributed to the high amount of Na (17.27%) in the synthesised geopolymer material.

CHAPTER FIVE

CHARACTERISATION OF ZEOLITE FAUJASITE AND GEOPOLYMER SYNTHESISED FROM COAL FLY ASH

5.1. Introduction

This chapter details the results obtained from Process 2. The process flow diagram for Process 2 is shown in Figure 3.1. Process 2 comprises the extraction of alumina and silica for the synthesis of zeolite faujasite while the resulting solid residue is used for the synthesis of geopolymer. The elemental composition of coal fly ash alumina extracts (CFAAEs) and coal fly ash silica extract before and after oxalic acid (CFASE2-BAT and CFASE2-AAT) extracted from coal fly ash (CFA), as detailed in Sections 3.3.2.1 and 3.3.2.2, are also examined in this chapter. The elemental composition of the CFA extracts was determined by ICP-AES after acid digestion. This is followed by a detailed discussion on the characterisation of zeolite faujasite synthesised from CFAAE and CFASE2-AAT used as the source of alumina and silica respectively. The last part of this chapter details the characterisation of geopolymer synthesised from the solid residue (SR3) obtained after the extraction of CFAAE and CFASE2-AAT.

5.2. Characterisation of coal fly ash extracts

The first part of this section details the elemental composition, XRD and SEM of alumina extracts from coal fly ash. Coal fly ash alumina extracts (CFAAEs) were obtained from coal fly ash by means of an acid leaching process using concentrated sulphuric acid (H_2SO_4). A weighed mass of 30 g of CFA was mixed with 60 mL of concentrated H_2SO_4 (95-99%) and reacted at 250 °C for 6 h. Upon completion, the mixture was filtered. The procedure was repeated four times with fresh CFA samples. Thus, a total starting mass of 120 g (4 X 30 g) of CFA was used for the extraction. The filtrates from all four extractions were poured into a beaker and allowed to stand in order to allow aluminium sulphate ($Al_2(SO_4)_3$) to precipitate. The precipitated aluminium sulphate extracts were recovered in a 24 hour time interval for 96 hours to give 4 batches of extracts coded CFAAE1 (24 h), CFAAE2 (48 h), CFAAE3 (72 h) and CFAAE4 (96 h). CFAAE1, CFAAE2, CFAAE3 and CFAAE4 were dried at 70 °C for 24 h and calcined at 800ºC for 2 h. The CFAAEs were obtained by leaching coal fly ash (CFA) with H_2SO_4, followed by calcination, as detailed in Section 3.3.2.1.

The second part of this section presents the elemental composition of coal fly ash silica extracts obtained from solid residue (SR2) using NaOH, as detailed in Section 3.3.2.2, herein

coded coal fly ash silica extract before oxalic acid treatment (CFASE2-BAT) and coal fly ash silica extract after oxalic acid treatment (CFASE2-AAT).

5.2.1. Elemental composition of coal fly ash alumina extracts (CFAAEs)

A portion of each of the extracts was digested, as described in Section 3.3.1.4, and analysed using ICP-AES in order to determine their elemental composition. The mass percentage of each element was calculated based on a dried mass basis using the equation presented below:

$$\%(i) = \frac{C_i}{C_T} * 100$$

Where i = Si, Al, Ca, Fe, Ti, Mg, P, K, Na, Mn and Cr, C_i = concentration of the element (i) determined by ICP, C_T = Total concentration of the elements present in the coal fly ash extract.

The results for analysis of CFA, CFAAE1, CFAAE2, CFAAE3 and CFAAE4 using ICP are presented in Figure 5.1.

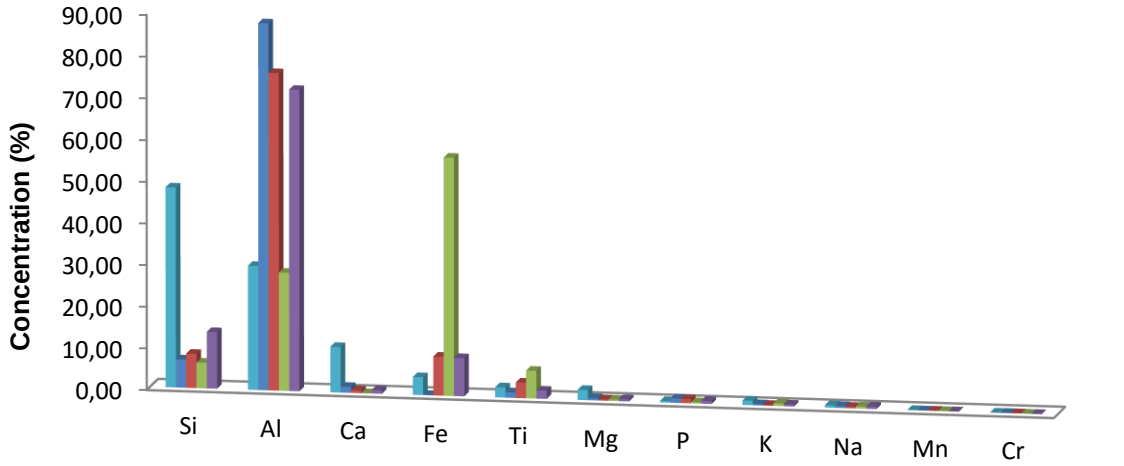

	Si	Al	Ca	Fe	Ti	Mg	P	K	Na	Mn	Cr
CFA	47,91	29,67	10,88	4,27	2,44	2,42	0,37	1,08	0,55	0,06	0,03
CFAAE1	6,74	88,03	1,41	0,08	1,31	0,53	1,04	0,30	0,46	0,05	0,06
CFAAE2	8,18	76,16	0,66	9,31	3,71	0,33	0,98	0,22	0,35	0,05	0,06
CFAAE3	6,12	28,26	0,05	57,11	6,63	0,34	0,31	0,63	0,50	0,04	0,02
CFAAE4	13,53	72,27	0,83	9,12	1,95	0,50	0,71	0,44	0,56	0,05	0,03

Figure 5.1: Elemental composition for coal fly ash (CFA), coal fly ash alumina extracts (CFAAE1, CFAAE2, CFAAE3 and CFAAE4) extracted using H_2SO_4 as the extraction medium

Figure 5.1 only presents the mass percentage of cations present in each sample as the ICP does not analyse anions. The figure showed that the mass percentage of Al in CFA, CFAAE1, CFAAE2, CFAAE3, and CFAAE4 dried extracts was 29.67, 88.03, 76.16, 28.26 and 72.27% respectively. Meanwhile, the mass percentages of Si were 47.91, 6.74, 8.18, 6.12 and 13.53% respectively. It is important to note that the mass percentage of Al was high in CFAAE1 and CFAAE2 at 88.03 and 76.16% respectively, showing the efficiency of Al extraction out of CFA, but decreased to 28.26% in CFAAE3. The mass percentage of Fe in CFAAE1, CFAAE2 and CFAAE3 was 0.08, 9.31 and 57.11% respectively. It can be seen from the results that Fe could only be extracted when the amount of aluminium in solution decreased, as seen in the case of CFAAE3. Therefore, the sequence of precipitation of Al and Fe could be predicted, as Fe precipitated from solution only after the bulk aluminium was precipitated and recovered in CFAAE1 and CFAAE2. It is also noteworthy that the mass percentage of Al in the extract (CFAAE4) increased to 72.27% while that of Si (6.12% in CFAAE3) doubled to 13.52%, while Fe decreased to 9.12% in the sample, showing that the sequence of precipitation of Si, Al and Fe was based on their concentration in the solution.

In this study, the high mass percentage of Al in CFAAE1, CFAAE2 and CFAAE4 showed that concentrated H_2SO_4 was a suitable medium to extract Al from coal fly ash. Based on the ICP results the extraction efficiency of the extracted Al in (CFAAE1, CFAAE2, CFAAE3 and CFAAE4) was calculated using the following formula:

$$\eta = \frac{Mass(Al)_{CFAAE}}{Mass(Al)_{CFA}} * 100$$

Where ŋ is the extraction efficiency.

The extraction efficiency of CFAAE1, CFAAE2, CFAAE3 and CFAAE4 was found to be 34.27, 23.12, 6.99 and 15.03% respectively, and the extraction efficiency totalled to 79.4%. Matjie *et al*, (2005) extracted 85% of Al from South African coal fly ash through calcination of the CFA/CaO mixture at a temperature ranging from 1000 to 1200 °C, followed by leaching of the obtained CFA/CaO mixture using 6.12 mol.dm^{-3} H_2SO_4 for 4 h at 80 °C. Wu *et al*., (2012) extracted 82.4% of Al from a Chinese CFA using 50% concentrated H_2SO_4 for 4 h at 180 °C while stirring. The high Al extraction efficiency of 85% reported by Matjie *et al*, (2005) could have been influenced by the calcination of CFA with calcium oxide at a temperature ranging from 1000 to 1200°C, prior to the leaching. Although the author reported a good extraction efficiency of Al from CFA, the employed method can constitute a barrier for its industrial application, due to the high energy usage. On the other hand, the high extraction efficiency of 82.4% reported by Wu *et al*., (2012) could be due to the stirring component during the Al leaching process; which enables the use of less severe extraction conditions than those

applied in the current study. However, the extracted 79.4% of Al in this study has proven that South African CFA can serve as a source of Al for the synthesis of high purity zeolites. The CFA Al extracts (CFAAE1, CFAAE2, CFAAE3 and CFAAE4) were further used as the source of Al in the synthesis of zeolite faujasite.

5.2.3. Physical appearance of CFAAEs extracts

Figure 5.2 presents the images for CFAAE1, CFAAE2, CFAAE3 and CFAAE4 to show the physical appearance of each extract. The CFA alumina extracts were sampled in a 24 h time interval for 96 h in this sequence: CFAAE1 (24 h), CFAAE2 (48 h), CFAAR3 (72 h) and CFAAE4 (96 h) respectively.

Figure 5.2: Images for the Coal fly ash alumina extracts extracted from CFA using sulphuric acid (H_2SO_4), A (CFAAE1), B (CFAAE2), C (CFAAE3) and D (CFAAE4).

It can be seen from Figure 5.4 that samples A, B, C and D are extracts exhibiting different physical appearances. It is important to note that all four extracts were obtained from the same resultant filtrate recovered after the leaching of CFA with sulphuric acid. Based on intensity

and prior knowledge of the appearance of aluminium species, the physical appearances as presented in Figure 5.2 show that A and B have high concentrations of Al (88.03 and 76.16% respectively) as indicated by the ICP result presented earlier in Figure 5.1. The appearance of extract C is different from A and B, a reddish colour was observed which may be attributed to the high content of Fe in the sample (57.11%). Extract D was yellowish in colour, correlating with the presence of alumina (72.27%) in the sample. These results agree with the ICP results presented in Figure 5.1.

5.2.3. XRD analysis of coal fly alumina extracts (CFAAE1, CFAAE2, CFAAE3 and CFAAE4)

The XRD analysis was performed on each of the alumina extracts to determine the mineral phase present in each sample, as detailed in Section 3.4.4. The XRD patterns for the alumina extracts are presented in Figure 5.3.

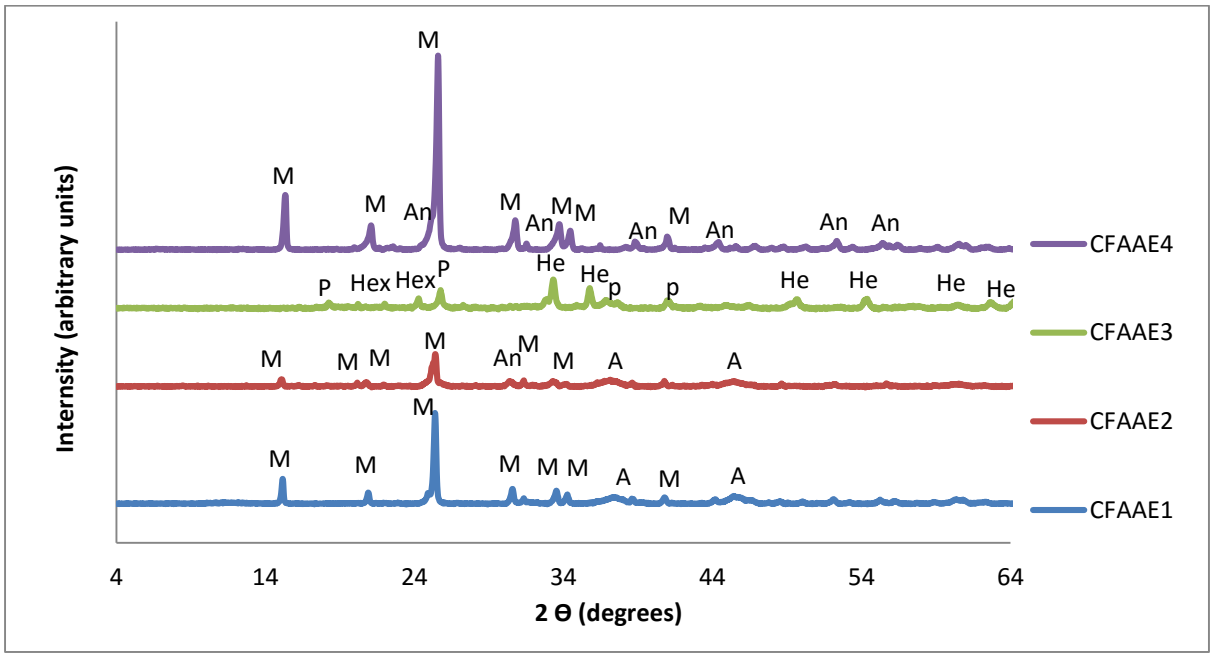

Figure 5.3: XRD patterns for coal fly ash alumina extracts (CFAAE1, CFAAE2, CFAAE3 and CFAAE4) synthesised from coal fly ash using sulphuric acid. Where M = Millosevichite ($Al_2(SO_4)_3$, A = Aluminium Oxide (Al_2O_3), An = Anhydrite ($CaSO_4$), P = Pseudobrookite (Fe_2TiO_5), Hex = Hexahydrate and He = Hematite

Figure 5.3 shows the XRD patterns of (CFAAE1, CFAAE2, CFAAE3, and CFAAE4) that were sampled in 24 h time intervals for 96 h. The XRD results for CFAAE1 correlated with the mineral phase of millosevichite and a trace mineral phase of aluminium oxide.

The presence of millosevichite shows that CFAAE1 was not completely converted to aluminium oxide during the calcination process. It can be seen from the XRD pattern of CFAAE2 that the mineral phases were similar to CFAAE1, with some trace mineral phases of anhydrite. However, it is evident that the peak intensity of the millosevichite reduced in CFAAE2. This could have been caused by the presence of anhydrite in CFAAE2, as shown in Figure 5.1. The XRD pattern of CFAAE3 showed a combination of pseudobrookite (Fe_2TiO_5), magnesium sulphate hexahydrate ($MgSO_4 \cdot 6H_2O$) and hematite (Fe_2O_3).

It was observed that hematite peaks in CFAAE3 had the highest intensity; this was expected, since the concentration of Fe in the CFAAE3 accounted for 57.11 mass% in the feedstock, which was twice the amount of the Al (28.26%).

The XRD pattern of CFAAE3 shows that the sample is mainly dominated by hematite, with some trace mineral phases of pseudobrookite and hexahydrite. These results confirmed the ICP results presented in Section 5.2.1. It can be seen from Figure 5.3 that the XRD pattern of CFAAE4 showed mainly millosevichite and anhydrite peaks. The high intensity peaks of millosevichite in CFAAE4 showed that aluminium was in a sulphate form, which proves that the calcination process was not effective. Therefore, the aluminium sulphates were not completely converted to aluminium oxide. The calcination conditions would need to be optimised, but this fell outside the scope of the study. It can also be seen from the results that the high intensity peak of millosevichite appeared in the region between 20 to 30 2Θ for the CFAAE1, CFAAE2 and CFAAE4. This observation was also reported by Li *et al*, (2011) after leaching of CFA with sulphuric acid.

5.2.4. Elemental composition of solid residue (SR2), coal fly ash silica extract before (CFASE2-BAT) and after (CFASE2-AAT) oxalic acid treatment

Silica was extracted from the solid residue (SR2) using 8 M NaOH solution. The solid residue SR2 was obtained after the extraction of alumina extract (CFAAE) from CFA using H_2SO_4, as detailed in Section 3.3.2.2. The precipitated silica recovered after filtration was dried at 70°C for 24 h, and the dried silica extract was coded as coal fly ash silica extract before oxalic acid treatment (CFASE2-BAT). The obtained CFASE2-BAT was further treated with a saturated oxalic acid solution to reduce the amount of Na present in the extract and also increase the mass percentage of silica, as detailed in Section 3.3.2.2. The elemental composition of SR2, CFASE2-BAT and CFASE2-AAT is presented in Figure 5.4.

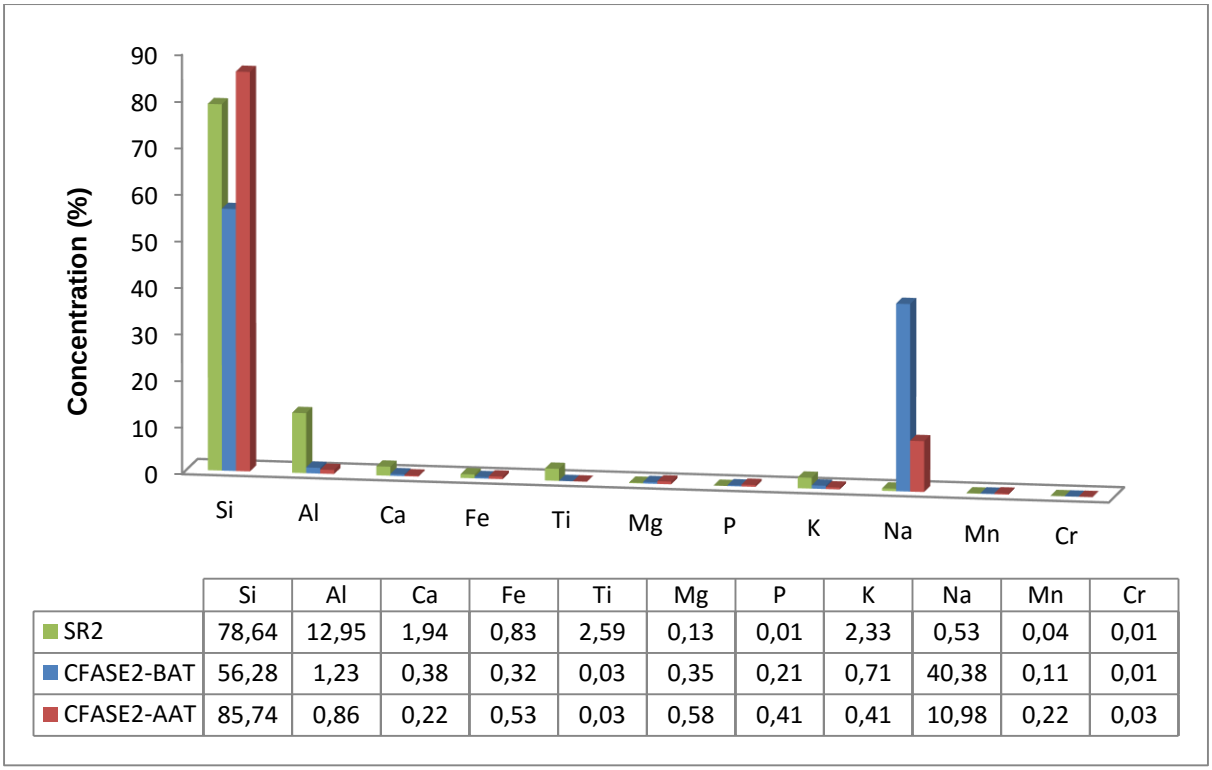

	Si	Al	Ca	Fe	Ti	Mg	P	K	Na	Mn	Cr
SR2	78,64	12,95	1,94	0,83	2,59	0,13	0,01	2,33	0,53	0,04	0,01
CFASE2-BAT	56,28	1,23	0,38	0,32	0,03	0,35	0,21	0,71	40,38	0,11	0,01
CFASE2-AAT	85,74	0,86	0,22	0,53	0,03	0,58	0,41	0,41	10,98	0,22	0,03

Figure 5.4: Elemental composition of dried CFA silica extract before oxalic acid treatment (CFASE2-BAT) and CFA dried silica extract after oxalic acid treatment (CFASE2-AAT) following Process 2.

Figure 5.4 represents the elemental composition of CFASE2-BAT and CFASE2-AAT. From these results, analysis of CFASE2-BAT revealed that Si and Na are the major elements in the dried powder obtained from the alkaline leaching of CFA, with 56.28 and 40.38 mass% respectively. The high mass% of Na in CFASE2-BAT sample can be attributed to the fact that an NaOH solution was used to adjust the pH of the solution to pH 10 in order to selectively recover silica from the solution. The mass percentage of Al coprecipitated was 1.23%, while the mass% of the rest of the elements in CFASE2-BAT was less than 1%, showing that the procedure was highly selective for Si separation, apart from Na contaminant. After the oxalic acid treatment of CFASE2-BAT, an increase in mass% of Si was observed. It can be seen that the mass percentage of Si increased to 85.74%, while that of Na decreased to 10.98%. Sodium is soluble in oxalic acid, hence, the use of saturated oxalic acid dissolved the Na and most of the Na in the silica extract was washed off during filtration. It can also be deduced that the use of saturated oxalic acid was effective to reduce the amount of Na in the final sample. In turn, after Na was reduced, the silica content in the extract increased from 56.23% to 85.74%, providing a high purity of silica.

The extraction efficiency of extracted Si was calculated using the formula presented in Section 4.3.2, and the extraction efficiency was found to be 92.65%. This efficiency is slightly higher

than that presented in Section 4.3.2. This could be due to the extraction of Al prior to the extraction of Si. The treated CFASE2-AAT was subsequently used as the source of silica in the synthesis of zeolite faujasite (FAU1, FAU2, FAU3 and FAU4), as detailed in Section 3.3.2.4.

5.2.5. XRD analysis for SR2, CFASE2-BAT and CFASE2-AAT

The solid residue (SR2) obtained after the extraction of CFAAE was used as a feedstock in the extraction of CFASE2-BAT. The XRD pattern of SR2, CFASE2-BAT and CFASE2-AAT is presented in Figure 5.5.

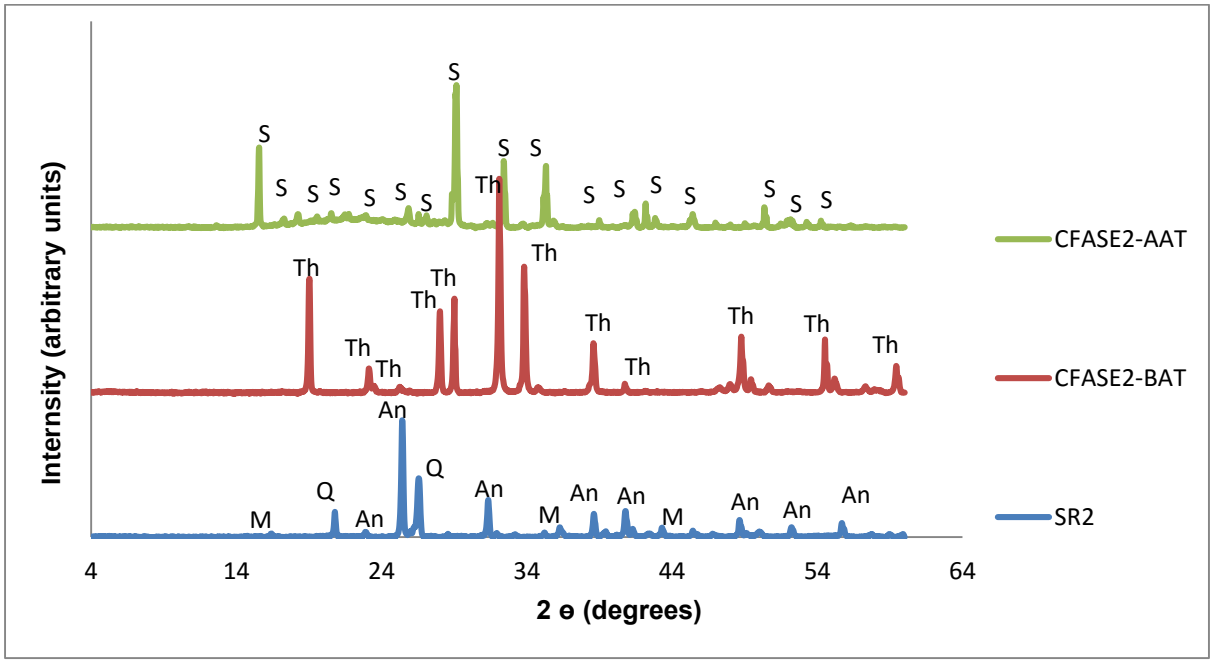

Figure 5.5: XRD pattern for solid residue (SR2) feedstock for the extraction of silica, CFASE2-BAT and CFASE2-AAT. Where S = Sodium Hydrogen Oxalate Hydrate ($C_2HNaO_4 \cdot H_2O$), Th = Thenardite (Na_2SO_4), M = Mullite ($Al_6Si_2O_{13}$), Q = Quartz (SiO_2) and An = Anhydrite ($CaSO_4$).

The XRD patterns for SR2, CFASE2-BAT and CFASE2-AAT are presented in Figure 5.5. It can be seen from the XRD pattern that SR2 was mainly dominated by anhydrite, mullite and quartz. The presence of mullite in the SR2 sample showed that the extraction of alumina using H_2SO_4 did not break all the mullite phases in the sample. The quartz mineral phases in the SR2 sample were expected, since they indicate the presence of silica.

The XRD pattern for CFASE2-BAT showed that the extract was composed of thenardite (Na_2SO_4) which was initiated by the use of NaOH during the extraction of silica from CFA.

The XRD result of CFASE2-BAT confirmed the ICP result in Section 5.2.4, which showed that the Na in CFASE2-BAT sample accounted to 42.86% of the total mass in the extract. It can be seen from the XRD result that the XRD pattern of CFASE2-AAT showed mineral phases of sodium hydrogen oxalate hydrate. The sodium hydrogen oxalate hydrate peaks in the extract occurred as a result of the oxalic acid treatment process during the removal of excess Na in the CFASE2-BAT extract. The absence of thenardite mineral phases in the CFASE2-AAT showed that the treatment of CFASE2-AAT with oxalic acid was efficient.

5.2.6. FTIR analysis for SR2, CFASE2-BAT and CFASE2-AAT

The FTIR spectra for SR2, CFASE2-BAT and CFASE2-AAT was analysed as described in Section 3.4.2. The FTIR spectra of these materials are presented in Figure 5.6.

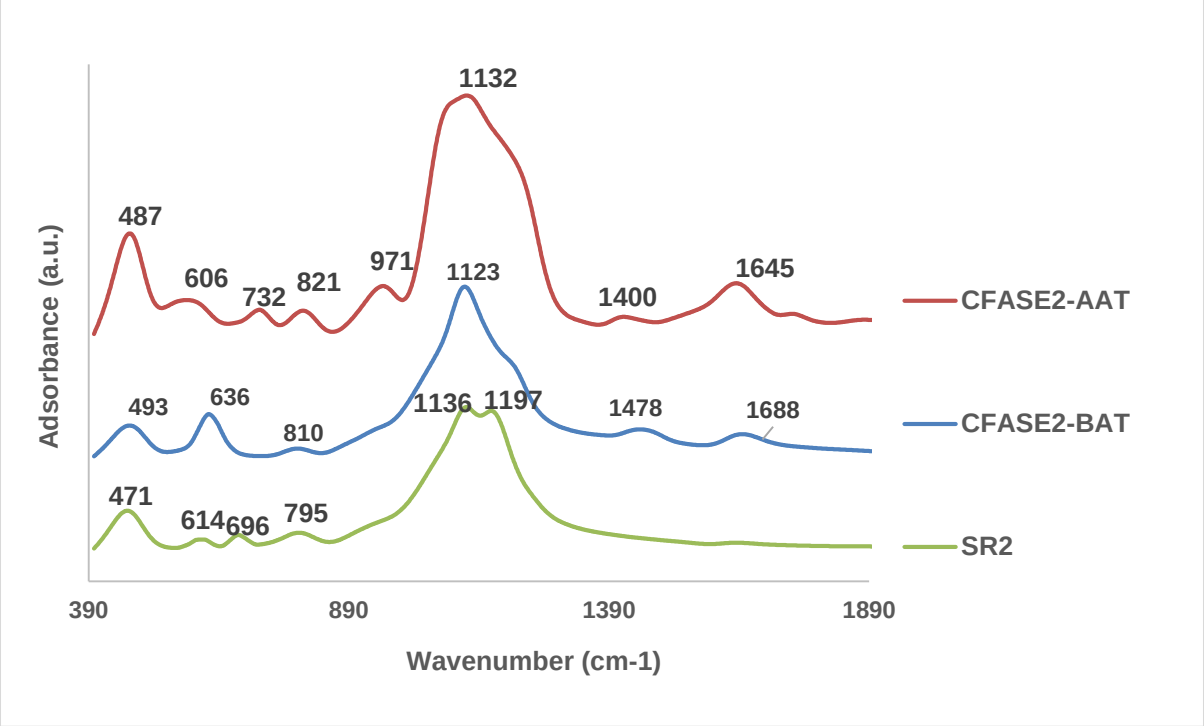

Figure 5.6: FTIR spectra for SR2, CFASE2-BAT and CFASE2-AAT extracts.

The FTIR spectrum of solid residue (SR2) showed some characteristic bands of aluminosilicates. The band appearing at 471 cm^{-1} could be assigned to the Si-O-Si or O-S-O bending vibration, the bands appearing at 614 and 696 cm^{-1} could be assigned to the asymmetric stretching vibration bend of Si-O or Al-O (Lee and Van Deventer, 2003). The band at 795 cm^{-1} could be assigned to the stretching vibration of the Al-O bands with aluminium ions in four-fold co-ordinated (Aronne *et al*., 1997). The bands at 1136 and 1197 cm^{-1} could be

associated with a silicon centre that is bonded to four other T atoms through oxo-bridges (Böke *et al*., 2015). It can be seen from these results that the SR2 samples were rich in silica and alumina. The FTIR spectrum of CFASE2-BAT showed four bands which are a characteristic of aluminosilicates. The band appearing at 493 cm^{-1} could be assigned to Si-O bending vibration, the adsorption bands appearing at 636 and 810 cm^{-1} are a characteristic of symmetric stretching vibration bend of Si-O or Al-O (Lee and Van Deventer, 2003). The band at 1123 cm^{-1} could be associated with a silicon centre that is bonded to four other T atoms through oxo-bridges (Böke *et al*., 2015). Two non-aluminosilicate peaks were identified in the region 1478 and 1688 cm^{-1} of CFASE2-BAT. In the FTIR spectrum, the peak at 1478 cm^{-1} could be associated with the carbonate, while that appearing at 1688 cm^{-1} can be assigned to the O-H deformation of water (Saikia and Parthasarathy, 2010). The FTIR spectrum of CFASE2-AAT showed six aluminasilicate bands appearing at 487, 606, 732, 821, 971 and 1132 cm^{-1} respectively. The adsorption band at 487 can be assigned to Si-O-Si or O-Si-O bending vibration, and the bands appearing at 606, 732 and 821 cm^{-1} are a characteristic of symmetric stretching vibration bend of Si-O or Al-O (Lee and Van Deventer, 2003). The band at 971 cm^{-1} could be associated with a silicon centre that is bonded to two other T atoms through oxo-bridges, while the band appearing at 1132 cm^{-1} could be associated with a silicon centre that is bonded to four other T atoms through oxo-bridges (Böke *et al*., 2015). And as in the case of CFASE2-BAT two non-aluminosilicate bands were observed for the CFASE2-AAT FTIR spectrum, the bands were identified at 1400 and 1645 cm^{-1}. The band at 1400 cm^{-1} could be associated with the carbonate, while that appearing at 1645 cm^{-1} could be assigned to the O-H deformation of water (Saikia and Parthasarathy, 2010). It can be seen from the FTIR result that the treated CFASE2-AAT revealed more peaks, which is a characteristic of aluminosilicate. The treated CFASE2-AAT would therefore be used as source silica in the synthesis of zeolite faujasite.

5.3. Characterisation of zeolite faujasite synthesised from coal fly ash alumina extracts (CFAAEs) and coal fly ash silica extract after oxalic acid treatment (CFASE2-AAT)

The dried extracts of CFAAE and CFASE2-AAT were used as the source of alumina and silica respectively in the synthesis of zeolite faujasite, as described in Section 3.3.2.4. The molar regime used in this study ($4.2Na_2O$: $1Al_2O_3$: $3SiO_2$:$180H_2O$) to prepare faujasite was adapted from Htun *et al*. (2012) with slight modifications. The hydrothermal temperature was optimised to reduce the energy input into the zeolite synthesis process. The molar regimes used in this study were calculated based on the alumina and silica content in the CFAAE and CFASE2-

AAT extracts. The obtained optimum conditions were employed in the synthesis of zeolite faujasite (FAU1, FAU2, FAU3 and FAU4). The results for characterisation of the precursors and the synthesised zeolite faujasite (FAU1, FAU2, FAU3 and FAU4) are presented in the subsections below.

5.3.2. Optimisation of the synthesis of zeolite faujasite using CFAAE1 and CFASE2-AAT

Zeolite faujasite was synthesised from CFAAE1 (dried coal fly ash alumina extract obtained by H_2SO_4 leaching methods) and CFASE2-AAT (coal fly ash silica extract obtained by alkaline extraction methods) following the experimental procedure detailed in Section 3.3.2.4. For the synthesis of zeolite faujasite: CFAAE1, CFASE2-AAT, NaOH and H_2O were mixed to get the molar ratio of 1Si: 1.1Al: 8.6Na: 102.7H_2O. The mixture was aged at room temperature for 3 h, and the resulting mixture was subjected to hydrothermal treatment at different temperatures (80, 90 and 100ºC) for 6 h. The zeolite product obtained was filtered and dried at 70ºC for 24 h. XRD analysis of the products was carried out. The XRD results for CFASE2-AAT, CFAAE1 and the zeolite products synthesised at different temperatures (80, 90 and 100ºC) from the same molar regime are presented in Figure 5.5.

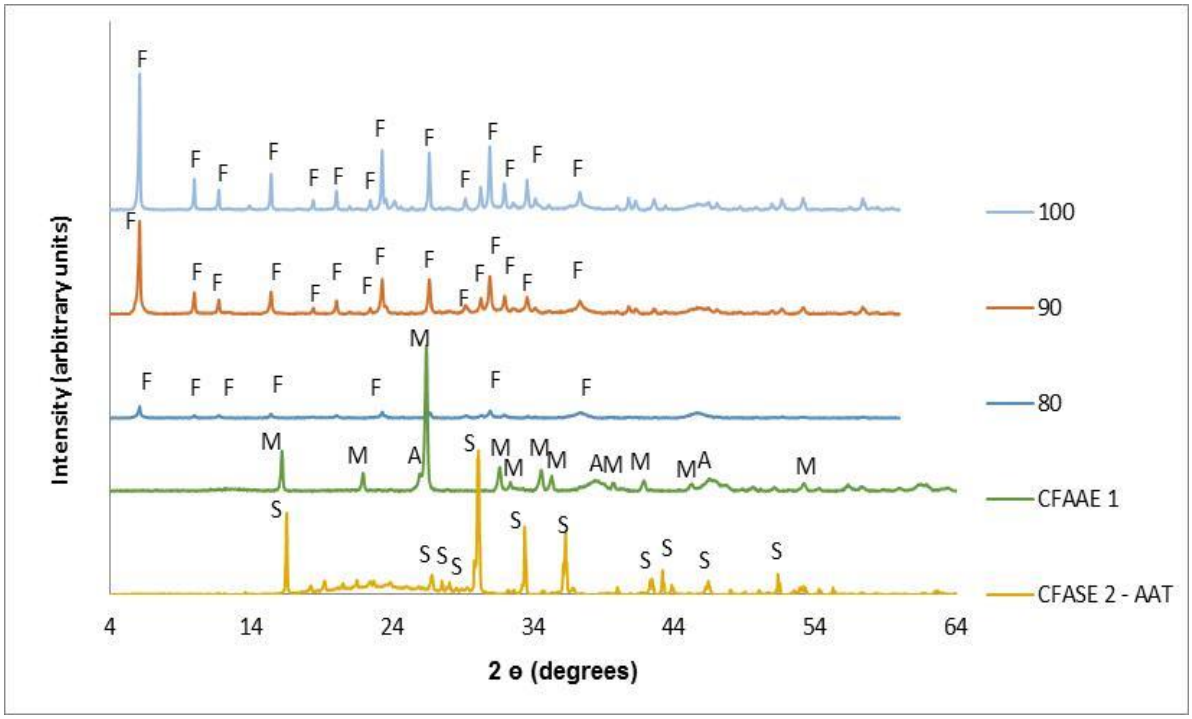

Figure 5.5: XRD patterns for CFAAE1, CFASE2-AAT and zeolite faujasite synthesised at different synthesis temperature (80, 90 and 100˚C). Where S = Sodium Hydrogen Oxalate Hydrate, M = Millosevichite, A = Aluminium Oxide, and F = Faujasite.

The XRD patterns for CFAAE1 and CFASE2-AAT were discussed in Sections 5.2.3 and 5.2.5 respectively. The XRD pattern results presented in figure 5.5 showed that a pure phase zeolite faujasite was obtained in each case after hydrothermal synthesis at 80, 90 and 100˚C for 6 h. It is important to note that, even though a pure phase zeolite faujasite was synthesised under these conditions, the intensity of the zeolite peaks increased with an increase in the hydrothermal temperature. The highest intensity peaks for the synthesised zeolite faujasite were attained at 100˚C. The condition which led to high zeolite peak intensity was chosen as the best condition and was employed to synthesise other zeolite faujasite products in this study. Molina and Poole (2004), synthesised zeolite faujasite (X type) from CFA using the fusion method, followed by a hydrothermal synthesis at 90˚C. Htun *et al*, (2012) successfully synthesised zeolite NaX, faujasite from hydrogel solution by using pure silica powder, aluminium hydroxide, sodium hydroxide and distilled water precursors under hydrothermal conditions at atmospheric pressure. The results obtained showed that it was possible to synthesise pure phase zeolite faujasite from coal fly ash extracts (CFAAE1 and CFASE2-AAT) without fusion in a process analogous to the pure chemical route, as shown in Figure 5.5.

5.3.3. XRD analysis of the synthesised zeolites FAU1, FAU2, FAU3 and FAU4

This section compares the XRD patterns of coal fly ash silica extract after oxalic acid treatment (CFASE2-AAT), alumina extracts (CFAAE1, CFAAE2, CFAAE3 and CFAAE4), as well as their respective synthesised zeolite products: FAU1, FAU2, FAU3 and FAU4. The zeolite products were synthesised using different molar regimes of (1Si: 1.1Al: 8.6Na: 102.7H_2O, 1Si: 1.1Al: 8.2Na: 101.1H_2O, 1Si: 1.1Al: 7.9Na: 96.2H_2O and 1Si: 1.1Al: 7.9Na: 97.4H_2O) respectively, based on the variation in the composition of the alumina extracts. The respective zeolite products were synthesised hydrothermally at 100°C for 6 h. The mineral phases present in the CFASE2-AAT, CFAAEs and the synthesised zeolite products (FAU1, FAU2, FAU3 and FAU4) are presented in the sub-sections below.

5.3.3.1. XRD analysis for zeolite FAU 1

Zeolite faujasite was synthesised from CFASE2-AAT and CFAAE1 extracts obtained from CFA. CFASE2-AAT and CFAAE1 were mixed with NaOH and H_2O to get a molar ratio of 1Si: 1.1Al: 8.6Na: 102.7H_2O. The mixture was aged for 3 h at room temperature, and thereafter subjected to hydrothermal synthesis at 100°C for 6 h. The zeolite product (FAU1) was recovered by filtration and dried at 70°C for 24 h. The dried FAU1 was analysed by XRD to determine the mineral phase present in the zeolite product. The XRD patterns of FAU1 and that of its precursors CFAAE1 and CFASE2-AAT are presented in Figure 5.6.

Figure 5.6 showed that a high crystalline pure phase of zeolite FAU1 could be synthesised from CFASE-AAT and CFAAE1, as discussed in Section 5.3.1. The XRD pattern for CFAAE1 and CFASE2-AAT was also discussed in Section 5.2.3 and 5.2.5 respectively. It was shown that the XRD pattern of CFAAE1 was mostly dominated by the millosevichite ($Al_2(SO_4)_3$) and trace mineral phase of aluminium oxide (Al_2O_3). The presence of millosevichite mineral phase showed that the calcination process for the CFAAE1 was not complete; and most of the aluminium was not converted to the oxide form. However, it is important to note that pure phase zeolite FAU1 was synthesised from the CFA extracts (CFAAE and CFASE2-AAT).

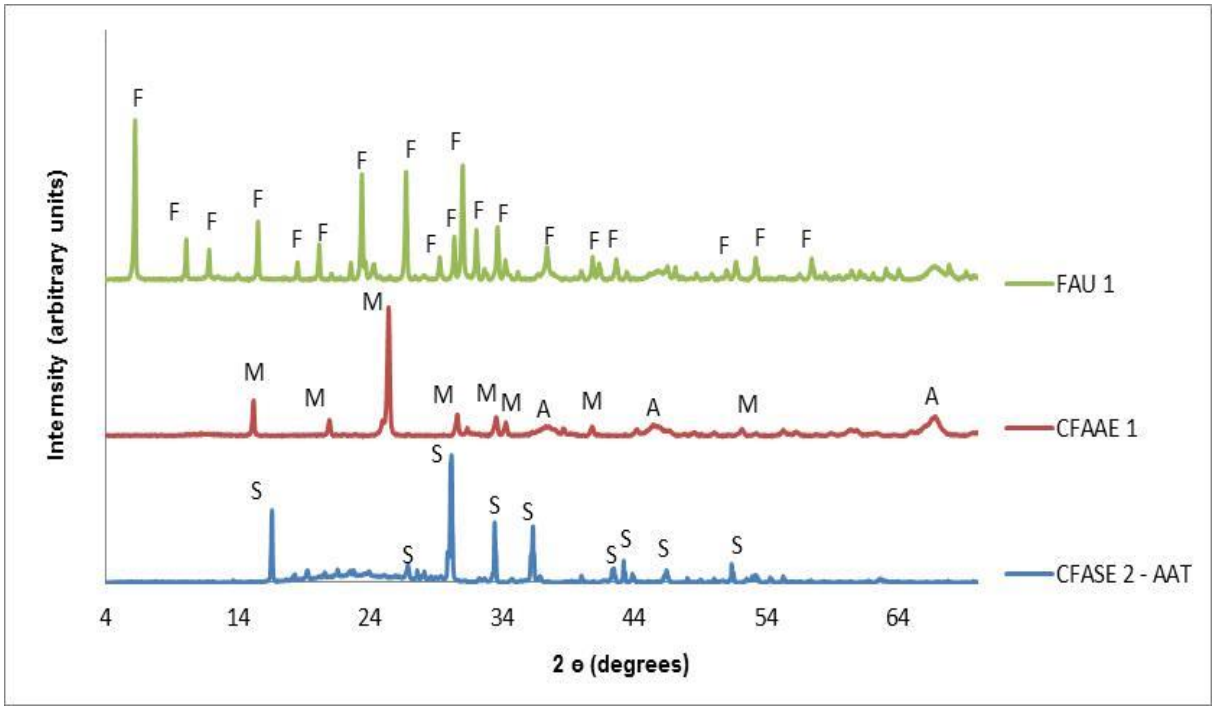

Figure 5.6: XRD patterns for zeolite Faujasite (FAU 1) synthesised from coal fly ash alumina extract (CFAAE1) and coal fly ash silica extract (CFASE 2-AAT). Where S = Sodium Hydrogen Oxalate Hydrate, M = Millosevichite, A = Aluminium Oxide, and F = Faujasite.

5.3.3.2. XRD analysis of zeolite FAU 2

Zeolite FUA2 was synthesised from CFAAE2 and CFAASE2-AAT extracts, obtained from acid and alkaline leaching of CFA respectively. To synthesise zeolite FAU2, a mixture of CFAAE2-AAT, CFAAE2, NaOH and H_2O was prepared to get a molar ratio of 1Si: 1.1Al: 8.2Na: 101.1H_2O. The prepared mixture was aged at room temperature for 3 h, and thereafter underwent a hydrothermal synthesis at 100°C for 6 h. The resulting zeolite product was recovered by filtration and dried at 70°C for 24 h. The obtained zeolites FAU2, CFASE2-AAT

and CFAAE2 were analysed using XRD to determine their mineral phase. The XRD patterns are presented in Figure 5.7.

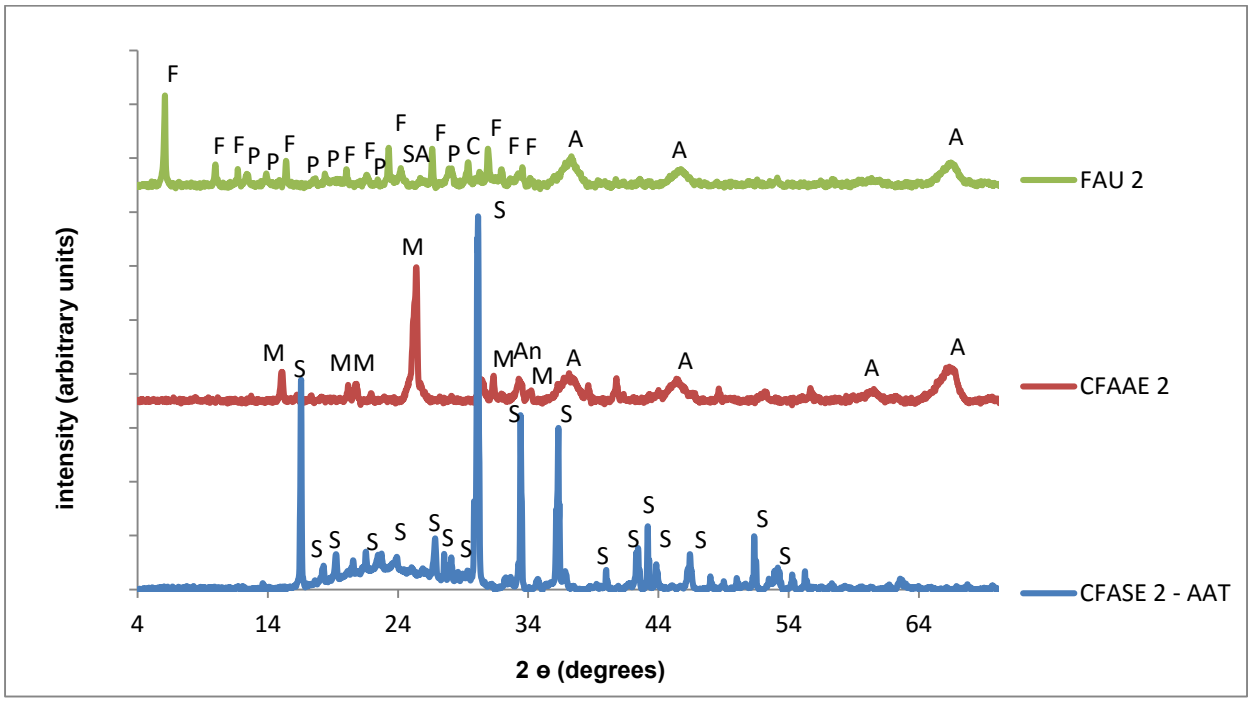

Figure 5.7: XRD patterns for zeolite faujasite (FAU 2) synthesised from coal fly ash alumina extract (CFAAE1) and coal fly ash silica extract (CFASE2-AAT). Where S = Sodium Hydrogen Oxalate Hydrate, M = Millosevichite, A = Aluminium Oxide, An = Anhydrite, P = Phillipsite, C = Calcite, F = Faujasite and SA = Sodium Aluminium Silicate Hydrate.

Zeolite FAU2 and FAU1 were synthesised using the same silica starting material (CFASE2-AAT). The XRD patterns of CFAAE2 and CFASE2-AAT were discussed in Section 5.2.3 and 5.2.5 respectively. The XRD pattern of FAU2 showed that zeolite FAU2 was mixed with other mineral phases, namely Faujasite, phillipsite ($(K,Na)_2(Si,Al)_8O_{16}\cdot 4H_2O$), sodium aluminium silicate hydrate and calcite ($Ca(CO_3)$) mineral phases. It was noteworthy that the hydrothermal gel of FAU1 and FAU2 had very similar molar regimes of 1Si: 1.1Al: 8.6Na: 102.7H_2O and 1Si: 1.1Al: 8.2Na: 101.1H_2O respectively. Figure 5.5 and 5.6 showed a pure phase of zeolite FAU1, and in contrast, Figure 5.7 showed a zeolite (FAU2) with a mixture of other mineral phases. The XRD pattern of FAU2 shows some mineral phase of aluminium oxide, which was also present in the feedstock (CFAAE2). This shows that not all the Al in CFAAE2 was completely converted into zeolite FAU2. The incomplete conversion of Al in CFAAE2 into zeolite FAU2 might have been caused by the applied synthesis conditions. It could be assumed that the optimisation of zeolite synthesis using different alumina extracts (CFAAE1, CFAAE2, CFAAE3

and CFAAE4) was necessary, since the mass composition and mineral phase of the extracts differs.

5.3.3.3. XRD analysis of zeolite FAU3

CFASE2-AAT and CFAAE3 were used as sources of silica and alumina respectively. Zeolite FAU3 was synthesised by mixing CFASE2-AAT, CFAA3, NaOH and H_2O to get a molar ratio of 1Si: 1.1Al: 7.9Na: 96.2H_2O. The obtained mixture was aged at room temperature for 3 hours, and thereafter underwent a hydrothermal synthesis at 100°C for 6 h. The zeolite product was recovered by filtration and dried at 70°C for 24 h. XRD analysis was used to identify the mineral phases present in CFAAE3 and FAU3. The XRD pattern of zeolite product (FAU3) and its starting materials CFAAE3 and CFASE2-AAT are presented in figure 5.8.

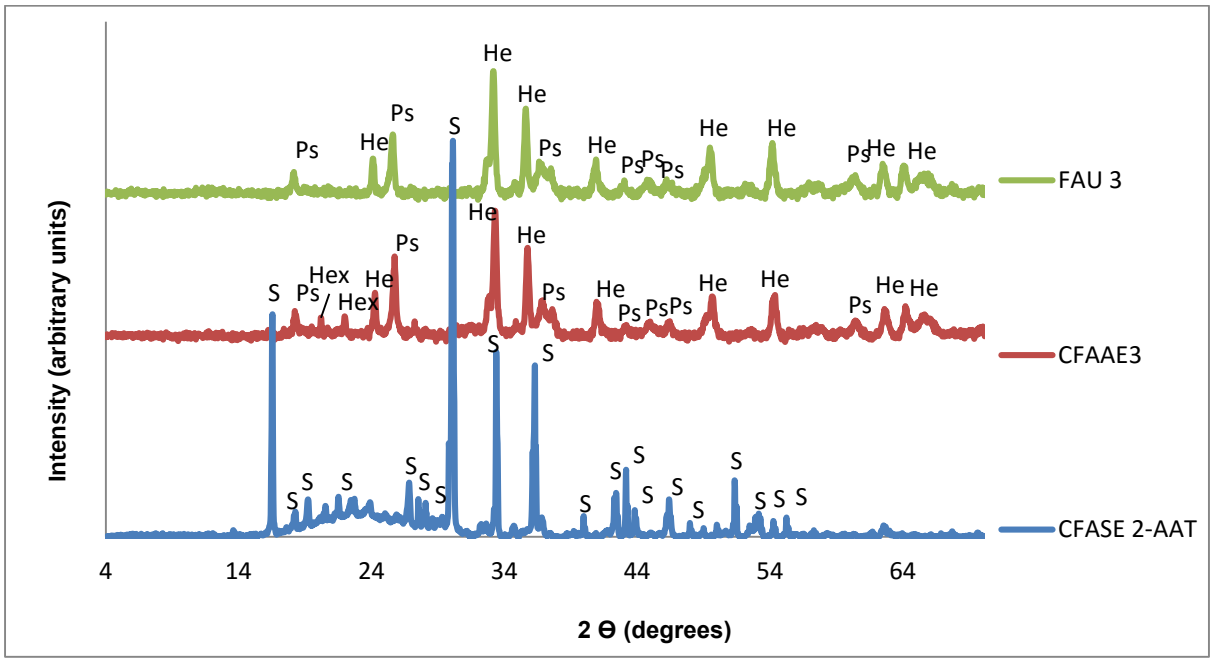

Figure 5.8: XRD pattern for zeolite Faujasite (FAU 3) synthesised from coal fly ash alumina extract (CFAAE3) and coal fly ash silica extract (CFASE2-AAT). Where S = Sodium Hydrogen Oxalate Hydrate, Ps = Pseudobrookite, Hex = Hexahydrite and He = Hematite.

Figure 5.8 presents the XRD pattern of CFASE2-AAT, CFAAE3 and zeolite product (FAU3). The XRD analysis of CFAAE3 and CFASE2-AAT has been discussed previously, in Section 5.2.3 and 5.2.5 respectively. It can be seen from Figure 5.8 that CFASE2-AAT and CFAAE3 were not converted to the targeted zeolite FAU3. The synthesised products (FAU3) showed the same mineral phases as those appearing on the XRD pattern of CFAAE3. However, the hexahydrate ($MgSO_4 \cdot 6H_2O$) peaks appearing on the CFAAE3 pattern were not identified in

the FAU3 pattern, which means that this phase dissolved during the hydrothermal synthesis process.

Although Fe is regarded as a zeolite contaminant, the literature has shown that it could be used to isomorphously substitute Al in the zeolite framework structure to produce materials with specific catalytic properties which can be used in oxidation and hydroxylation reactions (Ali *et al*., 2009, Aiello *et al*., 2005). However, as shown in the XRD result, the high Fe content in CFAAE3 extract prevented the formation of zeolite faujasite.

5.3.3.4. XRD analysis of zeolite FAU4

CFA extracts CFASE2-AAT and CFAAE4 were used as sources of silica and alumina in the synthesis of zeolite FAU4. A mixture with a molar regime of 1Si: 1.1Al: 7.9Na: 97.4H_2O was prepared and the synthesis of FAU4 is as described in section 5.3.3. The XRD patterns of CFASE2-AAT, CFAAE4 and the synthesised zeolite product (FAU4) are presented in figure 5.9.

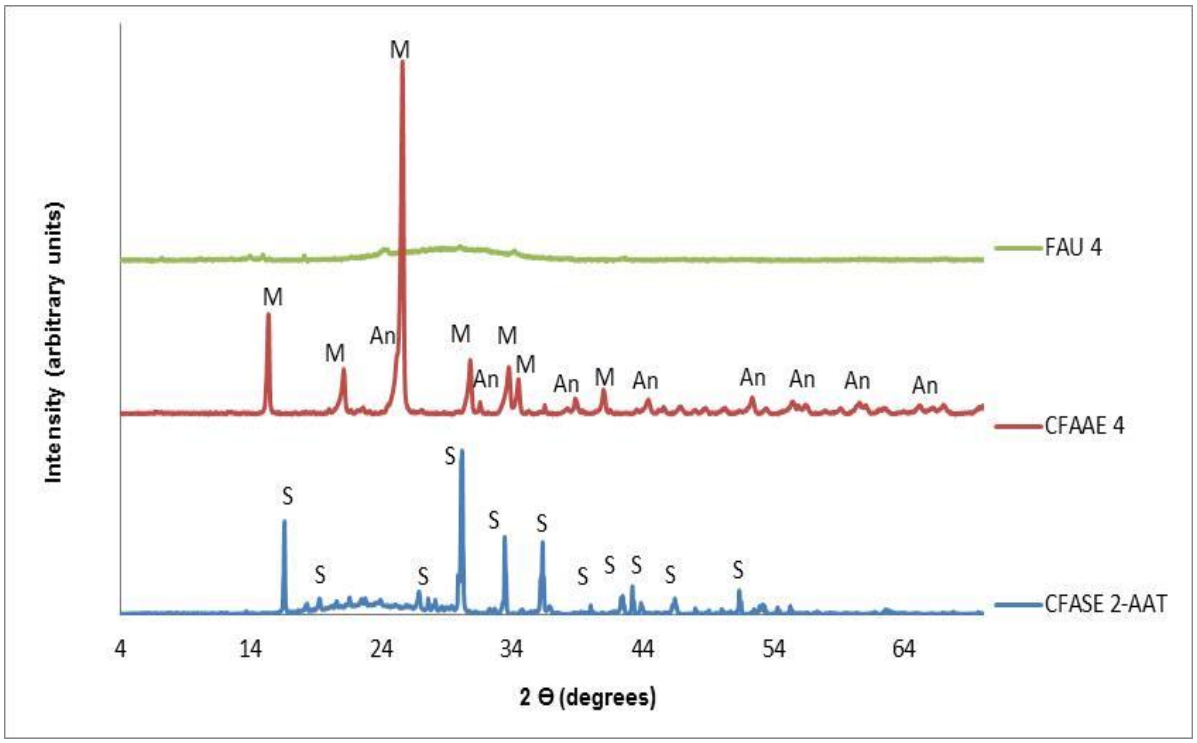

Figure 5.9: XRD patterns of the product (FAU 4) synthesised from coal fly ash alumina extract (CFAAE4) and coal fly ash silica extract (CFASE 2-AAT). Where S = Sodium Hydrogen Oxalate Hydrate, An = Anhydrite and M = Millosevichite.

The XRD patterns of CFAAE4 and CFASE2–AAT are discussed in section 5.2.3 and 5.2.5 respectively. It can be seen from the CFASE2-AAT and FAU4 patterns that there was a shift of the amorphous hump from 16 to 25º 2Θ in the CFASE2-AAT to 18 to 34º 2Θ in the FAU4 sample. It is also evident from the XRD spectra that CFASE2-AAT and CFAAE4 did not react to form a crystalline zeolite FAU4 under the applied conditions. It is therefore assumed that the mineral peaks (sodium hydrogen oxalate hydrate, anhydrite and millosevichite) in CFASE2-AAT and CFAAE4 dissolved in the zeolite precursor mixture and were washed off during the washing process after the synthesis. The peaks, therefore, do not show on the FAU4 pattern, except for the amorphous hump which indicates the presence of silica. From these results, it could be concluded that the zeolite product (FAU4) was not formed when CFAAE4 was used as the source of aluminium. This in part, may be due to the high Fe content (9.12 mass%) in the feedstock, and the presence of sulphates and anhydrite mineral phases (as shown in the XRD pattern). The presence of millosevichite in the CFAAE4 indicates that the calcination process of the feedstock was not complete. These results show that there was very little aluminium oxide in the extracts to initiate the formation of zeolite; hence only amorphous silica was revealed in the FAU4 XRD pattern.

The XRD results presented in Sections 5.3.3.1 and 5.3.3.2 show that CFAAE1, CFAAE2 and CFASE2-AAT can be successfully used as sources of alumina and silica respectively in the syntheses of zeolite products (FAU1 and FAU2). It is also shown that the CFAAE2 and CFASE2-AAT resulted in a mixed phase zeolite FAU2 as shown in Figure 5.7. CFAAE3 and CFAAE4 cannot be used in the synthesis of zeolite faujasite, as indicated in Section 5.3.3.3 and 5.3.3.4. As discussed in Section 5.3.3.3, the high Fe content in CFAAE3 limited the use of the extract as the source of alumina for the synthesis of zeolite faujasite. It was also shown that CFAAE4 contained mainly anhydrate and millosevichite, which prevented its use in the synthesis of zeolite faujasite. It is therefore important to optimise the conditions used for the calcination process in order to ensure complete conversion of $Al_2(SO_4)_3$ to Al_2O_3 in CFAAEs. These results have shown that even though CFAAE1 and CFAAE2 contained mainly $Al_2(SO_4)_3$, they contained trace mineral phases of Al_2O_3, which initiated the synthesis of zeolite faujasite, as shown in Figure 5.6 and 5.7. For this reason it was concluded that further characterisation of the zeolite products would be performed only on zeolite FAU1 and FAU2.

5.3.4. Scanning electron microscope (SEM) analysis for zeolite (FAU1 and FAU2), CFAAE1, CFAAE2 and CFASE2-AAT

This section presents the surface morphology of coal fly ash alumina extracts (CFAAE1 and CFAAE2), coal fly ash silica extract after oxalic acid treatment (CFASE2-AAT) and the synthesised zeolites FAU1 and FAU2. The SEM imaging results, which reveal the nature of the surface morphology of the extracts and the zeolites, is presented in the sub-sections below.

5.3.3.1. SEM for zeolite faujasite FAU 1

Zeolite FAU1 was synthesised using CFAAE1 and CFASE2-AAT as the source of alumina and silica respectively. SEM was used to analyse the surface morphology of CFAAE1, CFASE2-AAT and the synthesised FAU1. The SEM micrographs of the products are presented in Figure 5.10.

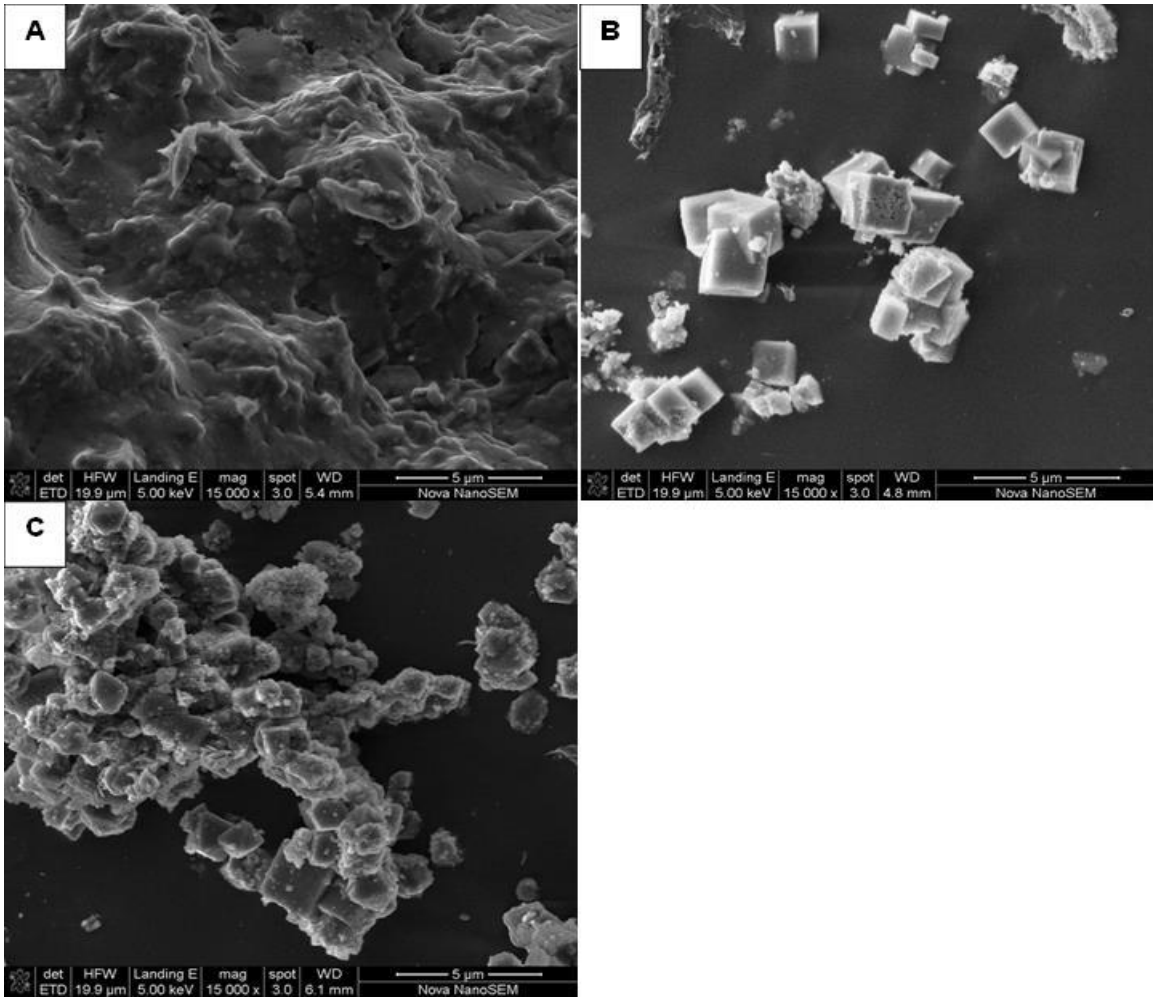

Figure 5.10: SEM micrographs of (A) CFASE2-AAT, (B) CFAAE1 and (C) FAU1.

CFAAE1 and CFASE2-AAT were used as the source of alumina and silica respectively during the hydrothermal synthesis of zeolite FAU1. It can be seen from Figure 5.10 (A) that CFASE2-AAT revealed an amorphous glassy phase. This was confirmed by the XRD, as presented in Figure 5.6. Figure 5.6 (B) shows dispersed cubic aluminium sulphate ($Al_2(SO_4)_3$) crystals that were formed after drying of the CFAAE1 extract. This result confirmed the XRD pattern of CFAAE1 presented earlier in Figure 5.6, where $Al_2(SO_4)_3$ was the dominant mineral phase in the extract. The cubic crystals of $Al_2(SO_4)_3$ in CFAAE1 also confirm the results obtained by Li *et al*, (2011), where CFA was leached with sulphuric acid to extract $Al_2(SO_4)_3$. Furthermore, the morphology of zeolite FAU1, as shown in Figure 5.6 (C), displays the typical octahedral crystals which are characteristic of zeolite faujasite. A similar observation was reported by Thuadaij and Nuntiya, (2012).

5.3.3.2. SEM for zeolite faujasite FAU 2

The surface morphologies of FAU2, CFAAE2-AAT, CFASE 2 were analysed using SEM. The SEM micrographs of the products are presented in Figure 5.11.

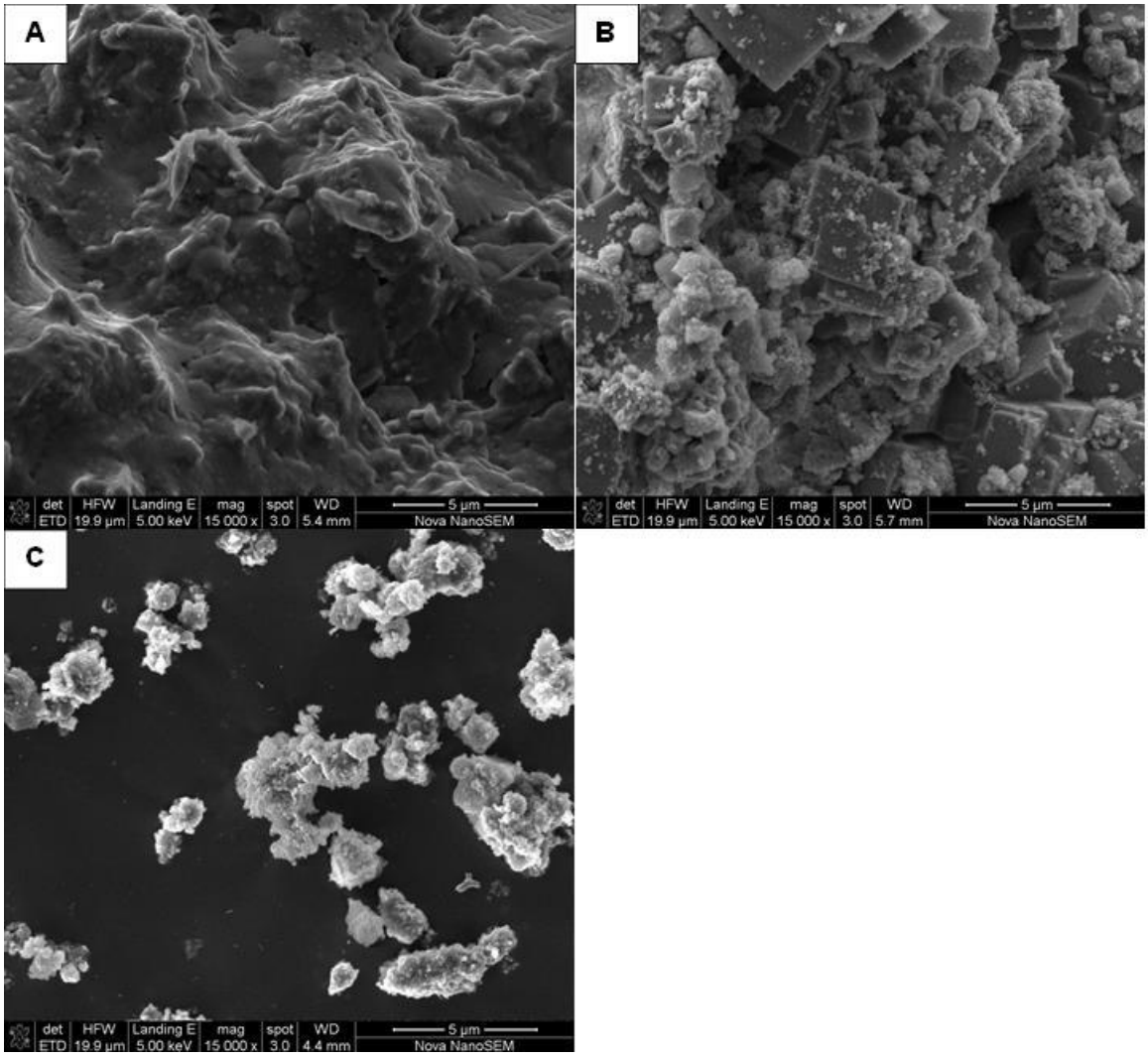

Figure 5.11: SEM micrographs of CFASE2-AAT (A), CFAAE2 (B) and FAU2 (C)

The source of silica (CFASE2-AAT) for the synthesis of zeolite FAU2 was the same as that used in the synthesis of zeolite FAU1, as discussed in Section 5.3.2.1. In Figure 5.11 (B), CFAAE2 shows cubic particles of $Al_2(SO_4)_3$ and Al_2O_3 with some impurities of $CaSO_4$. This interpretation was confirmed from the XRD results presented in Figure 5.7. The SEM of zeolite FAU2 contained octahedral crystals, which are characteristic of zeolite faujasite. The octahedral crystals of zeolite FAU2 were mixed with unreacted aluminium oxide from the CFAAE2 and some mixed phases of phillipsite and calcite. The presence of this impurity is confirmed by the XRD results (Figure 5.7).

5.3.5. Fourier transform infrared (FTIR) for CFA extracts and zeolites FAU1 and FAU2

FTIR analysis was performed on coal fly ash alumina extracts (CFAAE1 and CFAAE2), coal fly ash silica extract after oxalic acid treatment (CFASE2-AAT) and zeolite faujasite (FAU1 and FAU2), synthesised following the procedure detailed in Section 3.4.3. The determination of functional moieties and structural analysis of these materials is presented in the sub-sections below.

5.3.4.1. FTIR analysis for zeolite FAU 1

The FTIR analysis was carried out as described in Section 3.4.3 in order to determine the moieties of the structural configuration of FAU1 in comparison with CFAAE1 and CFASE2-AAT. The FTIR spectra of FAU1, CFAAE1 and CFASE2-AAT are presented in Figure 5.12.

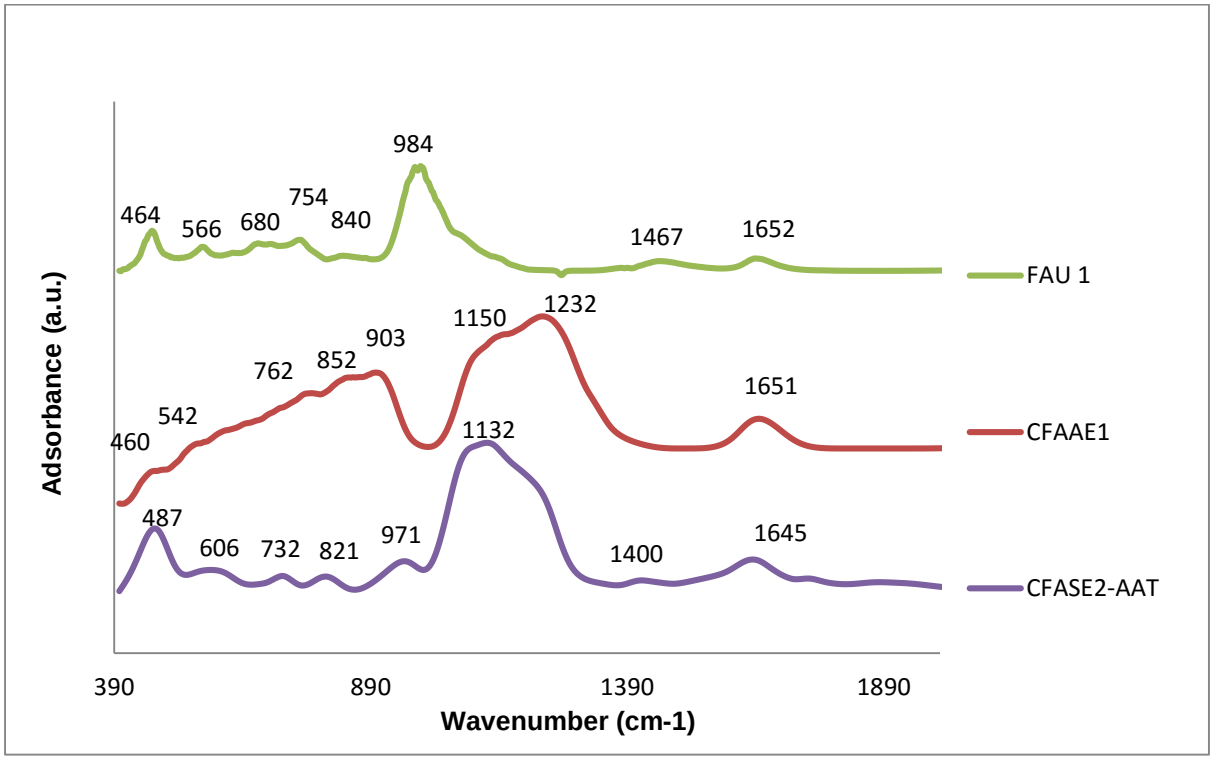

Figure 5.12: FTIR spectra for faujasite (FAU1), coal fly ash alumina extract (CFAAE1), coal fly ash silica extract (CFASE2-AAT)

The FTIR spectrum of CFASE2-AAT was discussed in Section 5.2.6. The FTIR spectrum of CFAAE1 shows peaks in the range of 400 to 1700 cm^{-1}, as illustrated in Figure 5.12. The bands appearing at 460, 542 and 903 cm^{-1} could be assigned to the Al-O stretching mode in the octahedral structure, while the band appearing at 762 cm^{-1} could be assigned to Al-O

stretching mode in the tetrahedral structure (Hosseini *et al*., 2011). It was found that the CFAAE1 extract was not pure alumina, but contained some elements such as Si, Ca, Mg, Fe, Na, and K in trace amounts, as shown in the elemental analysis (Figure 5.1). The FTIR spectrum of CFAAE1 showed a peak characteristic of amorphous silica at 852 cm^{-1}, which could be assigned to the SiO_4 tetrahedron (Aronne *et al*., 1997). CFAAE1 also showed the appearance of cyclic and polymeric anions appearing at 1150 and 1232 cm^{-1} respectively. The band at 1150 cm^{-1} indicated the presence of quartz in the CFAAE1 extract (Onisei *et al*., 2012), even though the quartz mineral phase could not be detected in the XRD pattern of CFAAE1, as presented in Figure 5.4. The presence of asymmetric T-O (T=Si, Al) stretching was observed at 1232 cm^{-1} and it could be assigned to the external tetrahedral TO_4 vibration (Bottazzi *et al*., 2011). The absorption band appearing at 1651 cm^{-3} is related to bending H–O–H vibration (El Didamony *et al*., 2012). Furthermore, the spectrum of FAU 1 shows bands characteristic of zeolite faujasite. The bands at 464, 566 and 680 cm^{-1} are attributed to the Al-O, Si-O-Al and Si-O-Al vibration bends respectively (Saikia and Parthasarathy, 2010, Flanigen *et al*., 1971). The bands appearing at 754, 840 and 984 cm^{-1} can be assigned to the symmetric, Si-O-Si and Si-O stretching band respectively (Rida and Harb, 2014, Flanigen *et al*., 1971). The band at 984 cm^{-1} is associated with either the dimer, trimer, tetramer and monomer anion type (Bass and Turner, 1997). Two peaks were also identified on the FAU spectrum; these peaks were identified at 1467 and 1652 cm^{-1}. The peak at 1467 $cm^{-1}$is assigned to the CH_2 scissoring deformation mode (Minet *et al*., 2004), while the peak at 1652 cm^{-1} is related to the O–H deformation of water (Attia *et al*., 2013, Saikia and Parthasarathy, 2010)**.** The FTIR result showed that the CFAAE1 and CFASE2-AAT feedstock were successfully transformed into a zeolite FAU1, which however still contained some amorphous species, as confirmed by SEM.

5.3.4.2. FTIR analysis for zeolite FAU2

FTIR analysis was performed for CFAAE2, CFASE2-AAT and FAU2, and the structural configuration is presented in Figure 5.13.

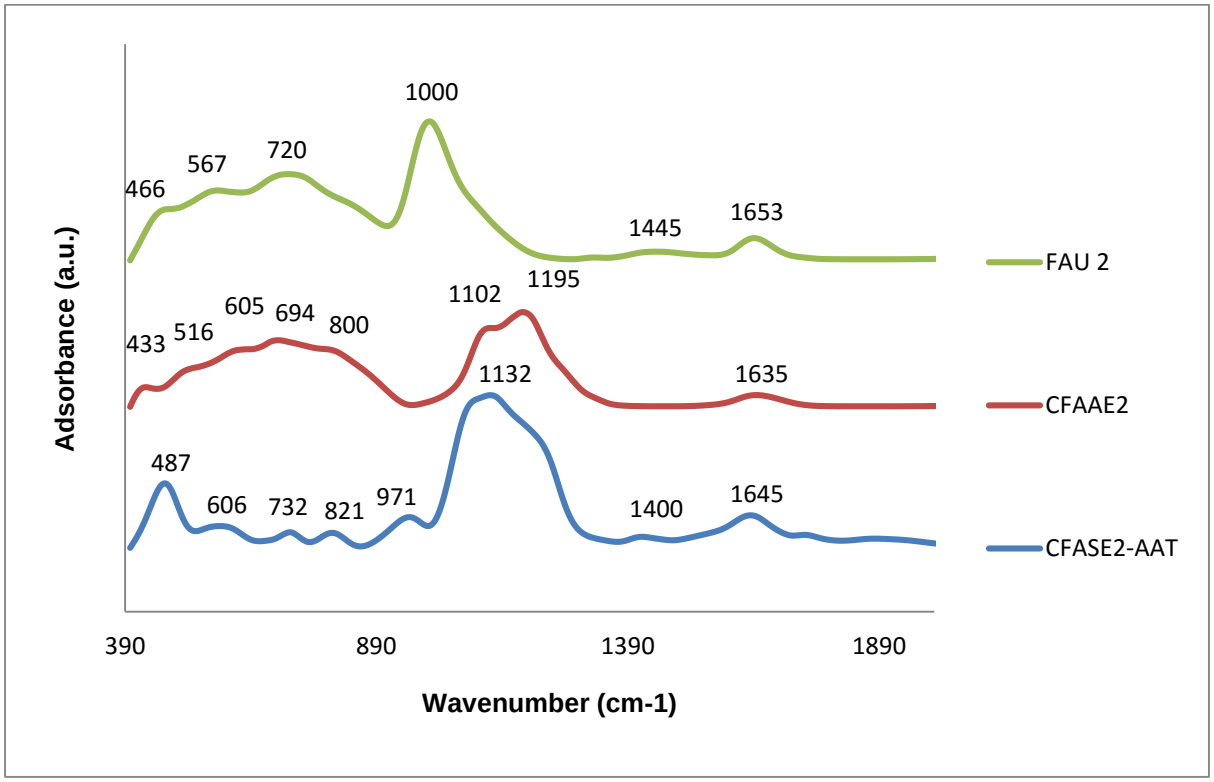

Figure 5.13: FTIR spectra for faujasite (FAU2), coal fly ash alumina extract (CFAAE2), coal fly ash silica extract after oxalic acid treatment (CFASE2-AAT)

The FTIR spectrum of CFASE2-AAT was presented and discussed in Section 5.2.6. The FTIR spectrum of CFAAE2 was composed of six absorption bands that were identified as follows: the bands appearing at 433 cm^{-1} can be assigned to Si-O, and 516 cm^{-1} can be assigned to the Si-O-Al vibration band (Hosseini *et al*., 2011). The bands appearing at 605, 694 and 800 cm^{-1} can be assigned to the stretching vibration of the Al-O bands with aluminium ions in four-fold co-ordination (Aronne *et al*., 1997). Furthermore, Aronne *et al*. (1997), demonstrate that the bands ranging from 800-1200 cm^{-1} could be assigned to the vibration of the SiO_4 tetrahedral with different numbers of bridging oxygen atoms (Farahmandjou and Golabiyan, 2015). The bands appearing at 1102 and 1195 cm^{-1} can be associated with the polymer anion (SO_4^-) (Bass and Turner, 1997). The FTIR spectrum of FAU2 identified four aluminosilicate peaks and two non-aluminosilicate peaks.

The peak appearing at 466 cm^{-1} could be assigned to the Si-O-Si and O-Si-O vibration bending (Lee and Van Deventer, 2003). The peak appearing at 567 cm^{-1} is identified as an external tetrahedral double ring vibration bend, while the peak appearing at 720 cm^{-1} is identified as an

internal tetrahedral symmetric stretching vibration band. Moreover the peak appearing at 1000 cm^{-1} is associated with the internal tetrahedral asymmetric stretching vibration band (Si-O-T) (Lee and Van Deventer, 2003, Flanigen *et al*., 1971) and is associated with the linear anion (Bass and Turner, 1997). The non-aluminosilicate peaks are identified at 1445 and 1653 cm^{-1} and could be associated with carbonate and OH^- respectively (Miller and Wilkins, 1952).

5.3.6. NMR analysis for the CFA extracts and the synthesised zeolites

Al and Si coordination of the zeolite precursors CFAAE1, CFAAE2 and CFASE2-AAT, and the synthesised zeolite faujasite FAU1 and FAU2, as detailed in Section 3.3.2.4, was investigated using ^{27}Al and ^{29}Si NMR analysis.

The ^{27}Al NMR analysis was carried out as described in Section 3.4.6. The ^{27}Al NMR spectra of CFAAE1, CFASE2-AAT and zeolite FAU1 is presented in Figure 5.14. The NMR spectra of the silica extract CFASE2-AAT (0.86% Al and 85.74% Si) showed an intense signal at 0 ppm, which corresponds to the extra-framework octahedrally coordinated Al, and a small broad signal at about 5 ppm that could correspond to penta-coordinated aluminium, due to the distortions of the octahedral symmetry of the AlO_6 units (Byrappa and Yoshimura, 2001). The presence of aluminium in the ^{27}Al NMR of the silica extract CFASE2-AAT corroborated the ICP results, which revealed the mass percentage of Al at 0.86% (Figure 5.2). It can also be seen from the ^{27}Al NMR spectrum of the alumina extract CFAAE1 (88.03% Al and 6.74% Si) that four signals were identified. The peaks were identified at 68, 40, -25 and 0 ppm, where 68 and 0 ppm correspond to the framework tetrahedrally coordinated, and extra-framework octahedrally coordinated respectively (Rodríguez-González *et al*., 2007). The peaks appearing at 40 and 25 ppm could correspond to penta-coordinated aluminium (Byrappa and Yoshimura, 2001). Lastly, the ^{27}Al NMR spectrum of FAU1 showed the presence of a single intense signal at about 60 ppm that corresponded to a tetrahedrally coordinated Al. These results indicated that the extra-framework aluminium, as well as the penta-coordinated aluminium, that were initially present in CFASE2-AAT and CFAAE1 were completely converted into the framework of tetrahedrally coordinated Al in FAU1. These results corroborate the XRD results, which showed that CFASE2-AAT and CFAAE1 were transformed into a crystallised zeolite faujasite (Figure 5.6).

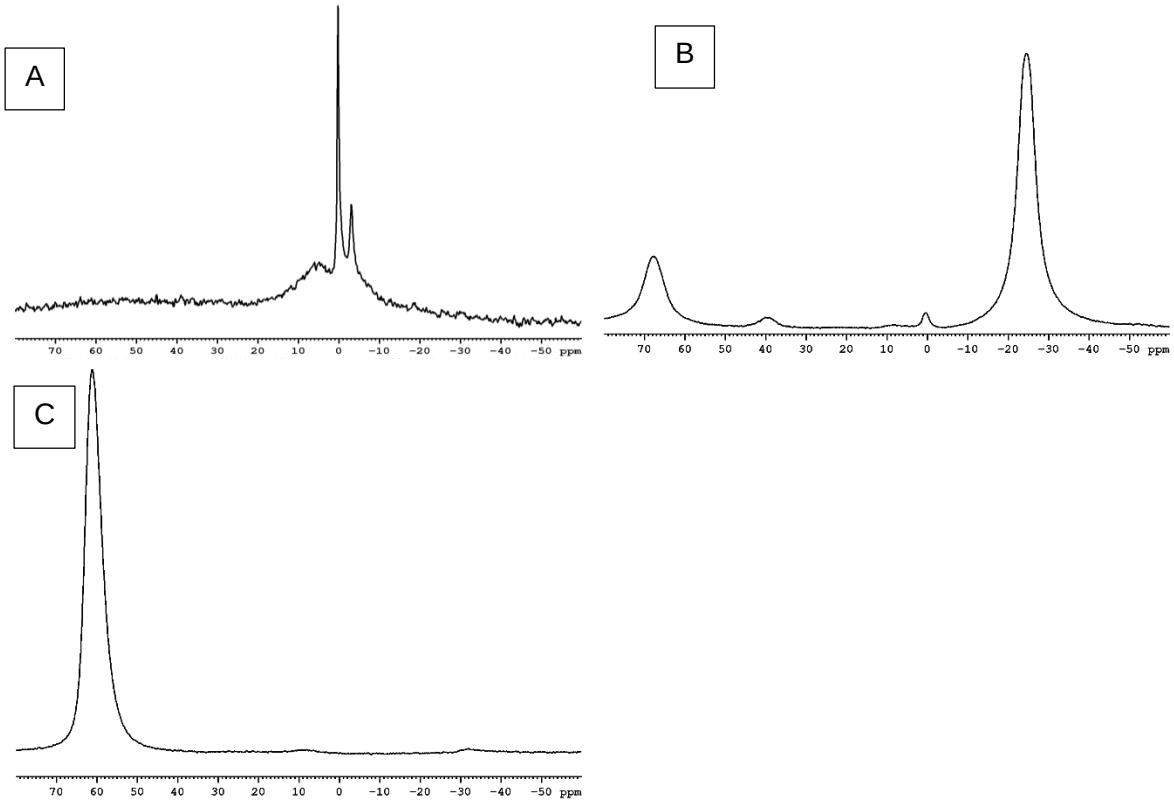

Figure 5.1411: The ^{27} Al NMR spectra of (A) CFASE 2-AAT, (B) CFAAE1 and (C) FAU1.

The ^{29}Si NMR spectra of CFASE2-AAT, CFAAE1 and zeolite FAU1 are presented in Figure 5.15. The ^{29}Si NMR spectrum of the silica extract CFASE2-AAT (85.74% Si and 0.86% Al) shows two signals around -100 and -110 ppm that correspond to Si(2Al) and Si(1Al) units respectively. The ^{29}Si NMR spectrum of the alumina extract CFAAE1 (6.74% Si and 88.03% Al) did not reveal any signal. This could be as a result of the lower silicon content in the CFAAE1 at 6.74%, as shown in the ICP results (Figure 5.1). It can be seen in the FAU1 ^{29}Si NMR spectrum that a signal appeared at -90 ppm, which corresponds to Si(3Al) units. The Si(2Al) and Si(1Al) units in CFASE2-AAT indicate that aluminium was not incorporated into any long range bonding in the precursor feedstock, but occurred as small monomers or dimeric species. On the other hand, the Si(3Al) in FAU1 spectrum was an indication of a more significant amount of Al that had been incorporated into the FAU1 framework. The additional Al that originated from the alumina extract CFAAE1 allowed the transformation of Si(2Al) and Si(1Al) in CFASE2-AAT into Si(3Al) in FAU1. This led to the conclusion that both extracts of CFASE2-AAT and CFAAE1 were involved in the synthesis of zeolite FAU1 as confirmed, by the XRD, SEM and FTIR results.

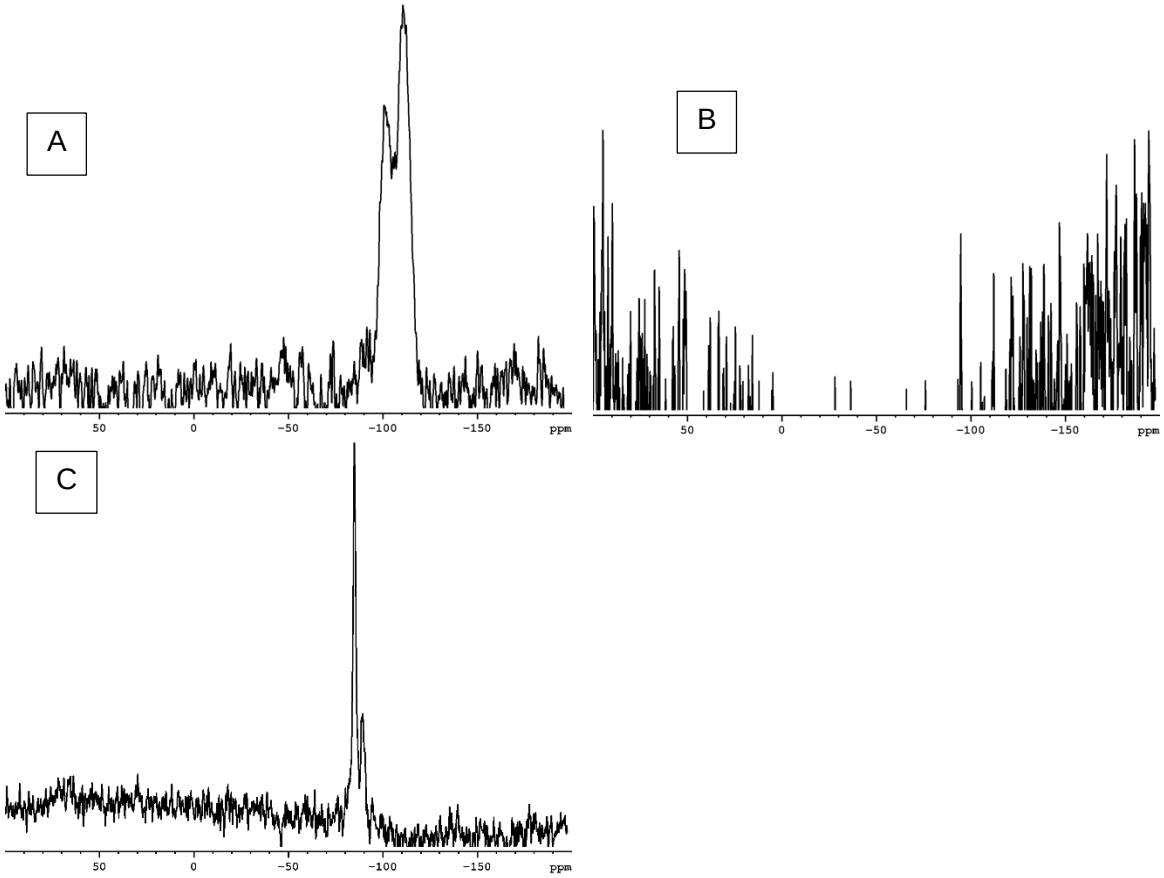

Figure 5.15: The 29Si NMR spectra of (A) CFASE2-AAT, (B) CFAAE1 and (C) FAU1.

5.3.7. NMR analysis for zeolite FAU2

This section presents the ^{27}Al and ^{29}Si NMR analyses of CFAAE2, CFASE2-AAT and FAU2. The ^{27}Al and ^{29}Si NMR analyses were carried out as described in Section 3.4.6.

The ^{27}Al NMR spectra of CFAAE2, CFASE2-AAT and zeolite FAU2 are presented in Figure 5.16. From Figure 5.16, the ^{27}Al NMR spectrum of the silica extract CFASE2-AAT (0.86% Al and 85.74% Si) reveals signals identified at 0 and -5 ppm, which correspond to the extract-framework Al and pentcoordinated respectively (Byrappa and Yoshimura, 2001). The alumina extract CFAAE2 (76.16% Al and 8.18% Si) ^{27}Al NMR spectrum showed the presence of framework coordinated, extra-framework coordinated and penta-coordinated aluminium. The peaks at 68 and 0 ppm correspond to the framework tetrahedral coordinated and extra-framework octahedral coordinated respectively, whereas the signal identified at 40 and -25 ppm correspond to the penta-coordinated aluminium (Byrappa and Yoshimura, 2001). The ^{27}Al NMR spectrum of FAU2 shows the presence of an intense signal at 65 ppm that corresponds to framework aluminium, while an unknown signal was also identified at -30 ppm.

These results showed that much of the alumina content present in the feedstock CFAAE2 and CFASE2-AAT was converted into a zeolite framework during hydrothermal synthesis. These results were confirmed by the XRD, SEM and FTIR result, as discussed in Section 5.3.2.2, 5.3.3.2 and 5.3.4.2.

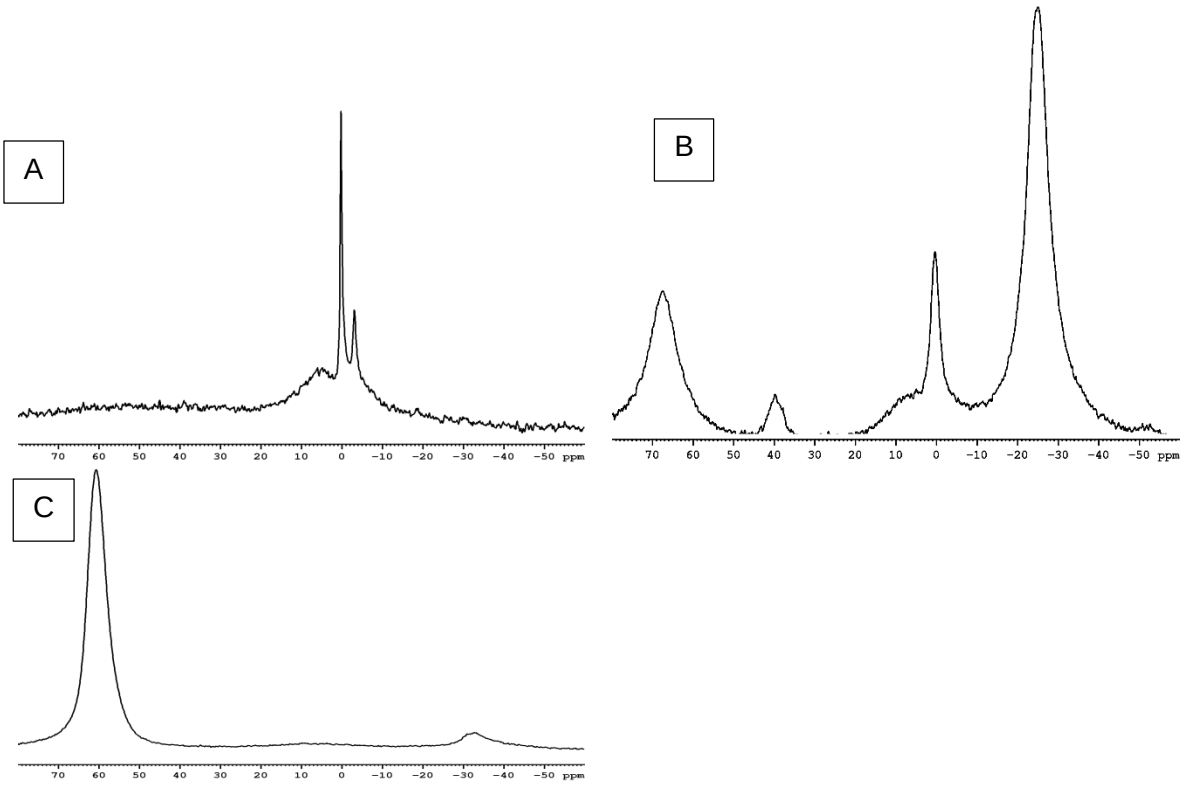

Figure 5.16: The 27Al NMR spectra of (A) CFASE2, (B) CFAAE2-AAT and (C) FAU2.

The ^{29}Si NMR spectra of CFAAE2, CFASE2-AAT and zeolite FAU2 is presented in Figure 5.17. In the ^{29}Si NMR spectrum of the silica extract CFASE2-AAT (85.74% Si and 0.86% Al), two signals were identified at -100 and -110 which correspond to the Si(2Al) and Si(1Al) units respectively. The presence of Si(2Al) and Si(1Al) units in the NMR spectra of CFASE2-AAT shows that aluminium and silica occurred as small monomers or dimeric species in the extract. The ^{29}Si NMR spectra of the alumina extract CFAAE2 (6.74% Si and 76.16% Si) show a lot of noise in the range between 50 to -50 ppm, hence no discernible signal was identified. The ^{29}Si NMR spectra of FAU2 identified a signal at -90 ppm which corresponds to the Si(3Al) unit in the zeolite structure. The Si(3Al) unit is an indication that a significant amount of alumina and silica from CFAAE2 and CFASE2-AAT respectively has been incorporated into the zeolite structure.

These results confirmed the XRD, SEM and FTIR characterisation results for zeolite FAU2. It is important to note that it is the first time anyone has correlated NMR signals for the feedstock silica and alumina extracts and then shown the zeolite product.

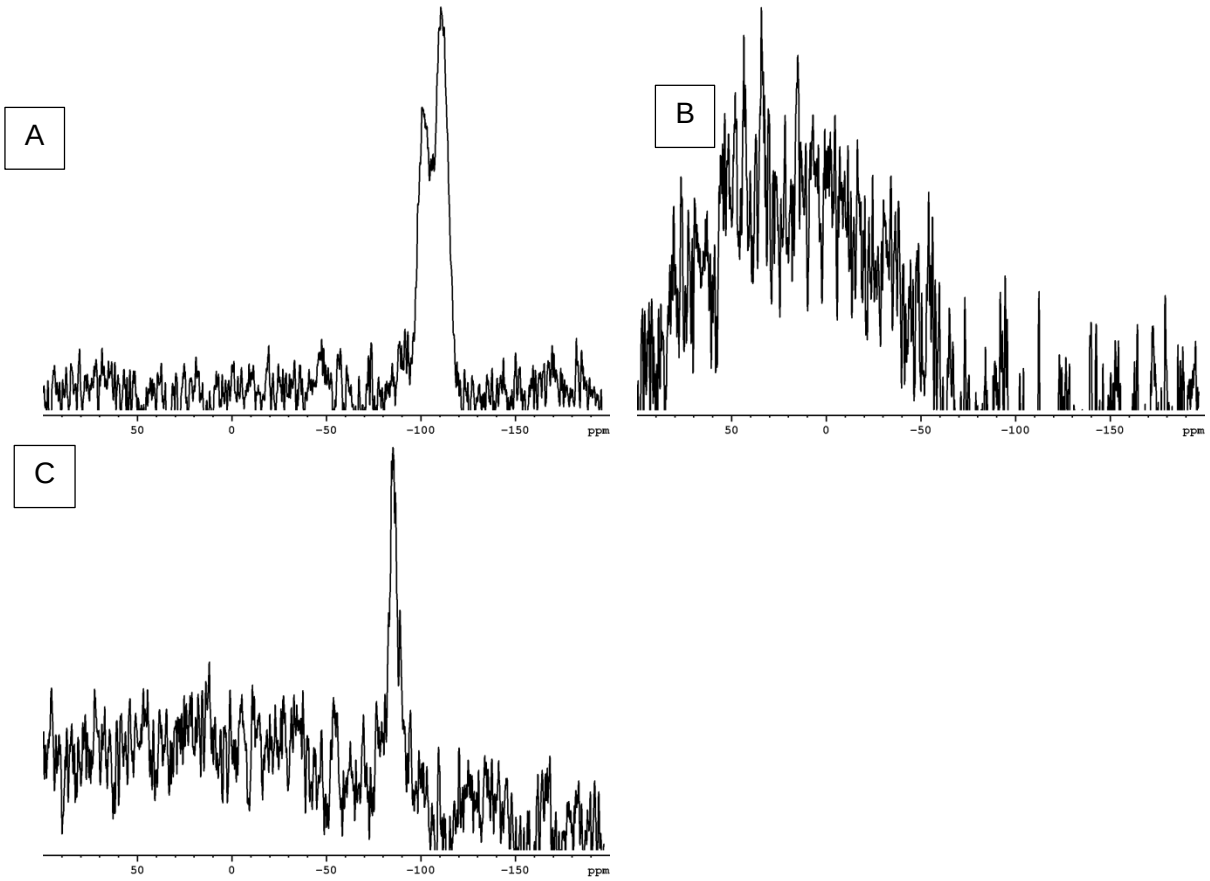

Figure 5.17: The ^{29}Si NMR spectra of (A) CFASE2-AAT, (B) CFAAE2 and (C) FAU2.

5.3.8. Mass balance for the synthesis of zeolite faujasite using CFAAE1 and CFASE1-AAT

This section presents the mass balances for the synthesis of zeolite FAU1 using CFAAE1 and CFASE2-AAT extracts from CFA. Figure 5.18 illustrates the block flow diagram (BFD) for the synthesis of zeolite FAU1 from CFAAE1 and CFASE2-AAT, obtained after the acid and alkaline leaching of CFA following Process 2.

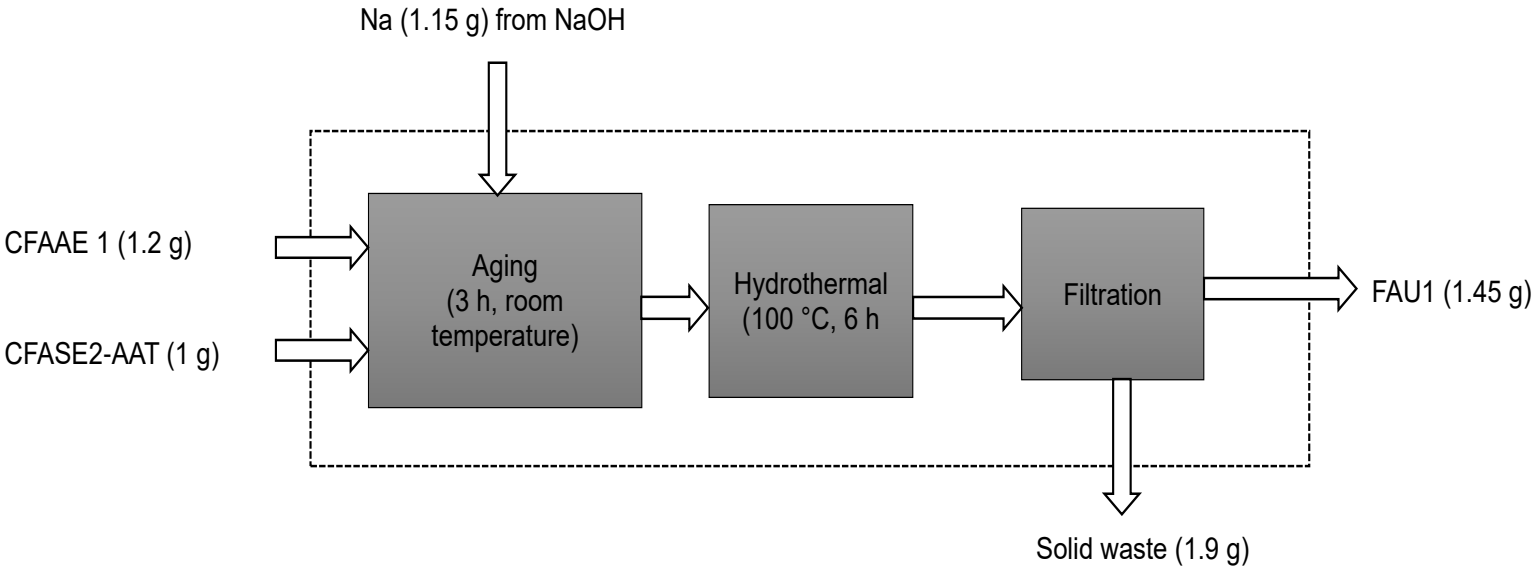

Figure 5.18: Mass balances for the synthesis of zeolite Faujasite (FAU1)

CFAAE1, CFASE2-AAT and Na (from NaOH) were mixed in a mass ratio of 1.20, 1.00 and 1.15 g respectively. The figure shows that 43.28% yield of the zeolite was obtained from this process. Therefore, it is necessary to proffer alternative process routes to recycle the solid waste stream back into the synthesis process. This is important to ensure that all available Si and Al in the extracts are utilised in the formation of the zeolite. In addition, efficient recycling will make the process more economically feasible by increasing the yield of the synthesised product and reduce wastage. Table 5.1 presents the mass balances for the synthesis of zeolite FAU1 from CFAAE1 and CFASE2-AAT. It should be noted that the mass percentage calculations were performed based on the abundance of each element available in the specified feedstock or product.

Table 5.1: The material balance on the synthesis of zeolite faujasite 1

Elements (%)	Feedstock streams				Product streams		
	CFAAE1	CFASE2-AAT	NaOH	Total feed stream	FAU1	Waste stream	Total product stream
Si	8.62	91.38	0.00	100.00	93.53	6.47	100.00
Al	99.19	0.81	0.00	100.00	37.39	62.61	100.00
Ca	88.39	11.61	0.00	100.00	25.15	74.85	100.00
Fe	14.53	85.47	0.00	100.00	0.00	100.00	100.00
Ti	98.21	1.79	0.00	100.00	100.00	0.00	100.00
Mg	52.15	47.85	0.00	100.00	77.34	22.66	100.00
P	75.09	24.91	0.00	100.00	12.46	87.54	100.00
K	46.71	53.29	0.00	100.00	30.95	69.05	100.00
Na	0.44	8.67	90.89	100.00	6.77	93.23	100.00
Mn	21.14	78.86	0.00	100.00	55.92	44.08	100.00
Cr	72.45	27.55	0.00	100.00	100.00	0.00	100.00

The mass balance was performed to trace the distribution of each element present in the feedstock and the final products. As illustrated in Table 5.1, the Si and Al fed into the synthesis process came from two sources, namely CFAAE1 and CFASE2-AAT. The CFAAE1 contained about 8.62 mass% and 99.19 mass% of Si and Al respectively, whereas the CFASE2-AAT contained 91.38 mass% and 0.81% of Si and Al respectively. It can be seen from the table that 93.53 mass% of the Si fed into the process reported to the zeolite product, while the remaining 6.47 mass% of the Si fed was contained in the waste stream. In contrast, an opposite observation was recorded for Al, whereby only 37.39 mass% of the Al available in the feed stream reported to the zeolite product, while the excess 62.61 mass% reported to the waste stream. From the results, the Si/Al ratio of the synthesised zeolite FAU1 was calculated and found to be 2.5. According to Jha and Singh, (2011) zeolite faujasite with a Si/Al ratio between 2 to 5 can be classified as Zeolite Y. It could also be seen from the table that Ti and Cr present in fly ash reported 100 mass% to the zeolite product. A significant amount of the Mg and Mn elements present in the fly ash (77.34 and 55.92 mass% respectively) reported to the zeolite product. It can also be seen that only 25.15, 12.46, 30.95 and 6.77 mass% of Ca, P, K, and Na reported to the zeolite product respectively, while the rest reported as waste in the waste stream. It is noteworthy that all the Fe from CFAAE1 and CFASE2-AAT from the feed stream reported to the waste stream, so the percentage of Fe in the synthesised zeolite Na-Y was below its ICP detection level. From the mass balance results, it can be seen that a large amount of Al and Na is lost in the waste stream. It is therefore important to devise ways to recycle the waste stream into the zeolite synthesis process in order to minimise the wastage of Si and Al. Du Plessis, (2014) showed that it was possible to recycle the supernatant waste resulting from the fusion-assisted process, into the hydrothermal synthesis of zeolite A. A high quality of zeolite A was produced from the recycling process. Therefore, Du Plessis's recycling study could be employed in this project in order to inform the recycling of the waste stream, which is rich in Al and Na, back into the zeolite synthesis process.

5.4. Characterisation of geopolymers synthesised from solid residue 2 (SR 2)

This section details the characterisation of the geopolymer that was synthesised from the alkaline waste (SR3) obtained after the extraction of CFASE2-AAT from CFA using 8 M NaOH. The employed synthesis procedure used for the synthesis of the geopolymer is detailed in Section 3.3.2.5. The synthesised geopolymer was analysed using different analytical techniques, namely XRD, SEM, ICP, FTIR and NMR. The results are presented in the subsections below.

5.4.1. XRD analysis of CFA and the synthesised geopolymers

A geopolymer (G2) was synthesised from the waste material (SR3) obtained after the extraction of Si from fly ash (CFASE2-AAT). CFASE2-AAT was extracted from CFA using 8 M NaOH solution at 150ºC under reflux condition for 24 h. The mixture was filtered and the moist solid slurry recovered as waste was poured in a 50 cm by 50 cm cubic mould. The mould was sealed and left to cure for five days at room temperature. After the 5 days was complete, the mould was placed in an oven for further curing and heated at 70ºC for five days. The procedure for geopolymer synthesis is detailed in Section 3.3.2.5. The resulting geopolymer was cooled after the five days and analysed using XRD. The XRD of the synthesised geopolymer in comparison with CFA is presented in Figure 5.19.

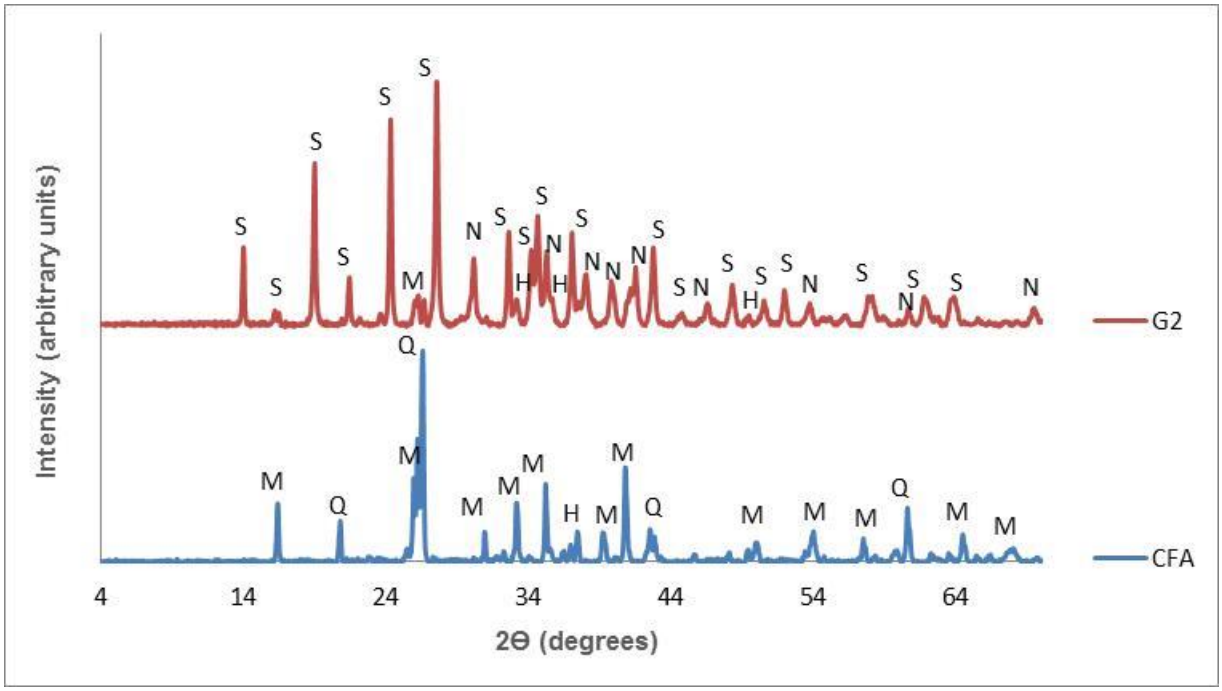

Figure 5.19: XRD patterns of CFA in comparison with G2. Where M = Mullite (3Al2O3. 2SiO2), Q = Quartz (SiO2), H = Hematite (Fe2O3), S = Sodium aluminium sulphide silicate hydrate (Na8(Al6Si6O24)S•4H2O) and N = Natrite (Na2CO3).

It can be seen that the XRD pattern of CFA was mainly dominated by mullite and quartz, as discussed in Chapter Four. The XRD pattern of G2 revealed the presence of sodium aluminium sulphide silicate hydroxide hydrate and natrite mineral phases, with only traces of unreacted mullite and hematite from CFA. It can be seen from the G2 XRD spectrum that most of the mullite and quartz mineral phase in the CFA was transformed during the curing phase of the process. Figure 5.19 also shows that the intensity of mullite decreased on the G2

spectrum at 26 º 2θ, indicating that most of the crystalline mineral phases in the fly ash were transformed. The XRD spectrum of G2 was similar to that of G1, as shown in Chapter Four, section 4.4.1.

5.4.2. SEM analysis for CFA and the synthesised geopolymers

The scanning electron microscope (SEM) was used to analyse the surface morphology of the synthesised geopolymer (G2). The SEM micrographs of G2 in comparison with CFA are presented in Figure 5.20.

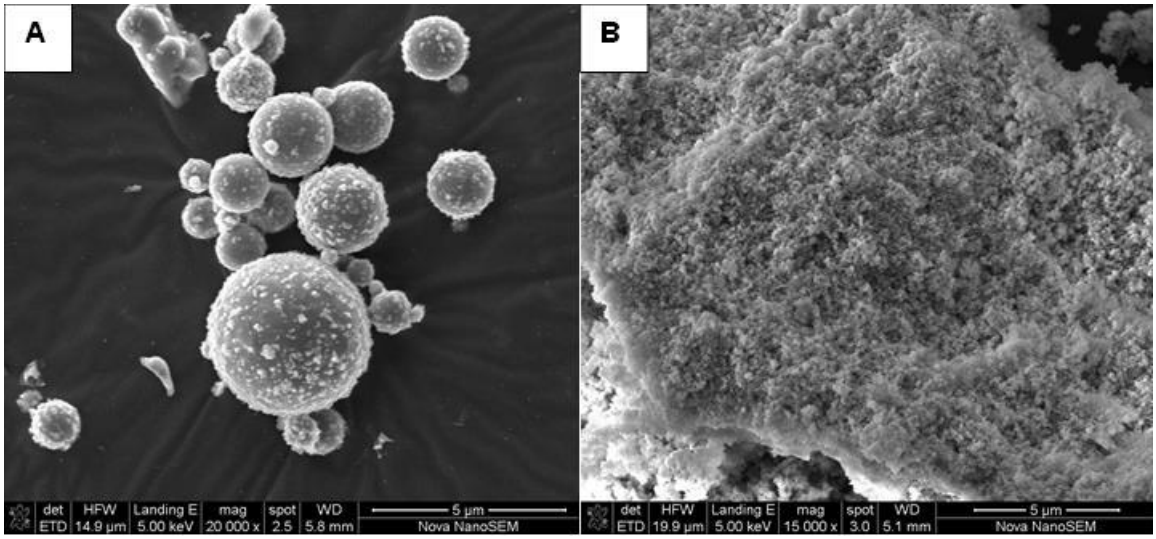

Figure 5.20: SEM micrographs of (A) CFA in comparison with (B) G2.

From SEM images presented in Figure 5.20, it can be seen that CFA was made up of dispersed rough spherical particles. The SEM micrograph of G2 showed that the surface of the geopolymer was amorphous and granular in the nanometre range. This could also be due to the influence of removal of alumina and silica through an earlier extraction process (for the synthesis of zeolites) or due to curing during geopolymer formation. Delair *et al*, (2012) mention that when the geopolymerisation process is not complete, excess Na^+ accumulates on the surface of the geopolymer in the form of a salt. The powder-like material on the surface of the geopolymer could be Na^+ salts resulting from the NaOH used during the CFASE2-AAT extraction. The SEM micrograph of G2 showed that the synthesis of geopolymeric material from the solid waste resulting from the extraction of CFAAEs and CFASE2-AAT respectively was not complete. The synthesis conditions could be optimised to improve the quality of the geopolymer synthesised from the solid waste.

5.4.3. FTIR analysis for CFA and the synthesised geopolymers

The FTIR spectroscopy was used as detailed in Section 3.4.3 to determine the surface functionalities and structural configuration of geopolymer (G2). The FTIR spectra of G2 in comparison with CFA are presented in Figure 5.21.

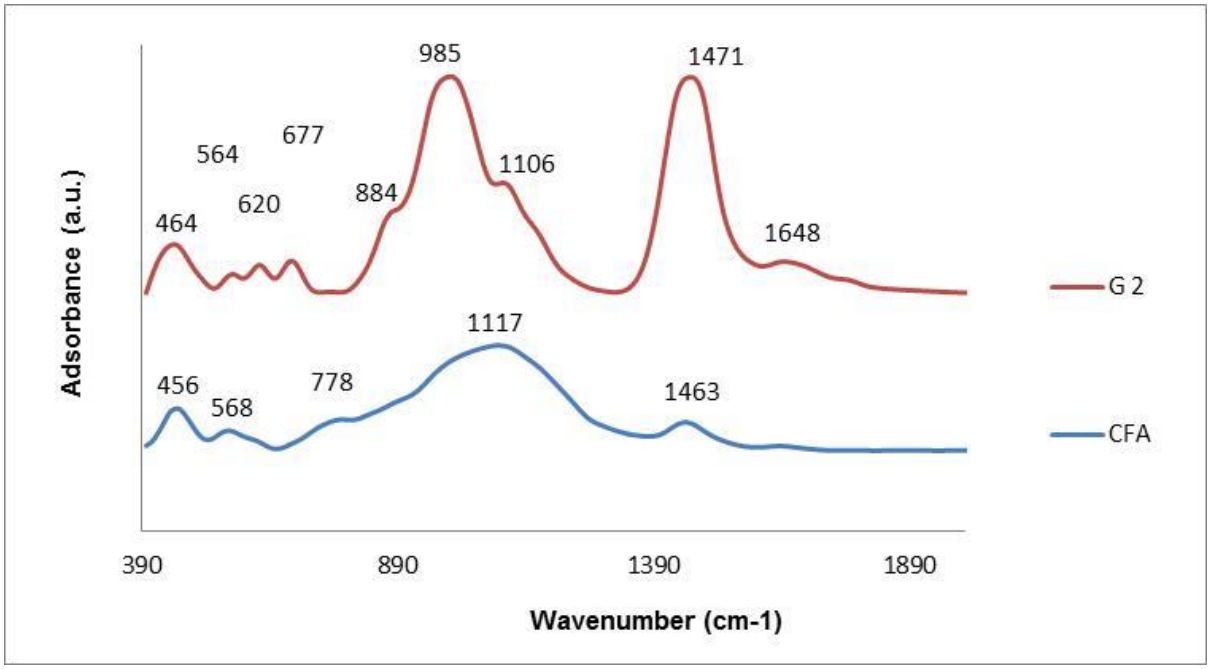

Figure 5.21: FTIR spectra of geopolymer (G2) in comparison with coal fly ash (CFA)

The FTIR spectrum of CFA is discussed in Chapter Four, Section 4.1.3. CFA and G2 had some similar bands in their spectra. The FTIR spectrum of G2 revealed bands at 464 cm^{-1}, 561 cm^{-1} that could be assigned to the T-O and Al-O-Si vibration band respectively (Fernández-Jiménez and Palomo, 2005, Flanigen *et al*., 1971). The band appearing at 620 cm^{-1} could be identified as a symmetric stretching (Si-O-Si and Al-O-Si) vibration bands (Lee and Van Deventer, 2003). The band appearing at 677 cm^{-1} is due to internal tetrahedral symmetric stretching band (Flanigen *et al*., 1971), while the band appearing at 884 cm^{-1} could be assigned to Si-O stretching and OH bending (Si-OH) (Lee and Van Deventer, 2003). Furthermore, the bands appearing at 985 and 1106 cm^{-1} could be associated with the internal tetrahedral stretching vibration bands and these bands can also be associated with the linear and polymer anion. The band appearing in the region of 1471 cm^{-1} is a new absorption band, which was also observed by Bondar *et al*, (2011). This absorbance could be due to a vibration of carbonate salts formed on the surface of the geopolymer (Lee and Van Deventer, 2003).

The absorption band in the region of 1648 cm^{-1} can be assigned to non-aluminosilicate bands, because its range falls outside the aluminosilicate range. This band characterises the

spectrum of stretching and deformation vibrations of OH group from the weakly bound water molecules, which are adsorbed on the surface or trapped in the large cavities between the rings of geopolymeric products (Palomo *et al*., 1999).

5.4.4. NMR analysis of CFA and the synthesised geopolymers

The ^{27}Al and ^{29}Si NMR analysis was used, as detailed in Section 3.4.6, to determine the framework and extra-framework Al and also identify the structure of silicate anions in the geopolymer material. The ^{27}Al and ^{29}Si NMR analyses of G2 in comparison with CFA are presented in the sub-sections below.

5.4.4.1. ^{27}Al NMR analysis

The ^{27}Al NMR spectra of G2 in comparison with CFA are presented in Figure 4.22 below. The ^{27}Al NMR spectrum of CFA is presented in Section 4.8.4.1. Figure 5.22 shows that the NMR spectrum of G2 is similar to that of G1, as discussed in section 4.8.4., with a signal at 55 ppm. The signal is assigned to framework aluminium. The signal at 60 ppm showed that most of the Al in the geopolymer was not soluble anymore, but formed part of the geopolymer framework. A small unknown broad peak at -30 ppm was also observed.

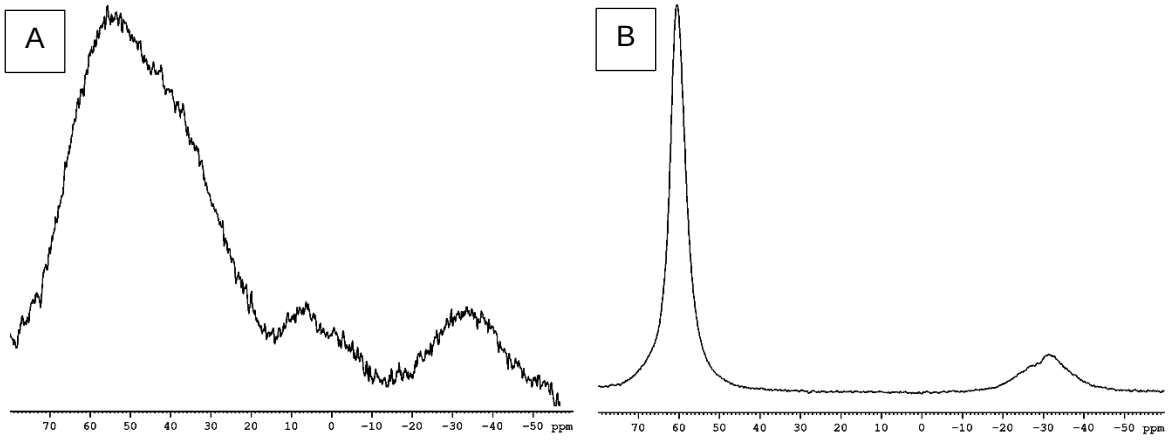

Figure 5.22: The ^{27}Al NMR spectra of CFA (A) and G2 (B)

5.4.4.2. ^{29}Si NMR analysis

The ^{29}Si NMR spectra of G2 in comparison with CFA are presented in Figure 5.23. Figure 5.23 shows that the spectrum of CFA (A) presented two signals at -110 and -160 ppm, corresponding to the Si(1Al) and Si(0Al) units respectively. The ^{29}Si NMR spectrum for G2 showed a prominent signal at -90 ppm, which corresponds to the Si(3Al) units. The Si(3Al) in the geopolymer material showed that Al was incorporated into the geopolymer framework.

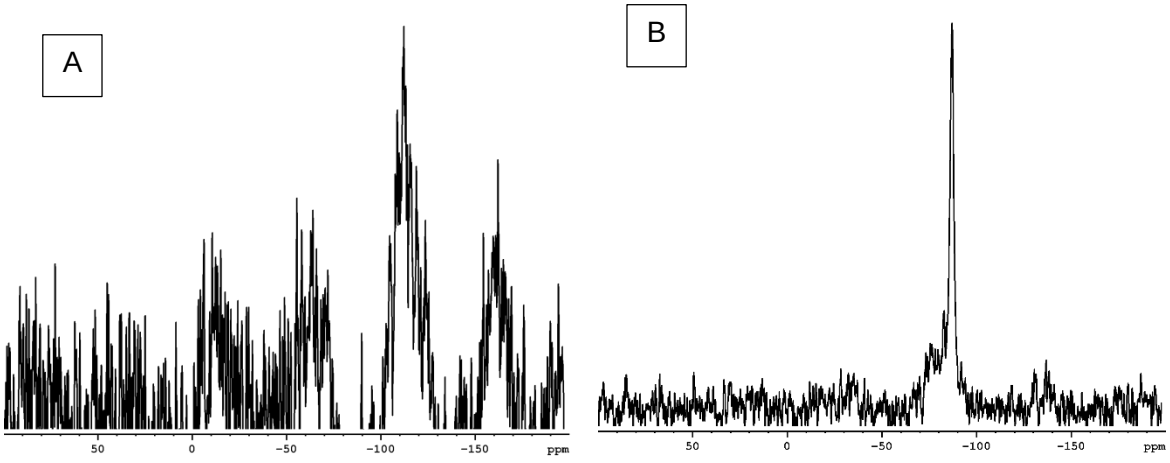

Figure 5.23: 29Si NMR spectra of (A) CFA and (B) G2.

5.4.5. Elemental composition of geopolymer 2 (G2) synthesised using the solid residue obtained after the extraction of CFAAEs and CFASE2-AAT

Geopolymer 2 (G2) was synthesised using the wet waste material obtained after the extraction of CFAAEs and CFASE2-AAT. A portion of the synthesised G2 was digested and analysed using ICP-AES to determine its elemental composition. The elemental composition of G2 is presented in Table 5.2 in mass percentage.

It can be seen from the results obtained that the synthesised geopolymer was mainly composed of Si and Fe at 69.22 and 14.86 mass% respectively. It also can be seen that the atomic percentage of Al, P, Na and Cr were below 10 mass% of the total composition with concentrations of 2.22, 1.97, 5.69 and 3.62 mass% respectively.

Table 5.2: Elemental composition of the synthesised G2

Elements mass (%)	G2
Si	69,22
Al	2,22
Ca	0,46
Fe	14,86
Ti	0,47
Mg	0,49
P	1,97
K	0,54
Na	5,69
Mn	0,47
Cr	3,62
Total	100,00

It can be seen from the results obtained that the synthesised geopolymer was mainly composed of Si and Fe at 69.22 and 14.86 mass% respectively. It also can be seen that the atomic percentages of Al, P, Na and Cr were below 10 mass% of the total composition, with concentrations of 2.22, 1.97, 5.69 and 3.62 mass% respectively. Also, the percentage of Ca, Ti, Mg, K and Mn amounted to less than 0.5 mass% each on the total concentration. The Si/Al ratio of the synthesised geopolymer was 31.18. It can be seen from the elemental composition that Na accounted for 5.69 mass%, which correlates to the discussion in Section 5.4.2, attesting to the fact that some of the powder-like material in the surface of the geopolymer could be the $Na^{+,}$ as indicated in Figure 5.20. According to Giannopoulou and Panias (2007), the applications of geopolymers are dependent on the geopolymer structure and the Si/Al ratio. Oudadesse *et al*. (2007), showed that amorphous geopolymers of the potassium-poly(sialate)-nanopolymer type with a mole ratio Si/Al = 31 were studied for their use as potential biomaterial in bone restoration.

This shows that the synthesised G2 from the slurry after the extraction of silica has the potential for application as a biomaterial in bone restoration.

This study has shown the possibility of developing and upscaling the synthesis of zeolite and geopolymer from South African coal fly ash in order to optimise the usage of CFA for the synthesis of valuable materials. This in turn will reduce the environmental burden caused by the disposal of CFA.

CHAPTER SIX

GENERAL CONCLUSION AND RECOMMENDATIONS

6.1. Introduction

The aims and objectives in this study were set out based on the gaps identified in the literature. In this chapter, major findings are presented in view of the objectives drawn up in Chapter One. The recommendations are also highlighted based on the findings obtained.

6.2. General findings

The main aim of this study was to synthesise ZSM-5 and faujasite zeolites from South African coal fly ash (CFA), which is not new. However, a new approach was used in order to avoid the addition of extra silica or alumina sources in the synthesis of zeolites, improving their yield and also minimising the waste generated during the synthesis process by using the remaining fly ash slurry, after extraction of Si and Al, in the synthesis of geopolymers. In this study, coal fly ash from Matla power station (South Africa) was used as the raw material for the extraction of silica and alumina. The raw material was characterised using different analytical techniques (XRF, ICP, XRD, SEM, FTIR and NMR). The characterisation of coal fly ash with these analytical techniques revealed the abundant presence of quartz and mullite, as well as an amorphous phase in the sample. The major oxides in coal fly ash determined by XRF were SiO_2 (53.1%) and Al_2O_3 (29.1%), accounting for 82.2% of the total CFA composition, with a SiO_2/Al_2O_3 ratio of 1.61. The coal fly ash used in this study was classified as class F, based on its CaO and (SiO_2+ Al_2O_3+ Fe_2O_3) content. It was made up of microscopic spherical particles.

In this study, two processes were investigated for the synthesis of zeolites (ZSM-5 and faujasite) from coal fly ash, depending on the type of extraction. Process 1 involved the extraction of silica from coal fly ash using 2, 4 and 8 M of NaOH solution, followed by precipitation of silica from the filtrate using concentrated H_2SO_4 (95-99%). It was found that the coal fly ash silica extract (CFASE1-BAT) obtained from the treatment with 8 M of NaOH solution had the highest Si content of 55.21%, followed by the 4 M NaOH extract (44.69%) and the 2 M NaOH extract (34.70%). Therefore, CFASE1-BAT obtained from 8 M NaOH was considered as optimum and was used for the rest of the experiments. It was noteworthy that CFASE1-BAT (8 M NaOH) contained a certain amount of Al (0.70%) enough for the extract (Si/Al = 79) to be used as a ZSM-5 precursor. However, the highest Na content of 42.86% could affect the product quality. Thus, CFASE1-BAT (8 M NaOH) was treated with oxalic acid solution in order to remove excess Na.

The obtained extract named CFASE1-AAT contained 86.84, 0.70 and 11.62% of Si, Al and Na respectively, with a Si/Al ratio of 124.06, and was used as a ZSM-5 precursor. The characterisation techniques (XRD, SEM and FTIR) revealed that CFASE1-AAT was amorphous and was used to synthesise ZSM-5 zeolite and the last step in the process was the synthesis of a geopolymer from the residual fly ash slurry (SR1) after silica extraction.

Conventionally, the synthesis of ZSM-5 zeolite from coal fly ash normally requires the addition of a silica source in order to adjust the Si/Al molar ratio in the starting mix. The synthesis of ZSM-5 requires an initial Si/Al ratio ≥ 10 in the hydrothermal gel. Unfortunately, the Si/Al ratio in CFA was found to be 1.61, which was insufficient for the synthesis of Zeolite ZSM-5. However, the method employed in this study showed that ZSM-5 could be synthesised from fly ash without the addition of an extra silica source. The selective extraction of CFASE1-BAT from CFA using 8 M NaOH was found to increase the Si/Al ratio from 1.61 to 78.87. A treatment of CFASE1-BAT with oxalic acid increased the purity of the extract (CFASE1-AAT), and the Si/Al ratio to 124.06. Thus it is noteworthy that the CFASE1-AAT was successfully transformed into ZSM-5 zeolite using tetraethyl ammonium hydroxide (TEAOH) as the structure directing agent.

The CFASE1-AAT and the synthesised Zeolite ZSM-5 were characterised using ICP, XRD, SEM, FTIR and NMR. The XRD spectra for CFASE1-AAT and ZSM-5 had shown that an amorphous XRD pattern of CFASE1-AAT, characterised by a broad hump of amorphous silica from 16 to 25 2Θ, was transformed into a characteristic pattern of pure phase Zeolite ZSM-5. CFASE1-AAT also had high intensity peaks of sodium hydrogen oxalate hydrate, which occurred as a result of the oxalic acid treatment of CFASE1-BAT which was undertaken to remove the excess Na content in the extract. The SEM analysis showed the amorphous CFASE1-AAT was transformed into lath-shaped crystals that are characteristic of Zeolite ZSM-5. The FTIR result of ZSM-5 showed aluminosilicate structural features of Zeolite ZSM-5 at the region of 462, 605, 724, 854, 957 and 1096 respectively, while the ^{27}Al NMR result for both CAFSE1-AAT and ZSM- showed that all extra-framework Al in CFASE1-AAT was transformed into framework Al in Zeolite ZSM-5, while the ^{29}Si NMR result showed that the two signals corresponding to Si(2Al) and Si(1Al) units in CFASE1-AAT were transformed into a signal corresponding to a Si(1Al) unit. The yield of the synthesised zeolite ZSM-5 was 35.9%.

Further, a geopolymer was successfully synthesised from the residual slurry (SR1) obtained after the extraction of CFASE1-BAT from CFA. The synthesised geopolymer was characterised by ICP, XRD, SEM, FTIR and NMR.

It was shown from the SEM analysis that the spherical fly ash particles were polymerised into a bulky mass in the geopolymer (G1). It was also revealed that the geopolymer was not

completely polymerised, since small spherical particles of CFA were partially observed in the SEM image of G1. The XRD result of G1 revealed the presence of sodium aluminium silicate hydroxide hydrate and natrite mineral phases, with some traces of unreacted mullite and hematite from CFA. The presence of mullite in G1 indicated that not all SiO_2 and Al_2O_3 participated in the geopolymerisation reaction. However, it is noteworthy that most of the mullite and quartz was converted into sodium aluminium silicate hydroxide hydrate to form a geopolymer. The FTIR result showed aluminosilicate structural features at 464, 561, 702, 888 and 990 cm^{-1}. Furthermore, the ^{27}Al NMR result showed that the extra framework Al in the starting material was converted into framework Al in the G1 structure; while the ^{29}Si NMR result showed that the Si(1Al) unit in the CFA was transformed to Si(3Al) and Si(0Al) as a result of the silica extraction and geopolymerisation process. The synthesised geopolymer had a Si/Al ratio of 9.4. However, the synthesised G1 was not that strong, as some fractures were observed in the final material, and this might be attributed to the high amount of Na (17.27%) in the material. These findings confirm that high purity zeolite ZSM-5 with a yield of 35.9% could be synthesised from the fly ash extract without the addition of a silica source. This study has also established the fact that the remaining slurry (SR1) could be used for the synthesis of a geopolymer, thus leading to a zero waste process.

Process 2 involved the extraction of alumina (CFAAEs) from coal fly ash using H_2SO_4 (95-99%), followed by calcination at 800 °C for 2 h. The Al extraction efficiency was found to be 79.4%, divided into four (4) alumina samples: CFAAE1 (34.27% of Al extraction efficiency), CFAAE2 (23.12% of Al extraction efficiency), CFAAE3 (6.99% of Al extraction efficiency) and CFAAE4 (15.03% of Al extraction efficiency). Thereafter, the solid residue was used as feedstock in the extraction of silica (CFASE2-BAT) using 8 M NaOH. CFASE2-BAT was treated with oxalic acid to reduce the Na content in the extract. The obtained extract (CFASE2-AAT) was used as a silica source in the synthesis of zeolite faujasite. Zeolite faujasite (FAU1, FAU2, FAU3 and FAU4) were synthesised from the silica extract (CFASE2-AAT) and alumina extract (CFAAE1, CFAAE2, CFAAE3 or CFAAE4). Finally a geopolymer was synthesised from the residual slurry (SR2) obtained after the alumina and silica extraction.

Zeolite faujasite (FAU1) was synthesised from CFAAE1 and CFASE2-AAT with a molar regime of 1Si: 1.1Al: 8.6Na: 102.7H_2O, while zeolite FUA2 was successfully synthesised from CFAAE2 and CFASE2-AAT with a molar regime of 1Si: 1.1Al: 8.2Na: 101.1H_2O.

Zeolite faujasite was not synthesised when CFAAE3 or CFAAE4 was used as source of alumina. This could be due to the low Al extraction efficiency, as well as the high percentage of other elements such as Fe or Ca in the extracts. The synthesised zeolites (FAU1 and FAU2) with their precursors (CFAAE1, CFAAE2 and CFASE2-AAT) were characterised using ICP,

XRD, SEM, FTIR, and NMR. The XRD results of CFAAE1 and CFAAE2 show that the sample mainly contained aluminium sulphate ($Al_2(SO_4)_3$) with trace amounts of aluminium oxide (Al_2O_3) and anhydrite. This was probably due to an incomplete calcination process. The XRD result of FAU1 showed pure phase zeolite faujasite, while that of FAU2 showed that the synthesised zeolite was mixed with other mineral phases such as phillipsite, sodium aluminium silicate hydrate and calcite mineral phases. It was shown from the SEM result that the alumina extracts (CFAAE1 and CFAAE2) exhibited cubic crystalline structures. Zeolite FAU1 displayed the typical octahedral crystals which are characteristic of zeolite faujasite, while on the other hand FAU2 showed that typical octahedral crystals observed by SEM were mixed with unreacted materials from its precursors (CFAAE2 and CFASE2-AAT). The FTIR result of FAU1 and FAU2 showed aluminosilicate structural features of zeolite faujasite. The ^{27}Al and ^{29}Si NMR result showed that the Al and Si in the CFAAE1, CFAAE2 and CFASE2-AAT were converted into zeolite faujasite. The presence of an impure phase in the synthesised zeolite FAU2 might have been caused by the incomplete conversion of CFAAE2 into zeolite faujasite. This suggests that the synthesis conditions of zeolite faujasite using different alumina extracts might need to be optimised, since the mass composition of the extracts differ. The synthesised zeolite FAU1 had a Si/Al ration of 2.5. Thus, FAU1 was classified as Y-type zeolite, since its Si/Al ranged between 2 and 5. The yield of the synthesised zeolite was 43.28%. The mass balance of FAU1 showed that most of the feedstock (CFAAE1 and CFASE2-AAT) reported to the waste stream of the process. It is therefore necessary to proffer alternative process routes to recycle the solid waste stream back into the synthesis process to ensure total conversion of the feedstock to the final product (FAU1).

A geopolymer (G2) was successfully synthesised from the residual slurry (SR3) obtained after the successive extraction of Al and Si from CFA. The synthesised geopolymer was characterised using ICP, XRD, SEM, FTIR, and NMR. It was shown from the XRD of G2 was mainly dominated by sodium aluminium sulphide silicate hydrate, natrite and trace minerals of mullite and hematite. The SEM analysis showed a polymerised G2 with the physical characteristic of white powder. The FTIR result showed the aluminosilicate structural features of a geopolymer at 464, 564, 620, 884, 985, and 1106 cm^{-1} respectively. Furthermore, it was shown in the ^{27}Al and ^{29}Si NMR result that the Al and Si in the starting material was converted into a geopolymer material.

The synthesised G2 had a Si/Al ratio of 31.18. Geopolymers with Si/Al ratio of 31.18 can potentially be used as a biomaterial in bone restoration.

It is important to note that the developed synthesis route was successfully used to synthesise zeolites (ZSM-5 and faujasite) and geopolymers, as intended. The synthesis condition may

need to be optimised to increase the yield and purity of the synthesised products and minimise wastage, making the synthesis of CFA based zeolites economically viable.

6.2. Recommendations and future work

This study has shown that coal fly ash alumina extracts (CFAAE1 and CFAAE2) and silica extracts (CFASE1-AAT and CFASE2-AAT) were successfully used in the synthesis of zeolites (ZSM-5 and faujasite) following the proposed methods (Process 1 and 2), and the remaining slurry was transformed into geopolymers. However, the processes still need to be optimised in order to increase the yield and purity of the zeolites, as well as the strength of the geopolymers. Therefore some recommendations need to be made, including:

- Optimisation of the CFAAE calcination process to ensure total conversion of $Al_2(SO4)_3$ to Al_2O_3.
- Optimisation of the synthesis conditions of zeolite ZSM-5 and faujasite to increase the yield of the final product and minimise wastage into the waste stream.
- Optimisation of the geopolymerisation process for G1 and G2 to increase the strength of the geopolymer.
- Mass balance should be performed for the overall process to determine the fate of each element and the efficiency of the process.

References

Abdullah, M., Hussin, K., Bnhussain, M., Ismail, K. & Ibrahim, W. 2011. Mechanism and chemical reaction of fly ash geopolymer cement-a review. *Int. J. Pure Appl. Sci. Technol,* 6**,** 35-44.

Ahmaruzzaman, M. 2010. A review on the utilization of fly ash. *Progress in Energy and Combustion Science,* 36**,** 327-363.

Aiello, R., Nagy, J. B., Giordano, G., Katovic, A. & Testa, F. 2005. Isomorphous substitution in zeolites. *Comptes Rendus Chimie,* 8**,** 321-329.

Aleem, M. A. & Arumairaj, P. 2012. Optimum mix for the geopolymer concrete. *Indian Journal of Science and Technology,* 5**,** 2299-2301.

Ali, I. O., Ali, A. M., Shabaan, S. M. & El-Nasser, K. S. 2009. Isomorphous substitution of Fe in the framework of aluminosilicate MFI by hydrothermal synthesis and their evaluation in p-nitrophenol degradation. *Journal of Photochemistry and Photobiology A: Chemistry,* 204**,** 25-31.

Alomayri, T., Vickers, L., Shaikh, F. U. & Low, I.-M. 2014. Mechanical properties of cotton fabric reinforced geopolymer composites at 200–1000° C. *Journal of Advanced Ceramics,* 3**,** 184-193.

Álvarez-Ayuso, E., Querol, X., Plana, F., Alastuey, A., Moreno, N., Izquierdo, M., Font, O., Moreno, T., Diez, S. & Vázquez, E. 2008. Environmental, physical and structural characterisation of geopolymer matrixes synthesised from coal (co-) combustion fly ashes. *Journal of Hazardous Materials,* 154**,** 175-183.

Anderson, J., Foger, K., Mole, T., Rajadhyaksha, R. & Sanders, J. 1979. Reactions on ZSM-5-type zeolite catalysts. *Journal of Catalysis,* 58**,** 114-130.

Andini, S., Cioffi, R., Colangelo, F., Grieco, T., Montagnaro, F. & Santoro, L. 2008. Coal fly ash as raw material for the manufacture of geopolymer-based products. *Waste management,* 28**,** 416-423.

Arafat, A., Jansen, J., Ebaid, A. & Van Bekkum, H. 1993. Microwave preparation of zeolite Y and ZSM-5. *Zeolites,* 13**,** 162-165.

Argauer, R. J. & Landolt, G. R. 1972. Crystalline zeolite ZSM-5 and method of preparing the same. Google Patents.

Aronne, A., Esposito, S. & Pernice, P. 1997. FTIR and DTA study of lanthanum aluminosilicate glasses. *Materials Chemistry and Physics,* 51**,** 163-168.

Attia, N. F., Menemparabath, M. M., Arepalli, S. & Geckeler, K. E. 2013. Inorganic nanotube composites based on polyaniline: Potential room-temperature hydrogen storage materials. *International Journal of Hydrogen Energy,* 38**,** 9251-9262.

Auerbach, S. M., Carrado, K. A. & Dutta, P. K. 2003. *Handbook of zeolite science and technology,* New York. Basel, CRC press.

Babajide, O., Petrik, L., Musyoka, N., Amigun, B. & Ameer, F. 2010. Use of coal fly ash as a catalyst in the production of biodiesel. *Petroleum & Coal,* 52**,** 261-272.

Bai, G., Qiao, Y., Shen, B. & Chen, S. 2011. Thermal decomposition of coal fly ash by concentrated sulfuric acid and alumina extraction process based on it. *Fuel Processing Technology,* 92**,** 1213-1219.

Barrer, R. M. 1948. 33. Synthesis of a zeolitic mineral with chabazite-like sorptive properties. *Journal of the Chemical Society (Resumed)***,** 127-132.

Bass, J. L. & Turner, G. L. 1997. Anion distributions in sodium silicate solutions. Characterization by 29Si NMR and infrared spectroscopies, and vapor phase osmometry. *The Journal of Physical Chemistry B,* 101**,** 10638-10644.

Baur, W. 1964. On cation+ water positions in faujasite. *American Mineralogist,* 49**,** 697.

Belviso, C., Cavalcante, F., Lettino, A. & Fiore, S. 2009. Zeolite synthesised from fused coal fly ash at low temperature using seawater for crystallization. *Coal Combustion and Gasification Products,* 1**,** 7-13.

Belviso, C., Cavalcante, F., Lettino, A. & Fiore, S. 2011. Effects of ultrasonic treatment on zeolite synthesized from coal fly ash. *Ultrasonics sonochemistry,* 18**,** 661-668.

Bergerhoff, G., Baur, W. & Nowacki, W. 1958. Neues Jahr. Mineral. *Mh,* 193.

Berkgaut, V. & Singer, A. 1996. High capacity cation exchanger by hydrothermal zeolitization of coal fly ash. *Applied clay science,* 10**,** 369-378.

Bhanarkar, A., Gavane, A., Tajne, D., Tamhane, S. & Nema, P. 2008. Composition and size distribution of particules emissions from a coal-fired power plant in India. *Fuel,* 87**,** 2095-2101.

Bhandari, R. B., Pathak, A. & Jha, V. K. 2013. A Laboratory Scale Synthesis of Geopolymer from Locally Available Coal Fly Ash from Brick Industry. *Journal of Nepal Chemical Society,* 29**,** 18-23.

Blissett, R. & Rowson, N. 2012. A review of the multi-component utilisation of coal fly ash. *Fuel,* 97**,** 1-23.

Böke, N., Birch, G. D., Nyale, S. M. & Petrik, L. F. 2015. New synthesis method for the production of coal fly ash-based foamed geopolymers. *Construction and Building Materials,* 75**,** 189-199.

Bondar, D., Lynsdale, C., Milestone, N. B., Hassani, N. & Ramezanianpour, A. 2011. Effect of type, form, and dosage of activators on strength of alkali-activated natural pozzolans. *Cement and Concrete Composites,* 33**,** 251-260.

Bottazzi, G. S. B., Martínez, M. L., Costa, M. B. G., Anunziata, O. A. & Beltramone, A. R. 2011. Inhibition of the hydrogenation of tetralin by nitrogen and sulfur compounds over Ir/SBA-16. *Applied Catalysis A: General,* 404**,** 30-38.

Breck, D. 1964. Crystalline molecular sieves. *Journal of Chemical Education,* 41**,** 678.

Bukhari, S. S., Behin, J., Kazemian, H. & Rohani, S. 2015. Conversion of coal fly ash to zeolite utilizing microwave and ultrasound energies: a review. *Fuel,* 140**,** 250-266.

Byrappa, K. & Yoshimura, M. 2001. Handbook of Hydrothermal Technology A technology for Crystal Growth and Materials Processing. *Byrappa, M. Yoshimura–Noyes Publications, Park Ridge, NJ*.

Carlson, C. L. & Adriano, D. C. 1993. Environmental impacts of coal combustion residues. *Journal of Environmental Quality,* 22**,** 227-247.

Chandrasekhar, S. & Pramada, P. 2008. Microwave assisted synthesis of zeolite A from metakaolin. *Microporous and Mesoporous Materials,* 108**,** 152-161.

Chang, H.-L. & Shih, W.-H. 2000. Synthesis of zeolites A and X from fly ashes and their ion-exchange behavior with cobalt ions. *Industrial & Engineering Chemistry Research,* 39**,** 4185-4191.

Chareonpanich, M., Jullaphan, O. & Tang, C. 2011. Bench-scale synthesis of zeolite A from subbituminous coal ashes with high crystalline silica content. *Journal of Cleaner Production,* 19**,** 58-63.

Chareonpanich, M., Namto, T., Kongkachuichay, P. & Limtrakul, J. 2004. Synthesis of ZSM-5 zeolite from lignite fly ash and rice husk ash. *Fuel processing technology,* 85**,** 1623-1634.

Charles, W. & Ho, G. 2013. Methyl ethyl ketone removal using microbial attached zeolite biofilter.

Corma, A. 2003. State of the art and future challenges of zeolites as catalysts. *Journal of Catalysis,* 216**,** 298-312.

Criado, M., Fernández-Jiménez, A. & Palomo, A. 2007. Alkali activation of fly ash: effect of the SiO 2/Na 2 O ratio: Part I: FTIR study. *Microporous and mesoporous materials,* 106**,** 180-191.

Crini, G. 2006. Non-conventional low-cost adsorbents for dye removal: a review. *Bioresource technology,* 97**,** 1061-1085.

Cundy, C. S. & Cox, P. A. 2003. The hydrothermal synthesis of zeolites: history and development from the earliest days to the present time. *Chemical Reviews,* 103**,** 663-702.

Daniels, W. L., Stewart, B., Haering, K. & Zipper, C. 2002. The potential for beneficial reuse of coal fly ash in southwest Virginia mining environments. *Virginia Cooperative Extension Publication***,** 460-134.

Davidovits, J. Properties of geopolymer cements. First international conference on alkaline cements and concretes, 1994. 131-149.

Davidovits, J. & Davidovics, M. 1991. Geopolymer: ultra-high temperature tooling material for the manufacture of advanced composites. *How Concept Becomes Reality.,* 36**,** 1939-1949.

Davis, M. E. & Lobo, R. F. 1992. Zeolite and molecular sieve synthesis. *Chemistry of Materials,* 4**,** 756-768.

Delair, S., Prud'homme, É., Peyratout, C., Smith, A., Michaud, P., Eloy, L., Joussein, E. & Rossignol, S. 2012. Durability of inorganic foam in solution: The role of alkali elements in the geopolymer network. *Corrosion Science,* 59**,** 213-221.

Du Plessis, P. W. 2014. *Process design for the up-scale zeolite synthesis from South African coal fly ash.* MTech Chemical Engineering Dissertations, Academic Cape Peninsula University of Technology.

Duxson, P., Fernández-Jiménez, A., Provis, J. L., Lukey, G. C., Palomo, A. & Van Deventer, J. 2007. Geopolymer technology: the current state of the art. *Journal of Materials Science,* 42**,** 2917-2933.

Dwyer, F. G. & Chu, P. 1985. *Synthesis of zeolite ZSM-5*. USA patent application US 4526879 A.

El-Naggar, M., El-Kamash, A., El-Dessouky, M. & Ghonaim, A. 2008. Two-step method for preparation of NaA-X zeolite blend from fly ash for removal of cesium ions. *Journal of Hazardous Materials,* 154**,** 963-972.

El Didamony, H., Assal, H., El Sokkary, T. & Gawwad, H. A. 2012. Kinetics and physico-chemical properties of alkali activated blast-furnace slag/basalt pastes. *HBRC Journal,* 8**,** 170-176.

Ensminger, D. & Bond, L. J. 2011. *Ultrasonics: fundamentals, technologies, and applications*, CRC press.

Fan, F., Feng, Z., Li, G., Sun, K., Ying, P. & Li, C. 2008. In situ UV Raman spectroscopic studies on the synthesis mechanism of zeolite X. *Chemistry–A European Journal,* 14**,** 5125-5129.

Farahmandjou, M. & Golabiyan, N. 2015. New pore structure of nano-alumina (Al2O3) prepared by sol gel method. *Journal of Ceramic Processing Research,* 16**,** 1-4.

Fernández-Jiménez, A. & Palomo, A. 2005. Composition and microstructure of alkali activated fly ash binder: effect of the activator. *Cement and Concrete Research,* 35**,** 1984-1992.

Ferreira, C., Ribeiro, A. & Ottosen, L. 2003. Possible applications for municipal solid waste fly ash. *Journal of Hazardous Materials,* 96**,** 201-216.

Fisher, G. L., Prentice, B. A., Silberman, D., Ondov, J. M., Biermann, A. H., Ragaini, R. C. & Mcfarland, A. R. 1978. Physical and morphological studies of size-classified coal fly ash. *Environmental Science & Technology,* 12**,** 447-451.

Flanigen, E. M., Khatami, H. & Szymanski, H. A. 1971. Infrared structural studies of zeolite frameworks.

Font, O., Moreno, N., Díez, S., Querol, X., López-Soler, A., Coca, P. & Peña, F. G. 2009. Differential behaviour of combustion and gasification fly ash from Puertollano Power Plants (Spain) for the synthesis of zeolites and silica extraction. *Journal of Hazardous Materials,* 166**,** 94-102.

Fouad, O., Mohamed, R., Hassan, M. & Ibrahim, I. 2006. Effect of template type and template/silica mole ratio on the crystallinity of synthesized nanosized ZSM-5. *Catalysis today,* 116**,** 82-87.

Freude, D., Fröhlich, T., Pfeifer, H. & Scheler, G. 1983. NMR studies of aluminium in zeolites. *Zeolites,* 3**,** 171-177.

García, E. J., Pérez-Pellitero, J., Jallut, C. & Pirngruber, G. D. 2013. Quantification of the confinement effect in microporous materials. *Physical Chemistry Chemical Physics,* 15**,** 5648-5657.

Gates, B. C., Katzer, J. R. & Schuit, G. C. 1979. *Chemistry of Catalytic Processes*, McGraw-Hill New York.

Georgiev, D., Bogdanov, B., Angelova, K., Markovska, I. & Hristov, Y. 2009. Synthetic zeolites–structure, classification, current trends in zeolite synthesis. Review. International Science Conference, 2009. Stara Zagora, BULGARIA, 4-5.06.

Giannopoulou, I. & Panias, D. Structure, design and applications of geopolymeric materials. Proceedings of the 3rd International Conference on Deformation Processing and Structure of Materials, 2007. 20-22.

Glukhovsky, V. D. Ancient, modern and future concretes. Proceedings of the First International Conference on Alkaline Cements and Concretes, 1994. Kiev, Ukraine, 1-9.

Golden, T. C., Taylor, F. W., Johnson, L. M., Malik, N. H. & Raiswell, C. J. 2000. Purification of air. Google Patents.

Goodarzi, F. 2006. Characteristics and composition of fly ash from Canadian coal-fired power plants. *Fuel,* 85**,** 1418-1427.

Hanson, A. 1995. Natural Zeolites. Many merits, meagre markets. *Industrial Minerals,* 339**,** 40-53.

Harada, Y., Kurata, N. & Furuno, G. 1993. Simultaneous determination of major constituents and impurities in high-purity mullite using pressure acid decomposition. *Analytical Sciences,* 9**,** 99-103.

Hardjito, D., Wallah, S. E., Sumajouw, D. M. & Rangan, B. V. 2004. On the development of fly ash-based geopolymer concrete. *ACI Materials Journal-American Concrete Institute,* 101**,** 467-472.

Hattori, T. & Yashima, T. 1994. *Zeolites and Microporous Crystals*, Elsevier.

Heebink, L. V. & Hassett, D. J. Coal fly ash trace element mobility in soil stabilization. Proceedings: 2001 International Ash Utilization Symposium, Center for Applied Energy Research, Univ. of Kentucky, Paper, 2001.

Holler, H. & Wirsching, U. 1985. Zeolite formation from fly-ash. *Fortschritte der Mineralogie,* 63**,** 21-43.

Hollman, G., Steenbruggen, G. & Janssen-Jurkovičová, M. 1999. A two-step process for the synthesis of zeolites from coal fly ash. *Fuel,* 78**,** 1225-1230.

Hosseini, S. A., Niaei, A. & Salari, D. 2011. Production of γ-Al2O3 from Kaolin. *Open Journal of Physical Chemistry,* 1**,** 23.

Htun, M. M. H., Htay, M. M. & Lwin, M. Z. Preparation of Zeolite (NaX, Faujasite) from Pure Silica and Alumina Sources. International Conference on Chemical Processes and Environmental issues 2012. 15-16.

Hui, K. & Chao, C. Y. H. 2006. Pure, single phase, high crystalline, chamfered-edge zeolite 4A synthesized from coal fly ash for use as a builder in detergents. *Journal of Hazardous Materials,* 137**,** 401-409.

Inada, M., Tsujimoto, H., Eguchi, Y., Enomoto, N. & Hojo, J. 2005. Microwave-assisted zeolite synthesis from coal fly ash in hydrothermal process. *Fuel,* 84**,** 1482-1486.

Iyer, R. 2002. The surface chemistry of leaching coal fly ash. *Journal of Hazardous Materials,* 93**,** 321-329.

Jacobsen, C. J., Madsen, C., Houzvicka, J., Schmidt, I. & Carlsson, A. 2000. Mesoporous zeolite single crystals. *Journal of the American Chemical Society,* 122**,** 7116-7117.

Jha, B. & Singh, D. 2011. A review on synthesis, characterization and industrial applications of flyash zeolites. *Journal of Materials Education,* 33**,** 65.

Kalapathy, U., Proctor, A. & Shultz, J. 2000. A simple method for production of pure silica from rice hull ash. *Bioresource Technology,* 73**,** 257-262.

Kruger, R. A. 1997. Fly ash beneficiation in South Africa: creating new opportunities in the market-place. *Fuel,* 76**,** 777-779.

Kuhn, E. M. 2005. *Microbiology of fly ash-acid mine drainage co-disposal processes.* Magister Scientiae (M.Sc.), University of the Western Cape.

Külaviir, M. 2014. *Geopolymerization of the Estonian oil shale solid heat carrier retorting waste ash: characterization of structural changes through infrared (ATR-FTIR) and nuclear magnetic resonance spectroscopic analysis.* Ecology and Earth Science BSc thesis, Tartu Ülikool.

Lee, W. & Van Deventer, J. 2003. Use of infrared spectroscopy to study geopolymerization of heterogeneous amorphous aluminosilicates. *Langmuir,* 19**,** 8726-8734.

Li, L.-S., Wu, Y.-S., Liu, Y.-Y. & Zhai, Y.-C. 2011. Extraction of alumina from coal fly ash with sulfuric acid leaching method. *The Chinese Journal of Process Engineering,* 11**,** 254-258.

Li, Y. & Yang, W. 2008. Microwave synthesis of zeolite membranes: a review. *Journal of Membrane Science,* 316**,** 3-17.

Lunsford, J. 1990. The catalytic conversion of methane to higher hydrocarbons. *Catalysis Today,* 6**,** 235-259.

Machado, N. R. C. F. & Miotto, D. M. M. 2005. Synthesis of Na–A and–X zeolites from oil shale ash. *Fuel,* 84**,** 2289-2294.

Madzivire, G. 2009. *Removal of sulphates from South African mine water using coal fly ash.* Magister Scientiae in Chemistry MSc Thesis, University of the Western Cape.

Madzivire, G., Petrik, L. F., Gitari, W. M., Ojumu, T. V. & Balfour, G. 2010. Application of coal fly ash to circumneutral mine waters for the removal of sulphates as gypsum and ettringite. *Minerals Engineering,* 23**,** 252-257.

Mainganye, D. 2012. *Synthesis of zeolites from South African coal fly ash: Investigation of scale-up conditions.* Magister Technologiae in Chemical Engineering MSc Thesis, Cape Peninsula University of Technology.

Mainganye, D., Ojumu, T. V. & Petrik, L. 2013. Synthesis of zeolites Na-P1 from South African coal fly ash: effect of impeller design and agitation. *Materials,* 6**,** 2074-2089.

Marchi, A. & Froment, G. 1991. Catalytic conversion of methanol to light alkenes on SAPO molecular sieves. *Applied Catalysis,* 71**,** 139-152.

Matjie, R., Bunt, J. & Van Heerden, J. 2005. Extraction of alumina from coal fly ash generated from a selected low rank bituminous South African coal. *Minerals Engineering,* 18**,** 299-310.

Medina, A., Gamero, P., Almanza, J. M., Vargas, A., Montoya, A., Vargas, G. & Izquierdo, M. 2010. Fly ash from a Mexican mineral coal. II. Source of W zeolite and its effectiveness in arsenic (V) adsorption. *Journal of Hazardous Materials,* 181**,** 91-104.

Miller, F. A. & Wilkins, C. H. 1952. Infrared spectra and characteristic frequencies of inorganic ions. *Analytical Chemistry,* 24**,** 1253-1294.

Minet, J., Abramson, S., Bresson, B., Sanchez, C., Montouillout, V. & Lequeux, N. 2004. New layered calcium organosilicate hybrids with covalently linked organic functionalities. *Chemistry of Materials,* 16**,** 3955-3962.

Misran, H., Singh, R., Begum, S. & Yarmo, M. A. 2007. Processing of mesoporous silica materials (MCM-41) from coal fly ash. *Journal of Materials Processing Technology,* 186**,** 8-13.

Molina, A. & Poole, C. 2004. A comparative study using two methods to produce zeolites from fly ash. *Minerals Engineering,* 17**,** 167-173.

Moliner, M., Franch, C., Palomares, E., Grill, M. & Corma, A. 2012. Cu–SSZ-39, an active and hydrothermally stable catalyst for the selective catalytic reduction of NO x. *Chemical Communications,* 48**,** 8264-8266.

Mondragon, F., Rincon, F., Sierra, L., Escobar, J., Ramirez, J. & Fernandez, J. 1990. New perspectives for coal ash utilization: synthesis of zeolitic materials. *Fuel,* 69**,** 263-266.

Moreno, N., Querol, X., Ayora, C., Alastuey, A., Fernández-Pereira, C. & Janssen-Jurkovicová, M. 2001. Potential environmental applications of pure zeolitic material synthesized from fly ash. *Journal of Environmental Engineering,* 127**,** 994-1002.

Moreno, N., Querol, X., Plana, F., Andres, J. M., Janssen, M. & Nugteren, H. 2002. Pure zeolite synthesis from silica extracted from coal fly ashes. *Journal of Chemical Technology and Biotechnology,* 77**,** 274-279.

Murayama, N., Yamamoto, H. & Shibata, J. 2002. Mechanism of zeolite synthesis from coal fly ash by alkali hydrothermal reaction. *International Journal of Mineral Processing,* 64**,** 1-17.

Muriithi, G. N., Petrik, L. F., Fatoba, O., Gitari, W. M., Doucet, F. J., Nel, J., Nyale, S. M. & Chuks, P. E. 2013. Comparison of CO 2 capture by ex-situ accelerated carbonation and in in-situ naturally weathered coal fly ash. *Journal of Environmental Management,* 127**,** 212-220.

Musyoka, N. 2012. *Zeolite A, X and Cancrinite from South African coal fly ash: mechanism of crystallization, routes to rapid synthesis and new morphology.* Doctor of Philosophy in Chemistry PhD thesis, University of Western Cape.

Musyoka, N., Petrik, L. & Hums, E. 2011. Ultrasonic assisted synthesis of zeolite A from coal fly ash using mine waters (acid mine drainage and circumneutral mine water) as a substitute for ultra pure water. *Proceedings of International Mineral Water Association, Aachen, Germany***,** 423-428.

Musyoka, N. M. 2009. *Hydrothermal synthesis and optimisation of zeolite Na-P1 from South African coal fly ash.* Magister Scientiae in Chemistry, University of Western Cape.

Musyoka, N. M., Petrik, L. F., Fatoba, O. O. & Hums, E. 2013. Synthesis of zeolites from coal fly ash using mine waters. *Minerals Engineering,* 53**,** 9-15.

Musyoka, N. M., Petrik, L. F., Gitari, W. M., Balfour, G. & Hums, E. 2012. Optimization of hydrothermal synthesis of pure phase zeolite Na-P1 from South African coal fly ashes. *Journal of Environmental Science and Health, Part A,* 47**,** 337-350.

Naik, V. 1993. Option valuation and hedging strategies with jumps in the volatility of asset returns. *The Journal of Finance,* 48**,** 1969-1984.

Narayanan, S., Sultana, A., Krishna, K., Mériaudeau, P. & Naccache, C. 1995. Synthesis of ZSM-5 type zeolites with and without template and evaluation of physicochemical properties and aniline alkylation activity. *Catalysis letters,* 34**,** 129-138.

Nazari, A. & Riahi, S. 2011. The effects of SiO 2 nanoparticles on physical and mechanical properties of high strength compacting concrete. *Composites Part B: Engineering,* 42**,** 570-578.

Nyale, S. M., Babajide, O. O., Birch, G. D., Böke, N. & Petrik, L. F. 2013. Synthesis and characterization of coal fly ash-based foamed geopolymer. *Procedia Environmental Sciences,* 18**,** 722-730.

Nyale, S. M., Eze, C. P., Akinyeye, R. O., Gitari, W. M., Akinyemi, S. A., Fatoba, O. O. & Petrik, L. F. 2014. The leaching behaviour and geochemical fractionation of trace elements in hydraulically disposed weathered coal fly ash. *Journal of Environmental Science and Health, Part A,* 49**,** 233-242.

Oboirien, B. O. 2011. *Gasification of high ash coal and chars from South African coals.* Doctor of Philosophy PhD, Faculty of Engineering and the Built Environment, University of the Witwatersrand.

Ojha, K., Pradhan, N. C. & Samanta, A. N. 2004. Zeolite from fly ash: synthesis and characterization. *Bulletin of Materials Science,* 27**,** 555-564.

Ojumu, T. V., Du Plessis, P. W. & Petrik, L. F. 2016. Synthesis of zeolite A from coal fly ash using ultrasonic treatment–A replacement for fusion step. *Ultrasonics sonochemistry,* 31**,** 342-349.

Oliveira, L. C., Petkowicz, D. I., Smaniotto, A. & Pergher, S. B. 2004. Magnetic zeolites: a new adsorbent for removal of metallic contaminants from water. *Water Research,* 38**,** 3699-3704.

Olson, D., Kokotailo, G., Lawton, S. & Meier, W. 1981. Crystal structure and structure-related properties of ZSM-5. *The Journal of Physical Chemistry,* 85**,** 2238-2243.

Onisei, S., Pontikes, Y., Van Gerven, T., Angelopoulos, G., Velea, T., Predica, V. & Moldovan, P. 2012. Synthesis of inorganic polymers using fly ash and primary lead slag. *Journal of Hazardous Materials,* 205**,** 101-110.

Oudadesse, H., Derrien, A. C., Lefloch, M. & Davidovits, J. 2007. MAS-NMR studies of geopolymers heat-treated for applications in biomaterials field. *Journal of Materials Science,* 42**,** 3092-3098.

Ouki, S. & Kavannagh, M. 1999. Treatment of metals-contaminated wastewaters by use of natural zeolites. *Water Science and Technology,* 39**,** 115-122.

Palomo, A., Blanco-Varela, M. T., Granizo, M., Puertas, F., Vazquez, T. & Grutzeck, M. 1999. Chemical stability of cementitious materials based on metakaolin. *Cement and Concrete Research,* 29**,** 997-1004.

Passaglia, E. & Sheppard, R. A. 2001. The crystal chemistry of zeolites. *Reviews in mineralogy and geochemistry,* 45**,** 69-116.

Pelrine, B. P. 1978. *Synthesis of zeolite ZSM-5*. United State patent application US4100262 A.

Petrik, L. 2004. Environmental impact of the placing of coal residue, fine coal residue and ash in mined out areas. *Journal of Environmental Science,* 43**,** 132-145.

Petrik, L., O'Connor, C. & Schwarz, S. 1995. The influence of various synthesis parameters on the morphology and crystal size of ZSM-5 and the relationship between morphology and crystal size and propene oligomerization activity. *Studies in Surface Science and Catalysis,* 94**,** 517-524.

Petrik, L. F., White, R. A., Klink, M. J., Somerset, V. S., Burgers, C. L. & Fey, M. V. Utilization of South African fly ash to treat acid coal mine drainage, and production of high quality zeolites from the residual solids. Proceedings of the Ash Utilization Symposium, Lexington, KY, USA, 2003a.

Petrik, L. F., White, R. A., Klink, M. J., Somerset, V. S., Burgers, C. L. & Fey, M. V. Utilization of South African fly ash to treat acid coal mine drainage, and production of high quality zeolites from the residual solids. International Ash Utilization Symposium, October 20-22, 2003b Lexington, Kentucky, USA. Center for Applied Energy Research

Pfenninger, A. 1999. Manufacture and use of zeolites for adsorption processes. *In:* DIVISION, Z. (ed.) *Structures and Structure Determination.* Uetikon, Switzerland: Springer.

Praharaj, T. K. & Ray, G. 2001. Percutaneous transluminal coronary angioplasty with stenting of anomalous right coronary artery originating from left sinus of valsalva using the voda guiding catheter: a report of two cases. *Indian Heart Journal,* 53**,** 79-82.

Purdon, A. 1940. The action of alkalis on blast-furnace slag. *Journal of the Society of Chemical Industry,* 59**,** 191-202.

Querol Carceller, X., Moreno, N., Valero, A., López-Soler, Á., Juan Mainar, R., Alastuey, A., Ayora, C., Gimeno, A., Manuel, J. & Medinaceli, A. 2007. Synthesis of high ion exchange zeolites from coal fly ash. *Geologica Acta,* 5**,** 0049-57.

Querol, X., Alastuey, A., Fernández-Turiel, J. & López-Soler, A. 1995. Synthesis of zeolites by alkaline activation of ferro-aluminous fly ash. *Fuel,* 74**,** 1226-1231.

Querol, X., Alastuey, A., López-Soler, A., Plana, F., Andrés, J. M., Juan, R., Ferrer, P. & Ruiz, C. R. 1997. A fast method for recycling fly ash: microwave-assisted zeolite synthesis. *Environmental Science & Technology,* 31**,** 2527-2533.

Querol, X., Moreno, N., Umaña, J. T., Alastuey, A., Hernández, E., Lopez-Soler, A. & Plana, F. 2002. Synthesis of zeolites from coal fly ash: an overview. *International Journal of Coal Geology,* 50**,** 413-423.

Querol, X., Umaña, J. C., Plana, F., Alastuey, A., Lopez-Soler, A., Medinaceli, A., Valero, A., Domingo, M. J. & Garcia-Rojo, E. 2001. Synthesis of zeolites from fly ash at pilot plant scale. Examples of potential applications. *Fuel,* 80**,** 857-865.

Ramesh, K., Damodar Reddy, D., Kumar Biswas, A. & Subba Rao, A. 2011. 4 Zeolites and Their Potential Uses in Agriculture. *Advances in Agronomy,* 113**,** 215.

Rattanasak, U. & Chindaprasirt, P. 2009. Influence of NaOH solution on the synthesis of fly ash geopolymer. *Minerals Engineering,* 22**,** 1073-1078.

Rida, M. A. & Harb, F. 2014. Synthesis and characterization of amorphous silica nanoparticles from aqueous silicates using cationic surfactants. *Journal of Metals, Materials and Minerals,* 24.

Rodríguez-González, L., Hermes, F., Bertmer, M., Rodríguez-Castellón, E., Jiménez-López, A. & Simon, U. 2007. The acid properties of H-ZSM-5 as studied by NH 3-TPD and 27 Al-MAS-NMR spectroscopy. *Applied Catalysis A: General,* 328**,** 174-182.

Run, M.-T. & Wu, G. 2004. Synthesis of mesoporous molecular sieve under ultrasonic. *Chinese Journal of Inorganic Chemistry,* 20**,** 219-224.

Ruthven, D. M. 1984. *Principles of adsorption and adsorption processes,* New York, John Wiley & Sons.

Saikia, B. J. & Parthasarathy, G. 2010. Fourier transform infrared spectroscopic characterization of kaolinite from Assam and Meghalaya, Northeastern India. *Journal of Modern Physics,* 1**,** 206.

Sang, S., Chang, F., Liu, Z., He, C., He, Y. & Xu, L. 2004. Difference of ZSM-5 zeolites synthesized with various templates. *Catalysis Today,* 93**,** 729-734.

Saravanan, G., Jeyasehar, C. & Kandasamy, S. 2013. Flyash Based Geopolymer Concrete–A State of the Art Review. *Journal of Engineering Science and Technology Review,* 6**,** 25-32.

Schiavon, N. 2007. Kaolinisation of granite in an urban environment. *Environmental Geology,* 52**,** 399-407.

Schlomach, J. & Kind, M. 2004. Investigations on the semi-batch precipitation of silica. *Journal of Colloid and Interface Science,* 277**,** 316-326.

Seidel, A., Sluszny, A., Shelef, G. & Zimmels, Y. 1999. Self inhibition of aluminium leaching from coal fly ash by sulfuric acid. *Chemical Engineering Journal,* 72**,** 195-207.

Sharma, S. K. & Kalra, N. 2006. Effect of flyash incorporation on soil properties and productivity of crops'. *Journal of Scientific and Industrial Research,* 65**,** 383-390.

Shigemoto, N., Hayashi, H. & Miyaura, K. 1993. Selective formation of Na-X zeolite from coal fly ash by fusion with sodium hydroxide prior to hydrothermal reaction. *Journal of Materials Science,* 28**,** 4781-4786.

Sibanda, V., Ndlovu, S., Dombo, G., Shemi, A. & Rampou, M. 2016. Towards the Utilization of Fly Ash as a Feedstock for Smelter Grade Alumina Production: A Review of the Developments. *Journal of Sustainable Metallurgy,* 2**,** 167-184.

Singer, A., Navrot, J. & Shapira, R. 1982. Extraction of aluminium from fly-ash by commercial and microbiologically-produced citric acid. *European Journal of Applied Microbiology and Biotechnology,* 16**,** 228-230.

Singh, P. S., Bastow, T. & Trigg, M. 2005. Structural studies of geopolymers by 29Si and 27Al MAS-NMR. *Journal of Materials Science,* 40**,** 3951-3961.

Singh, R. & Dutta, P. K. 2003. *MFI: a case study of zeolite synthesis,* Columbus, Ohio, USA, Marcel Dekker, Inc.

Singh, S., Verma, L. K., Sambi, S. & Sharma, S. Adsorption behaviour of Ni (II) from water onto zeolite X: kinetics and equilibrium studies. Proceedings of the World Congress on Engineering and Computer Science, October 22 - 24, 2008 San Francisco, USA. 22-24.

Swanepoel, J. & Strydom, C. 2002. Utilisation of fly ash in a geopolymeric material. *Applied Geochemistry,* 17**,** 1143-1148.

Tchadjié, L., Djobo, J., Ranjbar, N., Tchakouté, H., Kenne, B., Elimbi, A. & Njopwouo, D. 2016. Potential of using granite waste as raw material for geopolymer synthesis. *Ceramics International,* 42**,** 3046-3055.

Thuadaij, P. & Nuntiya, A. Synthesis of Na-x hydrate zeolite from fly ash and amorphous silica from rice husk ash by fusion with caustic soda prior to incubation. Proceeding of the International Conference on Chemistry and Chemical Process, Bangkok, 2011. 69-73.

Thuadaij, P. & Nuntiya, A. 2012. Preparation and characterization of faujasite using fly ash and amorphous silica from rice husk ash. *Procedia Engineering,* 32**,** 1026-1032.

Treacy, M. & Higgins, J. 2001. Collection of simulated XRD powder patterns for zeolites. Published on behalf of the Structure Commission of the 'International Zeolite Association'. *Powder Patterns, 203,* 204.

Triantafyllidis, K. S., Nalbandian, L., Trikalitis, P. N., Ladavos, A. K., Mavromoustakos, T. & Nicolaides, C. P. 2004. Structural, compositional and acidic characteristics of nanosized amorphous or partially crystalline ZSM-5 zeolite-based materials. *Microporous and Mesoporous Materials,* 75**,** 89-100.

Van Hamburg, H., Andersen, A. N., Meyer, W. J. & Robertson, H. G. 2004. Ant community development on rehabilitated ash dams in the South African Highveld. *Restoration Ecology,* 12**,** 552-558.

Van Jaarsveld, J., Van Deventer, J. & Lorenzen, L. 1997. The potential use of geopolymeric materials to immobilise toxic metals: Part I. Theory and applications. *Minerals Engineering,* 10**,** 659-669.

Venuto, P. B. & Habib Jr, E. T. 1979. *Fluid catalytic cracking with zeolite catalysts,* United States, Marcel Dekker, Inc., New York, NY.

Wang, S. & Wu, H. 2006. Environmental-benign utilisation of fly ash as low-cost adsorbents. *Journal of Hazardous Materials,* 136**,** 482-501.

Wdowin, M., Franus, M., Panek, R., Badura, L. & Franus, W. 2014. The conversion technology of fly ash into zeolites. *Clean Technologies and Environmental Policy,* 16**,** 1217-1223.

Weitkamp, J. 2000. Zeolites and catalysis. *Solid State Ionics,* 131**,** 175-188.

Wu, C.-Y., Yu, H.-F. & Zhang, H.-F. 2012. Extraction of aluminium by pressure acid-leaching method from coal fly ash. *Transactions of Nonferrous Metals Society of China,* 22**,** 2282-2288.

Xu, J. & Khor, K. A. 2007. Chemical analysis of silica doped hydroxyapatite biomaterials consolidated by a spark plasma sintering method. *Journal of Inorganic Biochemistry,* 101**,** 187-195.

Young, L. B. 1982. *From acid and olefin in presence of zeolite having high ratio of silica to alumina*. USA patent application US4365084 A.

Zhang, L. 2013. Production of bricks from waste materials–a review. *Construction and Building Materials,* 47**,** 643-655.

Zhao, X., Lu, G. & Zhu, H. 1997. Effects of ageing and seeding on the formation of zeolite Y from coal fly ash. *Journal of Porous Materials,* 4**,** 245-251.